

**INVESTIGATION OF THE POTENTIAL OF USING SEISMIC ATTENUATION  
AND VELOCITY TO IDENTIFY MASSIVE SULPHIDE ORE DEPOSITS**

By

© ASMA DEWAN

A Thesis submitted to the

School of Graduate Studies

in partial fulfillment of the requirements for the degree of

**Master of Engineering**

**Faculty of Engineering & Applied Science,**

Memorial University of Newfoundland

**October, 2014**

St. John's

Newfoundland and Labrador

بِسْمِ اللَّهِ الرَّحْمَنِ الرَّحِيمِ

In the name of Allah, the most Gracious, the most Compassionate

## ABSTRACT

Massive sulphide ore deposits are one of the major sources of valuable minerals. Therefore, identifying massive sulphide ores from their associated host rocks is of great interest in mineral exploration. The seismic P-wave velocity and density of massive sulphides and associated host rocks has been studied significantly but there has been very little work on attenuation. This thesis reports on a comprehensive assessment of attenuation and loss factor along with velocity for the sulphide minerals (pyrite, chalcopyrite, sphalerite and pyrrhotite) and the felsic and mafic host rocks. The Spectral Ratio Technique is used to measure attenuation. The relationships among velocity, attenuation and loss factor along with their sensitivity with hydrostatic confining pressure (10-600 MPa) will be discussed. Seismic P-wave velocity for silicates and massive sulphides shows positive change with pressure. Except for low pyrite,  $Q$  shows modest pressure dependence for other rocks. The low pressure results for  $Q$  are not systematic and low pyrite shows anomalous behaviour for  $Q$  and loss factor at low pressure. The changes in loss factor in felsic and mafic silicates are not pronounced compared to that in massive sulphides, however the response of  $Q$  with pressure is much more complicated than loss factor. The applicability of the joint interpretation of these parameters (velocity, attenuation and loss factor) to identify massive sulphides is the key of this research. Moreover the response of these parameters in low (below 100 Mpa) and high (above 100 Mpa) pressure zones are observed separately to observe their pattern of change and gradient with pressure to establish a relationship with pressure.

## **ACKNOWLEDGEMENT**

I am grateful to Allah S.W.T, the most gracious, the most merciful, for giving me the strength to complete this thesis. It is with His will, that I have completed this thesis after years of struggle and hard work.

I would like to thank my supervisors Dr. Stephen Butt and Dr. Charles Hurich for their relentless support in my Masters work. All the advice and assistance they gave, academically and non-academically, are really supportive and will never be forgotten. I would also like to thank the School of Graduate Studies and Faculty of Engineering and Applied Science, Memorial University of Newfoundland, for their financial and relevant support.

I would like to mention the names of several persons who were always beside me to encourage and support. My deepest gratitude goes to my mother for her inspiration and encouragement throughout my whole journey. I would like to mention the name of my daughter Fatimah who fills my life with all the sources of joy. Last, but not least, I would like to convey my thanks and appreciation to my husband, Hasan, who always stands beside and encourage me to pursue higher studies.

## Table of Contents

<b>Title</b>	<b>Page</b>
<i>ABSTRACT</i> .....	<i>iii</i>
<i>ACKNOWLEDGEMENT</i> .....	<i>iv</i>
<i>List of Tables</i> .....	<i>ix</i>
<i>List of Figures</i> .....	<i>x</i>
 <i>Chapter 1</i>	
<i>Introduction</i> .....	<i>1</i>
<i>1.1 Background</i> .....	<i>1</i>
<i>1.2 Importance of this study</i> .....	<i>3</i>
<i>1.3 Scope and Research Objectives</i> .....	<i>3</i>
<i>1.4 Organization of the thesis</i> .....	<i>4</i>
 <i>Chapter 2</i>	
<i>Literature Review</i> .....	<i>6</i>
<i>2.1 Necessity of a new massive sulphide exploration technique</i> .....	<i>6</i>
<i>2.2 Geophysical methods used in exploration:</i> .....	<i>7</i>
<i>2.3 Physical properties of massive sulphides</i> .....	<i>8</i>
<i>2.4 Attenuation and Q:</i> .....	<i>12</i>
<i>2.4.1 Mechanism and dependency of attenuation:</i> .....	<i>14</i>
<i>2.4.2 Application of attenuation</i> .....	<i>16</i>

## Chapter 3

<i>Methodology</i> .....	20
3.1 <i>Locations of investigations</i> .....	20
3.2 <i>High Pressure Laboratory</i> .....	21
3.2.1 <i>Equipment setup</i> .....	21
3.2.2 <i>Set up of the sample</i> .....	22
3.3 <i>Measurements of different parameter</i> .....	24
3.3.1 <i>The pulse transmission technique</i> .....	24
3.3.2 <i>Measurement of Attenuation</i> .....	26
3.3.3 <i>Measurement of loss factor</i> .....	29
3.4 <i>Test data</i> .....	30
3.4.1 <i>Selection of the reference sample</i> .....	30
3.4.2 <i>Selection of the rock samples</i> .....	32
3.4.3 <i>Method used to process and analyse data for Q factor calculation</i>	33
3.4.4 <i>Grading of the rock samples:</i> .....	38
3.4.5 <i>Summary of the grading and grouping</i> .....	42
3.5 <i>Summary data:</i> .....	42
<i>Chapter 4 Results and Discussion</i> .....	43
4.1 <i>Velocity versus pressure</i> .....	44
4.1.1 <i>Velocity Vs. pressure for the four groups of massive sulphides</i> .....	44
4.1.2 <i>Velocity for massive sulphides and silicates</i> .....	46
4.2 <i>Q versus pressure</i> .....	49

4.2.1	<i>Q</i> Vs. pressure for the four groups of massive sulphides .....	49
4.2.2	<i>Q</i> for massive sulphides and silicates.....	52
4.3	Loss factor versus pressure .....	56
4.3.1	Loss factor Vs. pressure for four groups of massive sulphides .....	56
4.3.2	Loss factor for massive sulphides and silicates.....	58
4.4	Summary of the velocity, <i>Q</i> and Loss factor plots.....	60
4.4.1	Summary results .....	60
4.5	Low pressure results.....	63
4.6	Sensitivity Analysis by Monte Carlo Approach: Sensitivity of <i>Q</i> for Silicates and Massive sulphides.....	67
4.7	Relationship among the parameters.....	72
4.7.1	Velocity and <i>Q</i> .....	73
4.7.2	Velocity and Loss factor.....	76
4.7.3	Loss factor and <i>Q</i> .....	78
4.7.4	Low and high pressure response .....	80
 <i>Chapter 5</i>		
<i>Conclusion</i> .....		
		84
5.1	Findings from the analysis: .....	85
5.2	Future recommendations.....	88
 <i>Bibliography</i> .....		
		89
 <i>Appendix A (Rock Properties)</i> .....		
		98

*Appendix B (Loss Factor)*..... 134

## List of Tables

<b>Table No.</b>	<b>Page</b>
<i>Table 4.2-1 Poisson's ratio of silicates and sulphide minerals .....</i>	<i>52</i>
<i>Table 4.4-1 Summary results for pyrite, chalcopyrite, sphalerite and pyrrhotite .....</i>	<i>61</i>
<i>Table 4.4-2 Summary results of Silicates and massive sulphides .....</i>	<i>62</i>
<i>Table 4.6-1 Distribution type and parameter for Grade A rock data.....</i>	<i>69</i>
<i>Table 4.6-2 Correlation coefficient of sample length, velocity and slope on Q .....</i>	<i>71</i>

## List of Figures

Figure No.	Page
<i>Figure 2.3-1 Velocity (Vp)-density fields for common sulfide ores and silicate host rocks at 200 MPa.....</i>	9
<i>Figure 3.2-1 The Pressure vessel (on left) and the Pressure Control panel (on right) of High Pressure Laboratory Dalhousie/GSC.....</i>	22
<i>Figure 3.2-2 The arrangement for the pulse transmission technique (Birch, 1960).....</i>	24
<i>Figure 3.3-1 Compressional velocity Vs. pressure for a typical sample (<a href="http://gdr.nrcan.gc.ca/rockprop/rock_e.php">http://gdr.nrcan.gc.ca/rockprop/rock_e.php</a>).....</i>	26
<i>Figure 3.4-1 The amplitude spectrum in near field for 25 mm length aluminum specimen (normalized) [Khondakar et al., 2010].....</i>	31
<i>Figure 3.4-2 Amplitude spectrum in far the field at different pressures for 55 mm length aluminum specimen (normalized) [Khondakar et al., 2010].....</i>	32
<i>Figure 3.4-3 Raw waveform (A) Reference Aluminum sample (B) Rock sample (Felsic Norite).....</i>	34
<i>Figure 3.4-4 Selection of signal from the waveform (reference aluminum sample) .....</i>	35
<i>Figure 3.4-5 Windowed waveform for (A) reference Aluminum and (B) rock sample.....</i>	36
<i>Figure 3.4-6 Amplitude spectrum of aluminum and rock (red denotes rock).....</i>	37
<i>Figure 3.4-7 Ln ratio of the amplitudes Vs frequency plot and the best-fitted line.....</i>	38
<i>Figure 3.4-8 Typical waveform for (top left) Grade A-Felsic norite and (top right) Grade B-Metatonalite and (bottom) Grade C rock-Basalt.....</i>	40

<i>Figure 3.4-9</i> Amplitude spectrums (left) Grade A and (right) Grade B rock.....	41
<i>Figure 3.4-10</i> Flow chart for the grading procedure .....	42
<i>Figure 4.1-1</i> Velocity vs. pressure for four groups of massive sulphides.....	45
<i>Figure 4.1-2</i> Velocity vs. pressure for silicate hosts (felsic and mafic) and massive sulphides (high and low pyrite).....	47
<i>Figure 4.2-1</i> $Q$ vs pressure for four groups of massive sulphides .....	50
<i>Figure 4.2-2</i> $Q$ vs pressure for silicate hosts (felsic and mafic) and massive sulphides (high and low pyrite).....	53
<i>Figure 4.2-3</i> $1/Q$ vs pressure for silicate hosts (felsic and mafic) and massive sulphides (high and low pyrite).....	54
<i>Figure 4.3-1</i> Loss factor vs pressure for four groups of massive sulphides.....	57
<i>Figure 4.3-2</i> $Q$ vs pressure for silicate hosts (felsic and mafic) and massive sulphides (high and low pyrite).....	59
<i>Figure 4.5-1</i> Velocity vs. pressure for silicate hosts (felsic and mafic) and massive sulphides (high and low pyrite) below 200 Mpa.....	64
<i>Figure 4.5-2</i> $Q$ vs. pressure for silicate hosts (felsic and mafic) and massive sulphides (high and low pyrite) below 200 Mpa.....	65
<i>Figure 4.5-3</i> Loss factor vs. pressure for silicate hosts (felsic and mafic) and massive sulphides (high and low pyrite) below 200 Mpa.....	66
<i>Figure 4.6-1</i> Distribution of (A) sample length, (B) velocity, (C) slope.....	70
<i>Figure 4.6-2</i> Graphical representation of sensitivity analysis by Monte Carlo method for Grade A rocks .....	72

<i>Figure 4.7-1 Q Vs Velocity for Massive Sulphides (Pyrite and Non pyrite) and Host rocks (Felsic and mafic) at pressures ranging from 10-600Mpa.....</i>	<i>74</i>
<i>Figure 4.7-2 Loss factor Vs Velocity for Massive Sulphides (Pyrite and Non pyrite) and Host rocks (Felsic) at pressures ranging from 10-600Mpa.....</i>	<i>77</i>
<i>Figure 4.7-3Q Vs loss factor for Massive Sulphides and Host rocks .....</i>	<i>79</i>
<i>Figure 4.7-4 Q Vs Velocity (Top left), Loss Vs Velocity (Top right) and Loss Vs Q (Bottom)for Massive Sulphides (Pyrite and Non pyrite) and Host rocks (Felsic and mafic) at pressures ranging from 10-100Mpa .....</i>	<i>81</i>
<i>Figure 4.7-5 Vs Velocity (Top left), Loss Vs Velocity (Top right) and Loss Vs Q (Bottom)for Massive Sulphides (Pyrite and Non pyrite) and Host rocks (Felsic and mafic) at pressures ranging from 100-600 Mpa .....</i>	<i>82</i>

# Chapter 1

## Introduction

### 1.1 Background

The mining industry has been using electrical, electromagnetic and potential field techniques to explore for new minerals for decades. These techniques are reasonably good for exploring for minerals at shallow depth. However, shallow mineral deposits are being depleted. Therefore, there is a need for geophysical tools that enable exploration at greater depths. The exploration for minerals at greater depths (>500m) requires high resolution techniques. Gravitational and magnetic methods are not effective at such depths because they lose resolution. Therefore techniques which retain resolution at greater depths are required. Currently, seismic techniques are playing an increasingly important role in deposit characterization and exploration [Salisbury et al., 1996; Milkereit et al., 1996; Eaton et al., 1997; Eaton et al., 2003; Duff et al., 2012; Salisbury and Snyder, 2007]. Detailed seismic imaging of the ore and the host rocks can be carried out with high frequency (200-2000Hz) seismic techniques which provide information on the existence of ore, changes of rock types, offset of mineralization, location of structures (faults, troughs), and the extent of shear zones [Greenhalgh and Mason, 1997]. Laboratory measurements of ultrasonic velocity and attenuation, as well as their relation

to confining pressure provide the baseline information for applying the seismic technique to mineral exploration.

When a seismic wave passes through the earth, the elastic energy associated with the wave is absorbed slowly by the passing medium. The higher frequency content of the wave attenuates. Therefore there is a reduction in amplitude and the wave loses its resolution as it propagates. This phenomenon is known as attenuation. It may cause total disappearance of the wave. The physical state and saturation condition of the rocks affect attenuation of compressional and shear waves. Measurement of attenuation is difficult because the amplitude is very sensitive to noise, scattering, receiver coupling effects and interference from other signals. Velocity on the other hand, can be measured easily, but it does not often provide the resolution needed to identify small changes that might occur in physical properties of rocks under varying conditions [Donald et al., 2004]. The laboratory measurement of attenuation indicates that attenuation coefficient is dependent on frequency [Toksöz et al., 1979].

Velocity and attenuation depends on elastic properties of the rocks, presence of any structures, pressure and temperature conditions, mineralogy, etc. Laboratory studies help to provide an understanding of how these parameters interact and which parameters are most important.

## 1.2 Importance of this study

Attenuation is an increasingly important parameter in seismic analysis. This is particularly true due to recent advances in full waveform inversions. While a lot of laboratory work has been done on the seismic velocity and density of rocks [Birch, 1960; Rybach, et al., 1982; Winkler and Plona, 1982; Duffy et al., 1989; Salisbury, 1997; Milkereit and Eaton, 1998; Vanorio et al., 2005], attenuation studies are relatively rare [Collins et al., 1956; Toksöz et al., 1979; Winkler and Plona, 1982; Butt, 2001]. Seismic attenuation studies of ore bearing rocks are very rare.

Some host rocks and sulphides have similar velocities. Therefore distinguishing them based on velocity might not be unique. Therefore seismic attenuation study along with velocity and density is required and may eliminate the non-uniqueness of velocity. This research aims to evaluate and compare the potential of using attenuation and loss factor of massive sulphide and the host rocks in conjunction with velocity to explore for massive sulphide deposits in the subsurface.

## 1.3 Scope and Research Objectives

The scope of this research is to carry out seismic attenuation analysis on massive sulphides and igneous and metamorphic host rocks. The database used for this research is

based on experiments conducted at the High Pressure Geophysics Laboratory (HPL) at Dalhousie University, managed by Dr. Matthew Salisbury, who conducted measurements of P and S wave velocity on massive sulphide and associated host rock drill cores. The velocities used in this thesis research were the values given in the database, however the author reprocessed the recorded full waveforms from the HPL measurements to determine the attenuation parameters, which form the primary objectives of the work.

The objectives of this research are:

- to determine the attenuation and loss factor for massive sulphides and their associated host rocks.
- To examine the response of attenuation and loss factor with respect to high (100-600Mpa) and low (10-100Mpa) confining pressures for massive sulphide ore and the host felsic and mafic rocks.
- to evaluate the potential of using seismic attenuation and loss factor to image massive sulphide ore in the hard rock regime.

#### 1.4 **Organization of the thesis**

[Chapter 1](#) deals with the research problem, importance, scope and the objectives of this research. [Chapter 2](#) reviews literature concerning the necessity of new massive sulphide exploration techniques and physical properties of massive sulphides. However, the main

focus of chapter two is attenuation. The mechanism, dependency and application of attenuation are reviewed. [Chapter 3](#) describes the measurement techniques. Details of the processing and grading of the data are demonstrated in that chapter. Chapter 4 discusses the detailed results of the attenuation analysis and presents an interpretation of the data. . Finally, [Chapter 5](#) discusses how we might apply the results along with some recommendations for future work.

# Chapter 2

## Literature Review

This chapter will discuss the necessity of a new massive sulphide exploration technique along with a brief description of the methods used in mineral exploration. Then the physical properties of massive sulphides are discussed. The major portion of this chapter will cover the literature review on attenuation mechanisms, factors affecting attenuation and finally the application of attenuation.

### 2.1 Necessity of a new massive sulphide exploration technique

The deposits of the present mining camps [such as Horne (Canada), Kidd (Canada) and Brunswick (Canada)] are depleting and they have been explored up to 300m depth. A need arises to search for new deposits due to the increasing demand of minerals around the world. In the existing mining camps, it is necessary to find additional deposits at deeper depth [[Gingerich et al., 2000](#)]. Geophysical methods have been used economically to identify ore deposits in the past. These methods give informative data on the physical properties of the subsurface due to the presence of geological structures and

mineralization. Seismic methods are more effective at deeper depths (between 300 to 1000m) due to their high resolution [Demerling, 2004].

## 2.2 Geophysical methods used in exploration:

Magnetic, gravity and electromagnetics are three major geophysical methods used for massive sulphide exploration. Another method, seismic with higher resolution and sensitivity is proposed here. A brief description of these methods is stated below.

The magnetic method is primarily dependent on the presence of magnetic minerals (mainly magnetite and pyrrhotite). In this method, the magnetic field of the earth is measured. The presence of magnetic minerals in the subsurface perturbs the earth's field resulting in detectable anomalies that are analyzed. Gravity methods are based on perturbation of the earth's gravity field due to the density contrasts between the different rock types. The gravity method is sensitive to large structures only. Therefore small ore bodies of massive sulphide deposits are hard to detect with this method. The most commonly used method in mineral exploration is electromagnetic. This method is responsive to secondary electromagnetic fields associated with rock bodies of varying conductivity. The depth of penetration of an electromagnetic survey is limited by high conductivity, near-surface zones. The present electromagnetic methods are not suitable for exploring at greater depths (over 500m) in crystalline terrains in Canada due to highly conductive glaciated overburden [Demerling, 2004; Telford et al., 1995].

Seismic methods are more expensive than other geophysical methods of mineral exploration but have the potential to provide much more detailed geological information because of higher resolution. Acquisition, processing and interpretation of the seismic data in hard rock exploration need to be modified according to the response of the ore body. Seismic methods play significant roles in detecting deep seated mineral deposits which are at greater depth of 800m [Malehmir et al., 2013]. A thorough understanding of the physical properties of a specific combination of ore and the host is required for the selection of a proper imaging technique. Duff et al., (2012) conducted an analysis on the sulphide ores and their associated host rocks from Voisey's Bay Ni-Cu-Co deposit (one of the most recent large-scale mineral discoveries of Canada). They showed that in the pyrrhotite-pentlandite rich assemblage (low pyrite sulphide), velocity is significantly lower than in felsic and mafic silicate hosts. Therefore tomographic imaging is better suited for this type of deposit instead of seismic reflection imaging due to the modest acoustic impedance contrasts. Often it is scattering that is important for location too.

### **2.3 Physical properties of massive sulphides**

Study of elastic properties for the host and the ore is a prerequisite for exploration as the elastic property contrast between the ore and the host rock can be significant [Eaton et al., 2003]. Salisbury et al., (1996) studied P wave velocities for massive sulphides and their associated hosts.

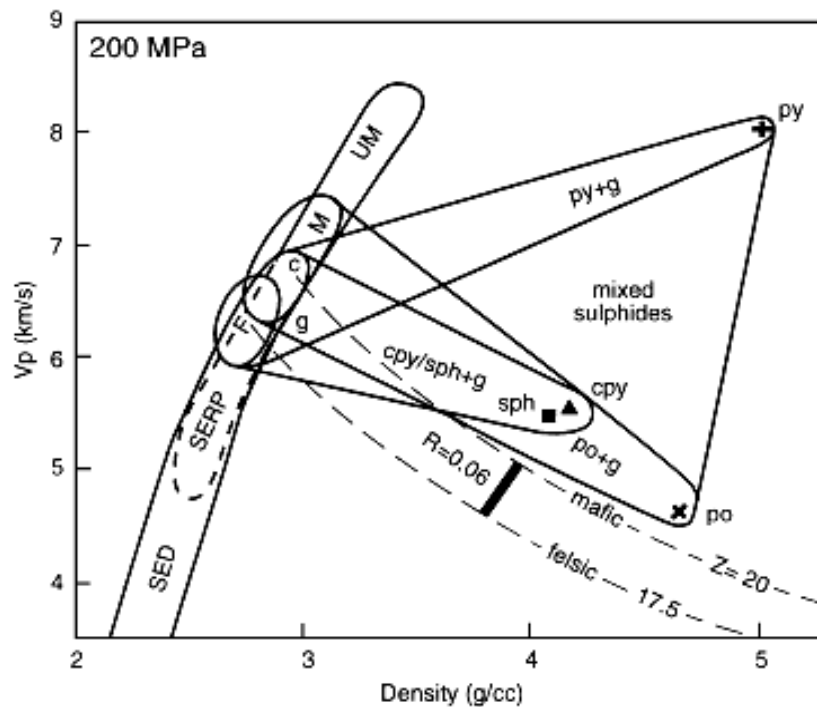


**Figure 2.3-1 Velocity ( $V_p$ )-density fields for common sulfide ores and silicate host rocks at 200 MPa. Ores: py=pyrite, cpy=chalcopyrite, sph=sphalerite, po=pyrrhotite. Silicate rocks along Nafe-Drake curve: SED=sediments, SERP= serpentine, F=felsic, M=mafic, UM=ultramafic, g=gangue, c=carbonate (Salisbury et al., 1996).**

**Figure 2.3-1** shows common velocity-density fields for silicates and sulphides. The v-d data shows that the behavior of the sulphides is different from that of the silicate hosts indicating that seismic techniques may be able to detect these differences .

Dashed lines ([Figure 2.3-1](#)) represent constant acoustic impedance ( $Z$ ) for felsic and mafic rocks. The bar shows the minimum impedance contrast required to give a detectable reflection ( $R=0.061$ ). An impedance difference of  $2.5E5 \text{ g/cm}^2\text{s}$  which is the contrast between mafic and felsic rocks, gives rise to the value  $R=0.06$  [Salisbury et al. (2000)]. Sulphides have a large velocity-density zone and mostly controlled by pyrite, pyrrhotite, sphalerite and chalcopyrite. Pyrite has density of  $5\text{g/cc}$  and velocity of  $8\text{km/sec}$ . Pyrrhotite is dense ( $4.6 \text{ g/cc}$ ) but it has low velocity of  $4.7 \text{ km/sec}$ . Sphalerite and chalcopyrite are intermediate. They have density and velocity around  $4.1 \text{ g/cc}$  and  $5.5 \text{ km/sec}$ . Pyrite content causes the velocity to increase. In contrast, pyrrhotite, sphalerite and chalcopyrite content cause it to decrease. Pyrite rich samples have high Bulk, Shear and Young's moduli. On the other hand, low pyrite sulphides have low Bulk, Shear and Young's moduli. Therefore, pyrite rich ore is resistant to changes in shape and volume, whereas low pyrite ores demonstrate the opposite nature. [Harvey \(1998\)](#) relates the high and low values (velocity and elastic constants) of pyrite-rich and low pyrite sulphides respectively to the crystal structures. The bonding in sulphides is mainly covalent. The dense structure and strong arrangement of pi-bonds may lead to the high elastic constants and wave velocity of pyrite. The low elastic moduli and velocity of chalcopyrite and sphalerite might be related to their rather open and weaker covalent bonds. The low elastic moduli of pyrrhotite are related with its molecular structure.

The ore in the study of [Salisbury et al., \(1996\)](#) shows a wide range of velocities ( $5.1\text{-}7.3 \text{ km/sec}$ ) due to the differing proportions of pyrrhotite and pyrite. Felsic and mafic hosts

also have a range of velocities and densities (ranging from 6.0 km/sec and 2.75 g/cm<sup>3</sup> (felsic) to 8.3 km/sec and 3.3 g/cm<sup>3</sup> (ultramafic). The impedance contrast between the ores and hosts can be large but that is not always the case. Therefore considering the acoustic properties, the contrast between ores and associated host rocks will often but not always produce strong seismic reflections.

The differing properties of massive sulphide ore compared to the host rocks is also reflected in the study of [Malehmir et al.\(2013\)](#). They measured P and S wave velocities for a series of rocks and ore samples from the Swedish crystalline environment at atmospheric and elevated pressure to see their dependency with pressure at depths of 2-3 km. These samples are collected from three regions ranging from metallic ore deposits, meta-volcanic and meta-intrusive rocks to deformed and metamorphosed rocks. They found that the samples do not exhibit much sensitivity with applied pressure but velocity and density show a positive correlation with pressure except for the massive sulphide samples. A massive sulphide ore sample shows low velocity in spite of having high density. They relate this with the mineral texture and lower pyrite content compared to another massive sulphide sample (obtained from Norway) which shows significantly higher velocity (both P and S wave). They found that massive sulphide deposits show very strong impedance contrast with most of the lithologies which gives privilege of applying seismic methods to describe the deposits.

## 2.4 Attenuation and Q:

When a propagating wave passes through the earth, the energy in the wave dissipates (attenuation) due to the propagation medium (physical state and saturation conditions). Attenuation of elastic waves tends to be frequency dependent resulting in the reduction of amplitude and the loss of the higher frequency content in the frequency band of the wave. Geometric attenuation associated with the spreading of the wave front as it propagates is a major consideration for normal seismic exploration scales. Geometric attenuation occurs at both the lab and field scale. However, the reduction in amplitude generally is not a function of frequency (i.e. uniform for all frequencies) and is related to the reciprocal of distance from the source. In the experimental data used in this research, the distance from the source to the receiver (the length of the sample) is approximately constant; therefore most of the amplitude changes observed are due to intrinsic anelasticity of the minerals, the frictional dissipation along cracks and grain boundaries and scattering. The intrinsic attenuation is related to the mineral anelasticity and the cracks and grain boundaries therefore more frequency dependent than geometrical spreading and give rise to the linear slope of the  $\ln (A_1/A_2)$  versus frequency curve ( $A_1$  and  $A_2$  are the final amplitudes after passing through the reference and rock samples respectively) that has been used to calculate Q and loss factor. As well, it is plausible that one of these two types of attenuation (intrinsic anelasticity or frictional dissipation) predominates in the regions above and below 100 MPa hydrostatic stress. Based on our

experimental data ‘which case will govern’ will be discussed in the results and discussion chapter.

Quality factor, Q, is a dimensionless parameter used to measure the attenuation which is inversely proportional to  $\alpha$  [frequency dependent attenuation co-efficient]. It is the ratio of the maximum energy stored during a cycle divided by the energy lost during the cycle. When the loss is large it is defined in terms of the mean stored energy and the energy loss.

$$Q = \frac{\pi f}{\alpha V} \dots \dots \dots (2.1)$$

Where, V=velocity, f=frequency,  $\alpha$ = attenuation coefficient.

The high value of Q for a rock indicates that the propagating wave undergoes less attenuation and vice versa. Attenuation coefficient is generally proportional to frequency (i.e., Q is independent of frequency).

Toksöz et al. (1979) conducted laboratory measurements on attenuation of P and S wave for sandstone and limestone in dry and saturated conditions at ultrasonic frequencies (0.1-1.0 MHz). Pulse transmission and spectral ratio methods were used for these measurements. The current research also measures attenuation of waves in massive

sulphide and silicate rocks following those techniques and considering the same assumptions and frequency range as described by Toksöz et al. (1979). To understand the mechanism of attenuation and extrapolate the lab data to field, the sensitivity of attenuation with pressure was described. They showed that attenuation decreases (Q increases) with differential pressure. At low pressure, the increase rate is higher and it levels off at higher pressure. Attenuation co-efficient is linearly proportional to frequency whereas Q remains constant in the frequency range of 0.1-1.0 MHz. The mechanism of attenuation was discussed by Johnston et al. (1979). The following section will describe some of the mechanisms associated with attenuation.

#### 2.4.1 *Mechanism and dependency of attenuation:*

A propagating wave may undergo attenuation in the rock matrix due to several factors: frictional dissipation across the crack surfaces and the grain boundaries, the intrinsic anelasticity of the matrix mineral and scattering. Frictional dissipation is the principal cause. It is difficult to define the precise mechanism of frictional dissipation across the crack and grain boundaries. The relative motion of two sides plays important role in frictional dissipation. In dry condition there is no sliding motion across the surface therefore attenuation is much lower in the dry state than the saturated condition. Intrinsic attenuation is very small but not negligible. When all the cracks diminish by the effect of pressure then intrinsic anelasticity plays the dominant role in attenuation of the wave. The other mechanisms responsible for the attenuation of wave in rocks might be fluid flow,

viscous relaxation, and scattering. [Johnston et al. \(1979\)](#) applied a model of these mechanisms to the laboratory data and showed that friction at the thin cracks and grain boundaries is the dominant attenuation.

The pressure dependence of these mechanisms is very important. We would like to see how pressure affects attenuation of waves in the rock. When pressure increases the elastic and anelastic properties of a rock undergo changes. Due to the applied hydrostatic or overburden pressure, the number of thin cracks decreases. Thus attenuation by friction at the crack decreases. The more the pressure increases the more the cracks close, resulting in additional decrease in attenuation. The point at which attenuation reaches a limiting value defines the intrinsic aggregate anelasticity. This is due to the unaffected grain boundary and fine structure. The decrease of attenuation with increasing pressure is verified by several experiments [[Gardner et al., 1964](#); [Klima et al., 1964](#); [Levykin, 1965](#); [Gordon and Davis, 1968](#); [Al-Sinawi, 1968](#); [Walsh et al., 1970](#); and [Toksöz et al., 1979](#); [Molyneux and Schmitt, 1999](#)].

A clear decrease in attenuation co-efficient is found for diabase and greywacke up to 100 Mpa by [Klima et al. \(1964\)](#). Rocks with very low porosity and with reasonable crack porosity may show an exponentially decreasing relationship of attenuation with pressure. For granite rocks [Gordon and Davis \(1968\)](#) showed that attenuation decreases with differential pressure. However for the other types of rocks, the intrinsic anelasticity must be considered where cracks are closed. Therefore attenuation is not zero at higher

pressure. In that case attenuation might not be decreasing exponentially with pressure. This non-zero value of attenuation at very high pressure remains constant with pressure and determined empirically by [Toksöz et al., \(1979\)](#). He fitted a model for dry Berea sandstone, Q with differential pressure (difference between the confining and pore fluid pressure) shows that around over 41Mpa the changes of Q with pressure becomes linear. Below 41 Mpa higher changes are observed in Q with increase of differential pressure. Generally the relationship is exponentially decreasing up to the pressure indicated earlier at which the thin cracks are generally closed and then the relationship is nearly linear. In the current research, the sensitivity of attenuation with pressure will be observed for silicate rocks and sulphide minerals in both low and high pressure due to the difference in behaviour in these pressures.

Frequency is another important parameter to be considered. Several studies discussed the relation of Q with frequency [[Butt, 2000](#)]. Q factor is independent of frequency over a broad range of frequency ( $10^{-2}$ - $10^{-7}$  Hz) for dry rocks [[Birch and Bancroft, 1938](#)].

#### 2.4.2 *Application of attenuation*

Different branches of engineering and geoscience have used attenuation. Attenuation is used for providing the information about the strata [[Sarma and Ravikumar, 2000](#)], lithology and saturation conditions [[Stainsby et al., 1985](#)], reservoir characterization

[Carcione et al., 2003], non-destructive testing [Molina and Wack, 1982], fracture detection [Pyrak, 1990] and the stability of the rock structure [Kaneko et al., 1979]. In the present research, we will try to investigate the potential of using attenuation in identifying massive sulphide ore. For that purpose the following paragraphs will present some background study on application of attenuation along with a study on delineation of massive sulphide ore.

Butt (2001) conducted an experiment on a diabase sample (very low micro crack density) to measure velocity, attenuation and fracture closure. This experiment was done to evaluate the potential of using attenuation to indicate roof failure in excavation of a fractured rock mass. He examined the influence of fracture on P-wave attenuation by observing the change of Q with stress level and frequency. Both the velocity and Q have similar trends. The change in attenuation is greater than velocity due to the sensitivity of attenuation to coupling between the transducer and the sample, source waveform, geological structure, reflection, beam spreading in small sized laboratory specimen etc. In this paper the spectral ratio (The relationship of the  $\ln \left( \frac{A_1(f)}{A_2(f)} \right)$  with frequency) is plotted against frequency ranging from 100-300KHz, and from the linearity of the spectral ratio curve it is shown that Q remains constant over this frequency range for both intact and fractured specimens. Q in fractured specimen is lower than that of intact specimen. This implies that attenuation is higher in fractured specimen. Above 20 Mpa normal stress, this difference in Q values between fractured and intact specimens reduces. This study

provides an important background in our current research by demonstrating changes of velocity and attenuation with non-hydrostatic stress and fracture.

The changes of attenuation and velocity with pressure are related with the closure of cracks [Meglis et al., 1996]. Increase in confining pressure causes cracks to close which causes the velocity to increase and attenuation to decrease. The velocity and the attenuation of the propagating wave in the intact rock and the cracked rocks are different. It may be noted that the response of the cracks with pressure is dependent on the nature of the cracks [Batzle et al., 1980]. The amplitude and the velocity of the wave are dependent on how the cracks are distributed and oriented and the sizes and geometry of the cracks.

Another application of attenuation is in describing the crystalline crust [Holliger and Buhnemann, 1996]. Their study on attenuation of a wave which employed high quality seismic data ( $S/N \gg 1$ ) in a band of 50-1500Hz on a near surface crystalline granite body implies high attenuation (Q values of 20-60 with standard error of 20%). These low values of Q (high attenuation) demonstrate that below the weathering zone the dampening of the wave in the crystalline crust is quite strong. The present research measures attenuation of crystalline hosts, the range of Q provided by Holliger and Buhnemann (1996) will give a base for this analysis. The range of attenuation for massive sulphides is still unknown in the literature except one study done by Khondakar

et al., (2010). However velocities for the massive sulphides have been studied significantly [Salisbury et al., 1996; Salisbury et al., 2000; Malehmir et al., 2013].

Salisbury et al. (2000) provided three parameters for the prediction of the resolution of seismic reflection technique in imaging massive sulphides: acoustic impedance, body diameter and minimum thickness. The acceptable limit of these parameters for easy imaging of the ore are described in that paper. They found that most of the massive sulphides have higher impedance than the silicate hosts. Therefore if the deposits are within the geometric restriction which means known subsurface condition, then seismic reflection techniques can be used directly. Sulphides occupy a large velocity-density field and lie far to the right of the Nafe Drake curve representing silicate rocks. This velocity-density field is controlled mainly by four massive sulphide minerals: pyrite, pyrrhotite, sphalerite and chalcopyrite. The detailed properties of these sulphides are presented in [section 2.3](#). This research established a relation between the acoustic properties and reflectivity of massive sulphides. We will work on the attenuation of wave in sulphide minerals and felsic and mafic silicates to find out correlation between velocity and attenuation and to observe whether attenuation alone or together with velocity can provide important information on imaging massive sulphides. These are the baseline information for applying seismic techniques. Also their study provides basis for the grouping of sulphide minerals in the present research.

# Chapter 3

## Methodology

This chapter covers the methodology we have used for attenuation studies including the location of the sample collections, laboratory set-up, test procedure, processing and sorting of the data. The database used in the present research is developed from experiments conducted in the High Pressure Laboratory at Dalhousie University by Geological Survey of Canada in cooperation with Dalhousie University. The aim of these experiments was to measure the acoustic properties (velocities, density) of the rocks. The resulting data base includes over 1000 rock samples collected from around the world. The samples include a wide variety of igneous, metamorphic and sedimentary rocks from the continental and oceanic crust, plus a large suite of ores provided by the mining industry.

### 3.1 Locations of investigations

Massive sulphide samples in the present study consist of a suite of rocks containing pyrite, chalcopyrite, sphalerite, pentlandite and pyrrhotite. The host rocks range from basalt to rhyolite. Eighteen locations have been chosen for this investigation. The locations are Bathurst suite, Bathurst NB, Ecsoot'96 Labrador, Ecsoot'96 Labrador-Nakvakfjord Nain, Kidd Creek, Inco-Sudbury Basin, Kapuskasing, Mattagami, Liscomb

complex, Norada 99-Bathurst, Selbaie, Selbaie mine study, Suleivan area, Sudbury sample, Sudbury-Inco BH 85534, Thompson mn, Thompson Nickel Belt-Manitoba and Tally Pond.

## 3.2 High Pressure Laboratory

The following sections will describe the equipment set up and the test procedures carried out in High Pressure Laboratory.

### 3.2.1 *Equipment setup*

The High Pressure Laboratory of Dalhousie University consists of a pressure vessel that operates over a pressure range of 0- 1400 Mpa for pressure curing and velocity measurements. The main pressure vessel is 7 ton in weight and has a sample chamber that is 40 cm long ×10 cm diameter. Hydraulic oil is pumped into the sample chamber with the assistance of a two-stage intensifier. The oil acts as the pressure medium. Six samples can be measured in this chamber at a time. Electrical contact to the source and receiver transducers is made by eight insulated cone feeds.. They are attached through the closure of the vessel end. The entire arrangement is situated in a reinforced concrete cellar. The system is monitored by a control panel situated in the adjacent lab. **Figure 3.2-1** shows the setup of the High Pressure Laboratory.

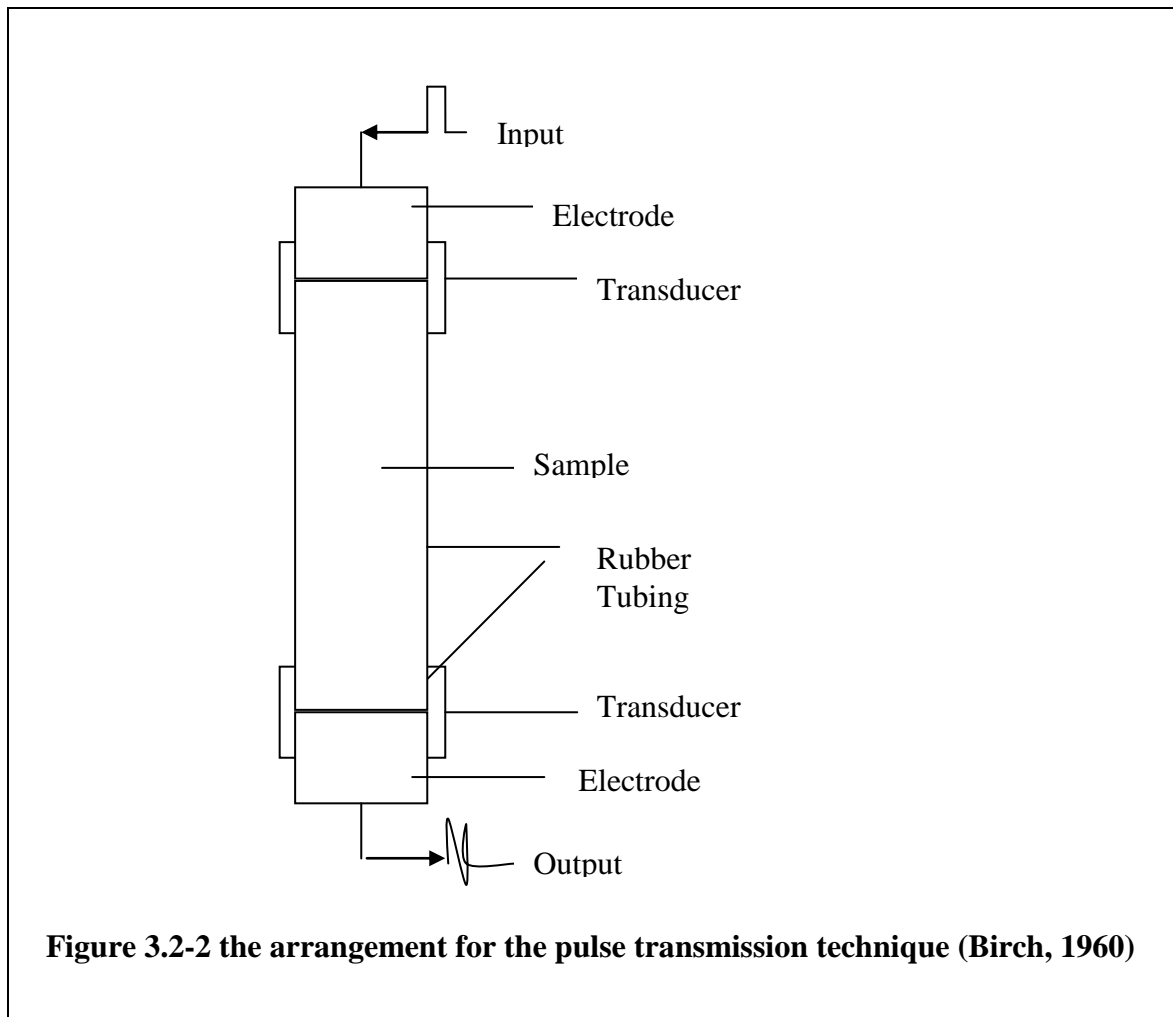


**Figure 3.2-1**The Pressure vessel (on left) and the Pressure Control panel (on right) of High Pressure Laboratory Dalhousie/GSC ([http://gdr.nrcan.gc.ca/rockprop/rock\\_e.php](http://gdr.nrcan.gc.ca/rockprop/rock_e.php))

### 3.2.2 *Set up of the sample*

The samples used in this experiment were cored with diamond core drills. They are right circular cylinders with sufficiently smooth flat surfaces and have the dimension of 2.5-6.0cm long  $\times$  2.5 cm diameter. They are covered by copper foil. The transducers and electrodes are attached to the sample and even contact is maintained. Electrodes are the ungrounded terminals for the transducers. The transducers are made of circular plate. Two types of transducers have been used in this experiment: one for the P wave

measurement and the other is for the S wave measurement. It may be noted that 1 MHz Lead Zirconate and 1 MHz Lead Zirconate Titanate transducers are used for P and S wave measurements respectively. The transducer covers the end of the specimen. A pulse of voltage is applied to the transducer and the disturbance is transmitted to the other transducer on the other end of the sample and the mechanical signal is converted to electrical signal and after amplification it is read on the oscilloscope. The whole arrangement of the sample, transducer and electrode is put in neoprene tubing. The arrangement is then kept closed in the pressure vessel. The arrangement of the sample, transducer and electrode are shown in [Figure 3.2-2](#).



### 3.3 Measurements of different parameters

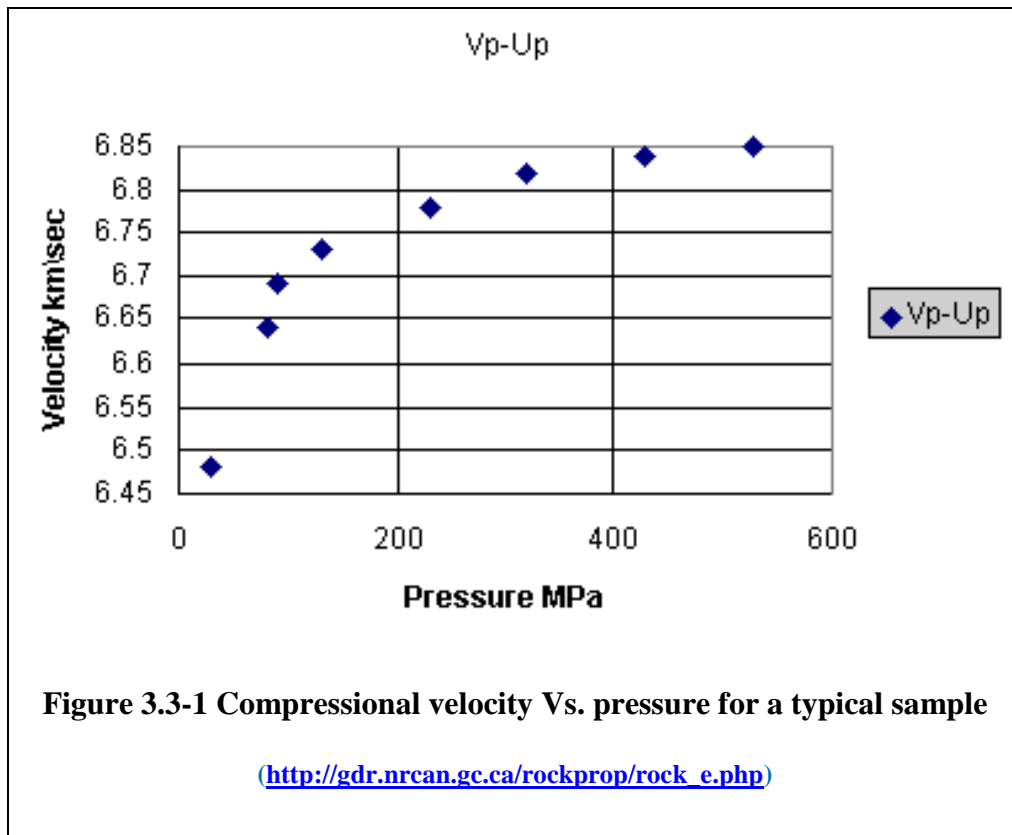
Measurement of velocity, attenuation and loss factor will be discussed here.

#### 3.3.1 *The pulse transmission technique*

The pulse transmission technique [Birch, 1960; Christensen, 1985] is used to measure the velocity of the propagating wave. A pulse voltage is applied to the source transducer

which initiates an elastic wave in the sample that is received at the receiving transducer. The time of flight of the pulse is recorded on a digital oscilloscope. Velocity is calculated from the ratio of the sample length to the travel time at room temperature with pressure ranging from 10-1000 Mpa. The velocity is measured primarily for the dry samples at room temperature. A few samples are saturated with water and the velocities for these wet samples are measured to simulate the field conditions.

Shear and compressional wave velocities are measured in one direction for the samples which do not have any definite fabric. They are measured in various directions for the samples with distinct fabric. Velocities are determined for both the compression and decompression cycles but the decompression cycle is considered to provide better results. The time of first arrival is chosen and then travel time is measured from the oscilloscope from the calibrated time marker. For a typical sample it is observed that velocity increases rapidly for pressure up to 200MPa and then the velocity gradient decreases which is shown in **Figure 3.3-1**. At the beginning, the increase in velocity is due to the closure of micro cracks. However at higher pressure the velocity becomes linear due to the intrinsic properties of the rock minerals. [Birch, 1960; [http://gdr.nrcan.gc.ca/rockprop/rock\\_e.php](http://gdr.nrcan.gc.ca/rockprop/rock_e.php)]



### 3.3.2 *Measurement of Attenuation*

The spectral ratio technique is the most commonly used method for attenuation measurements.  $Q$  which is a measure of attenuation, related inversely with attenuation coefficient is measured by this technique from the slope of the spectral ratio curve. As  $Q$ -factor is considered independent of frequency, the dispersion of the waves is not considered [Frempong et al., 2005, Johnston et al., 1980] in the spectral ratio model. This technique is reliable for negligible noise [Tonn, 1989]. Two types of samples are used in

this technique: one is the rock sample and the other is the reference sample. Both the rock and reference samples have the same dimensions. The reference sample is assumed to have no attenuation. The spectral ratio is derived from the ratio of the reference and sample amplitude spectrum. Quality factor Q can be calculated using the method described by [Butt \(2001\)](#) which is described below.

The change in amplitude as a function of frequency is expressed by the following formula:

$$A(f) = A_0(f) \cdot G(x) \cdot \exp\left(\frac{\pi f x}{cQ}\right) \dots\dots\dots (3.1)$$

Where,

$A_0(f)$  =initial amplitude,

$A(f)$  = the final amplitude after passing through the sample

$G(x)$  =geometrical factor which is a function of spreading, reflection etc.

$f$ = frequency

$x$ =sample length

$c$ =velocity

$Q$ =quality factor

Now we consider natural logarithm on both sides of equation [\(3.1\)](#),

$$\ln A(f) = \ln A_0(f) + \ln G(x) + \frac{\pi f x}{cQ} \dots \dots \dots (3.2)$$

Equation (3.2) can be rewritten for reference and rock samples as equations (3.2A) and (3.2B) respectively.

$$\ln A_1(f) = \ln A_{01}(f) + \ln G_1(x) + \frac{\pi f x}{c_1 Q_1} \dots \dots \dots (3.2A)$$

$$\ln A_2(f) = \ln A_{02}(f) + \ln G_2(x) + \frac{\pi f x}{c_2 Q_2} \dots \dots \dots (3.2B)$$

Now subtracting equation (3.2B) from equation (3.2A) and assuming  $Q_1 = \infty$ , we get the equation

$$\ln A_1(f) - \ln A_2(f) = \ln A_{01}(f) - \ln A_{02}(f) + \ln G_1(x) - \ln G_2(x) + \frac{\pi f x}{c_2 Q_2}$$

From which,

$$\ln \left( \frac{A_1(f)}{A_2(f)} \right) = \ln \left( \frac{A_{01}(f)}{A_{02}(f)} \right) + \ln \left( \frac{G_1(x)}{G_2(x)} \right) + \frac{\pi x}{c_2 Q_2} f \dots \dots \dots (3.3)$$

The basic assumption is that Q for the reference is essentially infinite. That provides a reference that gives a ratio that is independent (approximately) of all the other things going on in the wave propagation. The relationship of the  $\ln \left( \frac{A_1(f)}{A_2(f)} \right)$  with frequency

defines the spectral ratio and in this case equation (3.3) represents a straight line with slope  $\frac{\pi x}{c_2 Q_2}$ . The quality factor for rock sample  $Q_2$  can be calculated from this slope.

### 3.3.3 *Measurement of loss factor*

Loss factor represents the energy loss of a seismic wave per unit distance and it is frequency dependent. Loss factor can easily be used to measure attenuation per unit distance. We measured loss factor at 1 MHz because that was the resonant frequency of the transducers. It can be measured at any frequency but most always be referenced to that frequency.

Loss factor is measured using the following **equation 3.4**, derived by Dr. Stephen D. Butt (Professor at Faculty of Engineering and Applied Science, Memorial University of Newfoundland).

$$\text{Loss factor (dB/m @ 1 MHz)} = 5.4366 \times 10^7 * \frac{S}{x} \dots\dots\dots (3.4)$$

Where, S is the slope of the spectral ratio curve and x is the length of the specimen. The details of the derivation and the relationship of loss factor and Q are demonstrated in the Appendix B.

### 3.4 Test data

The database contains thousands of rock samples. The physical properties (weight, length, diameter, density, and volume) of the rocks, P and S wave velocities at hydrostatic confining pressures ranges from 10 to 600MPa are provided in the database. From this database, the test data are sorted for the present research considering the sample length. Selections of the reference and rock samples are described in the following sections.

#### 3.4.1 *Selection of the reference sample*

The reference aluminum samples used in the database consists of eight different lengths: 60, 55, 50, 45, 40, 35, 30 and 25 mm. The 55 mm aluminum sample is chosen as the reference sample based on the near and far field consideration [Khondakar et al., 2010]. In the near field, the uneven distribution of the energy is found in the wave front and ripples are observed in the Fourier amplitude curve due to this uneven distribution (Figure 3.4-1).

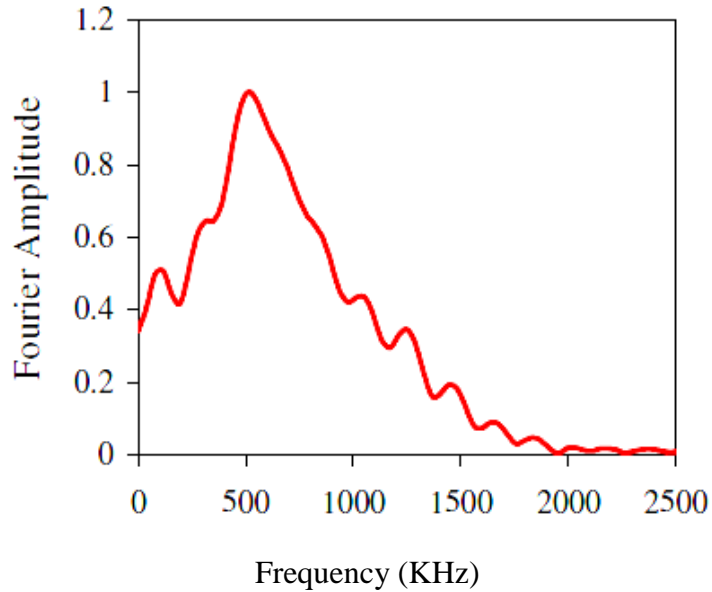
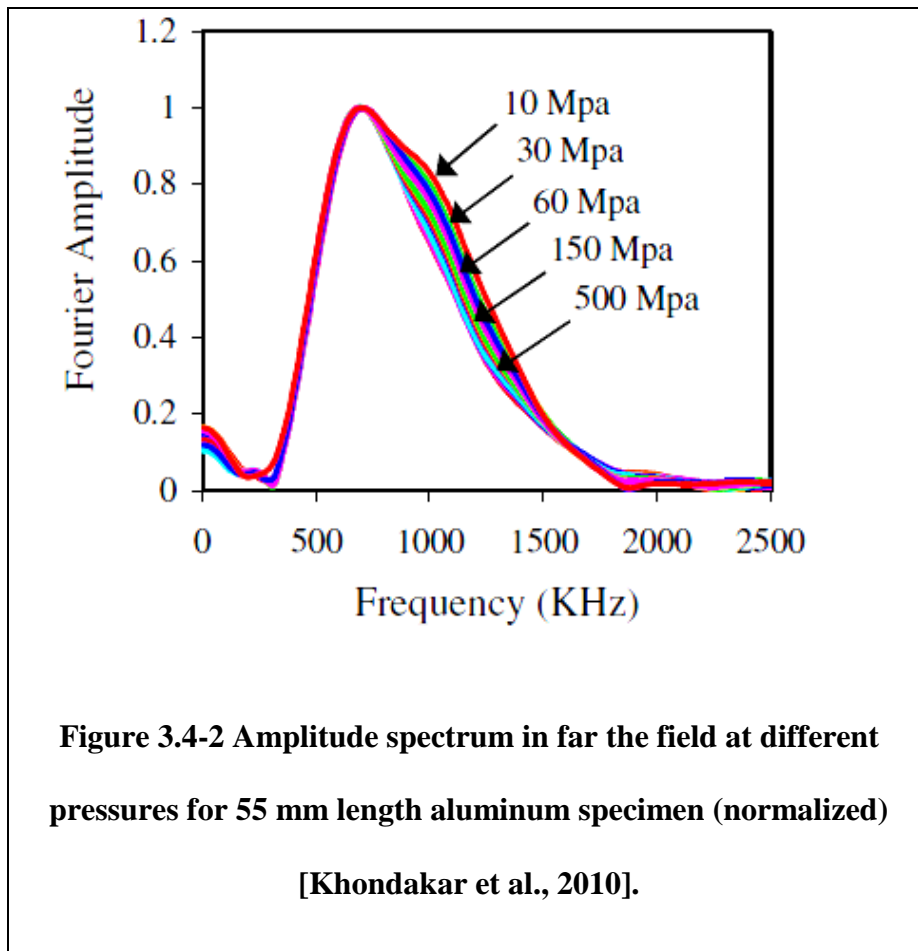


**Figure 3.4-1 The amplitude spectrum in near field for 25 mm length aluminum specimen (normalized) [Khondakar et al., 2010].**

It is observed that in the far field, the energy distributions are more even and Fourier amplitude curves look relatively smooth. The amplitude spectra become nice and smooth with increasing confining pressure ([Figure 3.4-2](#))



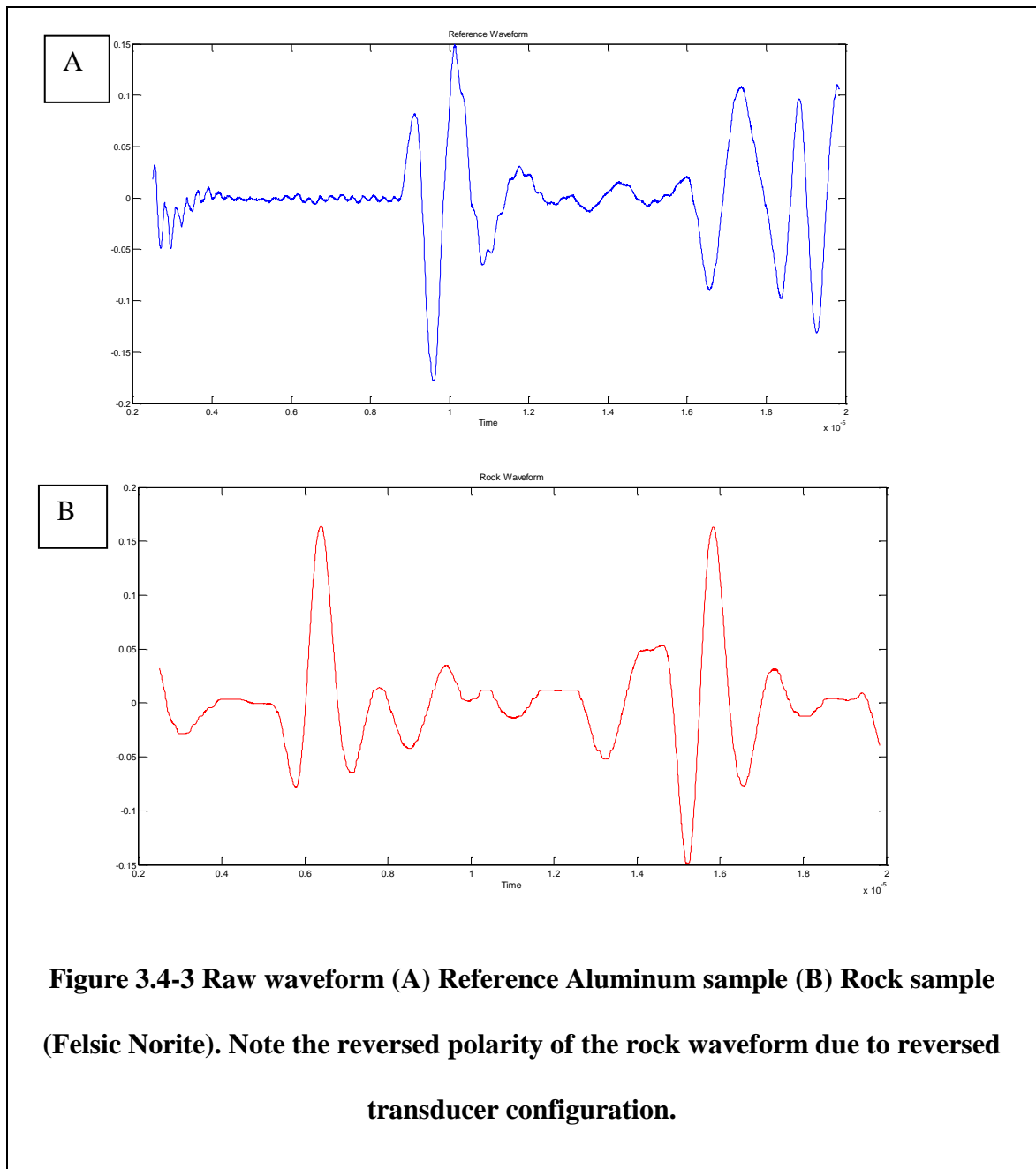
### 3.4.2 Selection of the rock samples

The same criteria (sample length consideration) of the reference aluminum sample have been used for the selection of the rock samples. Therefore, rock samples, greater than 38mm lengths are chosen for the analysis [Khondakar et al., 2010].

### 3.4.3 *Method used to process and analyse data for Q factor calculation*

A MATLAB code has been developed to process and analyse the data by Dr. Charles Hurich (Associate Professor at Department of Earth Sciences, Memorial University of Newfoundland). This code is the convenient implementation of the spectral ratio method. The database contains ultrasonic waveform data recorded at the High Pressure Laboratory. Prior to the analysis the program allows removal of DC and low frequency components of the data introduced by the acquisition system. The specific waveform of interest is windowed and tapered and Fast Fourier Transform (FFT) is carried out to determine the amplitude spectrum. The selected portion is usually one full oscillation of the wave. This selection should be done very carefully for the nice and smooth Fourier amplitude spectrum. Then the natural logarithm ratio of the amplitudes of reference and rock samples is plotted against the frequency, the linear portion of the spectral ratio plot is chosen and a linear fit determined. The slope of the spectral ratio provides the data required to determine Q using equation 3.3. An example of this procedure is shown in **Figure 3.4-3** through **Figure 3.4-7**

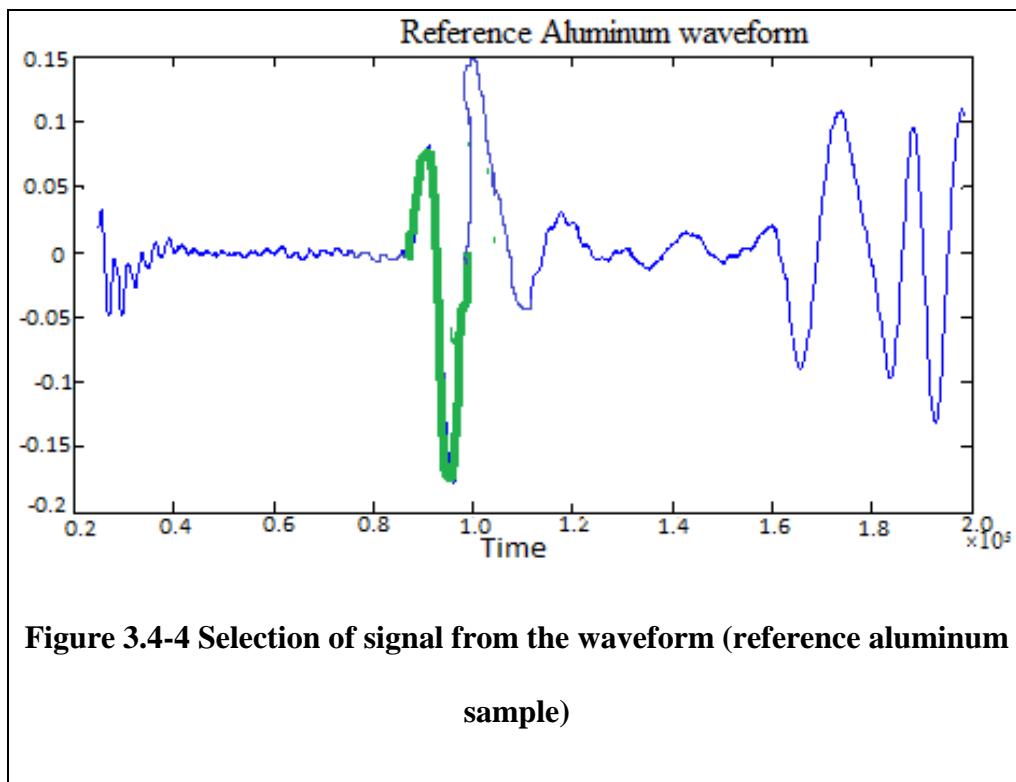
The reference and rock waveforms are shown in **Figure 3.4-3**. If we observe the



reference aluminum waveform (A), it is apparent that the very beginning part of the waveform is noise. Then distinct signal portion (5-8 microseconds) is observed and the

last part is the reflection of the signal (14.5-17 microseconds). The same is observed for the rock waveforms (B).

Figure 3.4-4 shows the selection of the desired signal portion from the reference aluminum and the same has been done for the rock waveform. One full oscillation is chosen starting from zero, which is illustrated by green color. The analysis was also performed considering two full oscillations. But the amplitude spectrum does not appear as it should be and it shows two peaks. Therefore after analyzing a good number of samples with two cycles, one cycle was chosen for the analysis.



The desired signal portion is shown both for the reference and rock waveform in Figure 3.4-5 (A) and (B). They represent waveform in time domain.

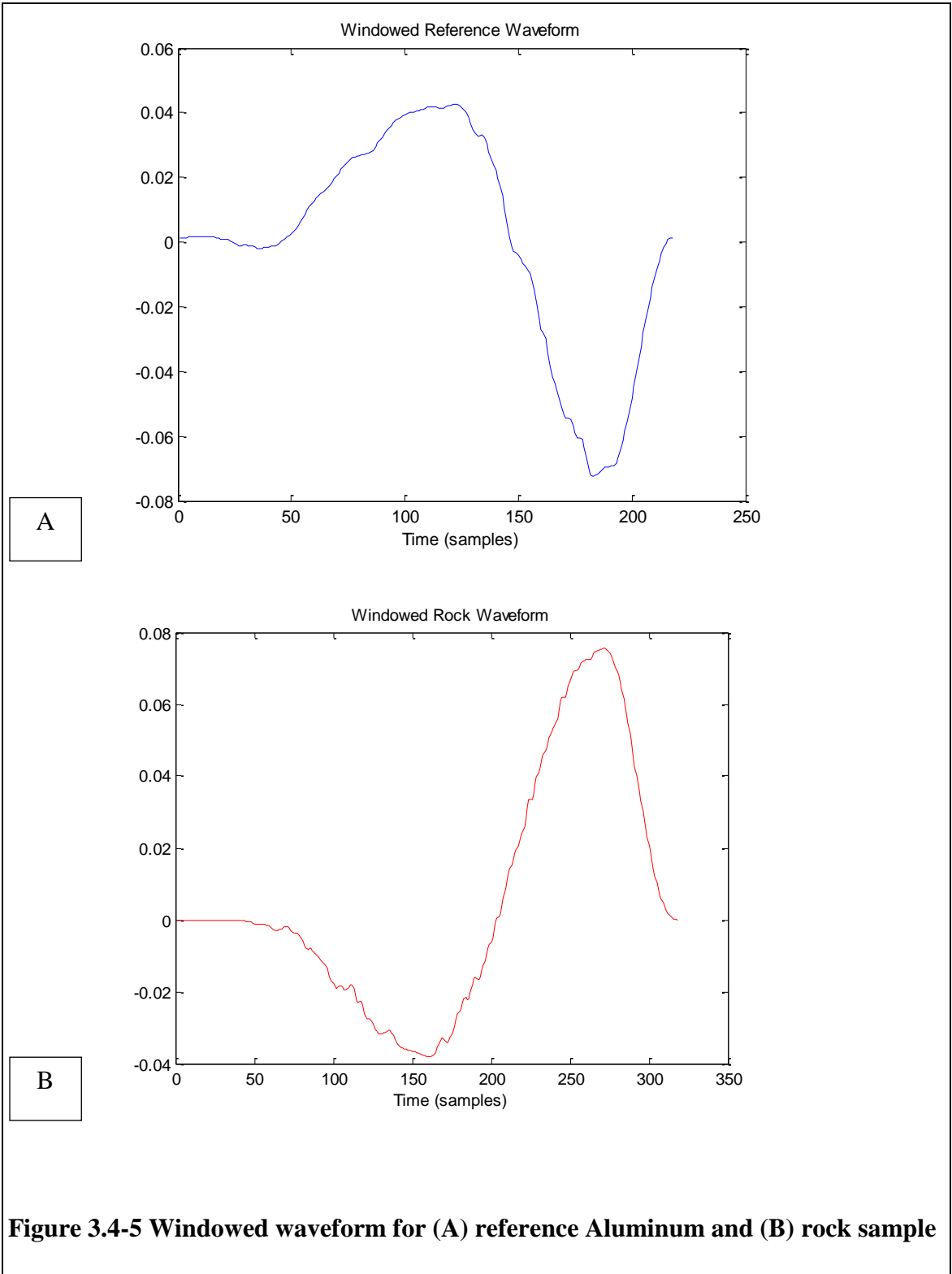
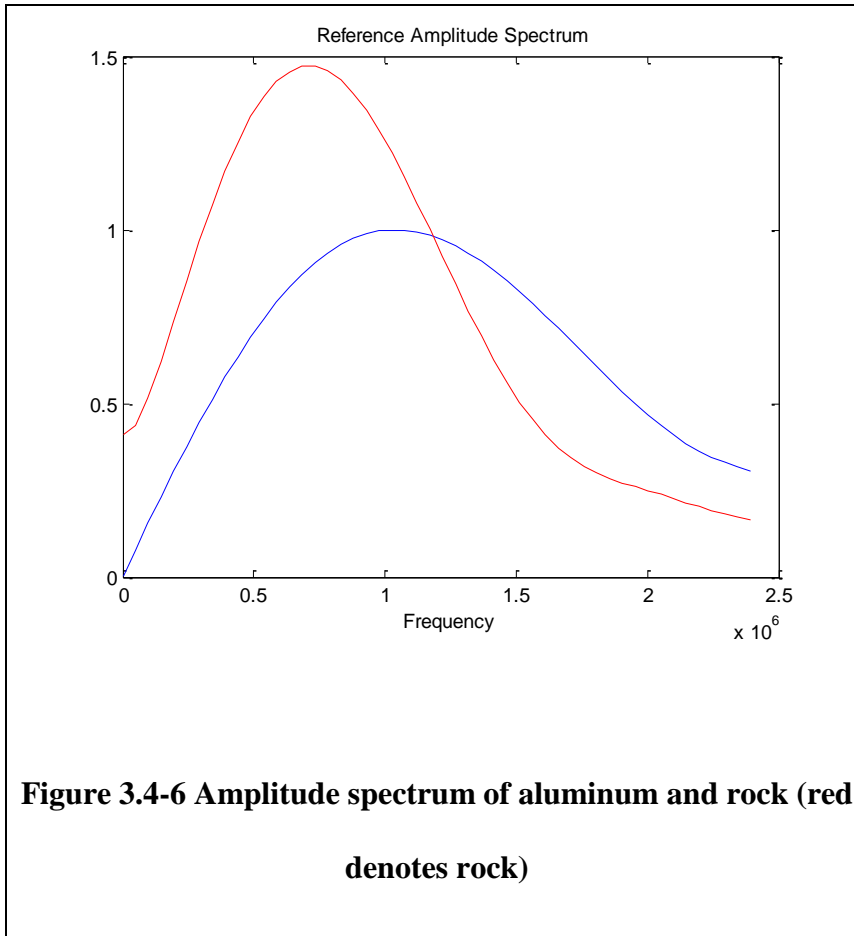


**Figure 3.4-6** shows the amplitude spectrums of the aluminum and rock samples. The rock spectrum has not started from zero due to the presence of non-zero offset that still remains after applying taper.



The natural logarithm of the spectral ratio with respect to frequency is plotted in **Figure 3.4-7** and a best fit straight line is drawn to the straight portion of the frequencies between 0.5-1.5 MHz for determining the slope of the curve. The line is chosen in such

way that it remains between the frequency ranges of 0.5-1.5 MHz because most of the signal lies in this frequency range.

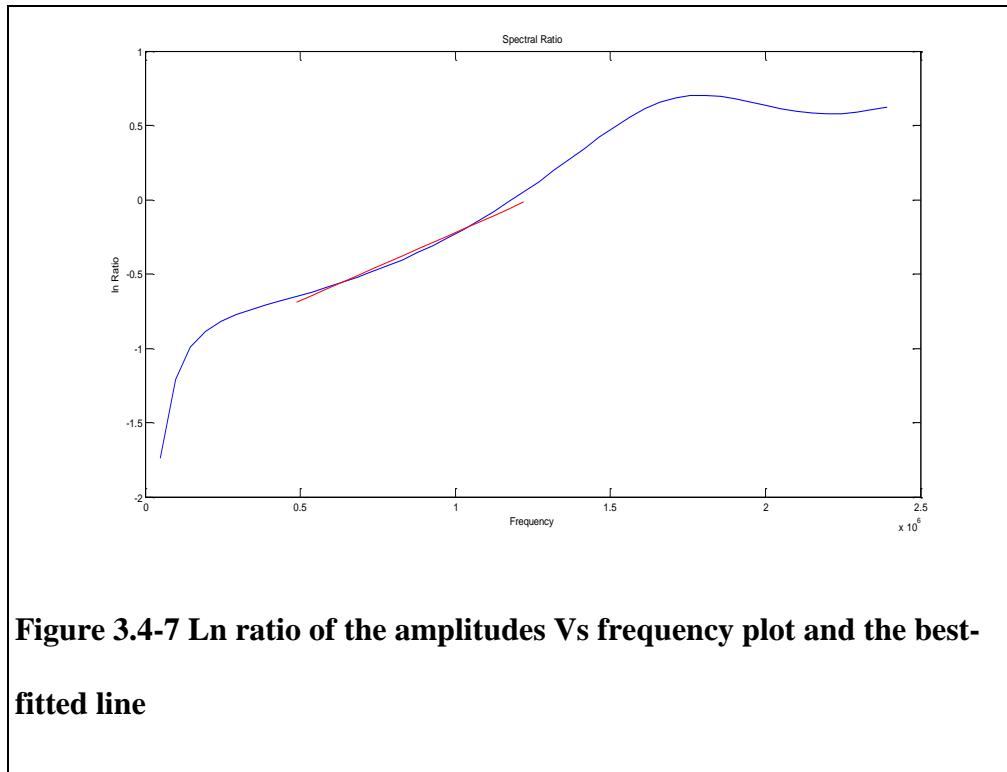


**Figure 3.4-7 Ln ratio of the amplitudes Vs frequency plot and the best-fitted line**

#### 3.4.4 *Grading of the rock samples:*

The selected rock samples ([Section 3.4.2](#)) are graded based on the quality of the recorded signal. Depending on the nature of the signal in the waveform, three grades (Grade A, B and C) are made. If the signal in the waveform is clear and distinct, therefore easily separated from the noise, then it is considered as Grade A. In Grade B sample, signal is

still distinguishable although noise is getting more pronounced than Grade A sample. Grade C mostly contains noise; therefore signal cannot be separated from the noise. Please note that these are largely subjective measure.

The waveforms and the amplitude spectra for the reference and rock samples (Grade A, B and C) are illustrated in the subsequent figures ([Figure 3.4-8](#) and [Figure 3.4-9](#)). It may be noted that 55mm length aluminum waveform ([Figure 3.4-3 \(A\)](#)) has been chosen as the reference for the spectral ratio technique.

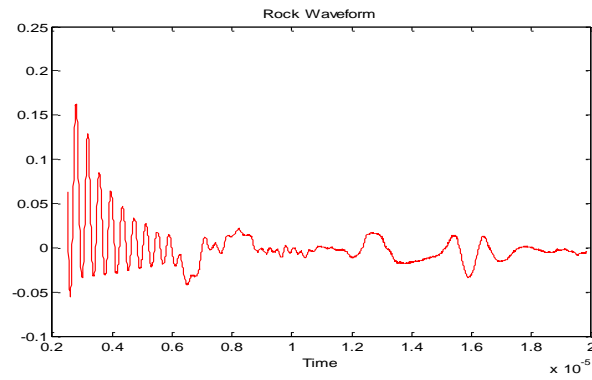
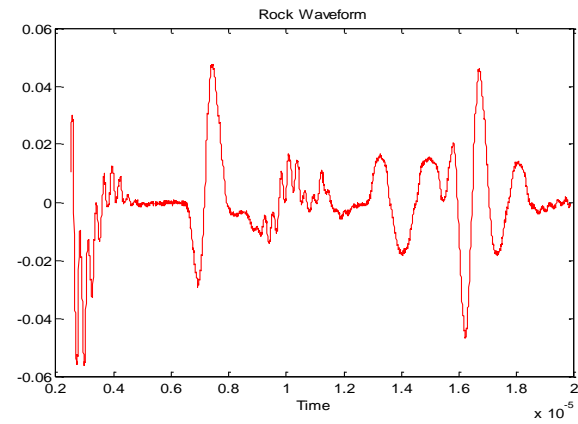
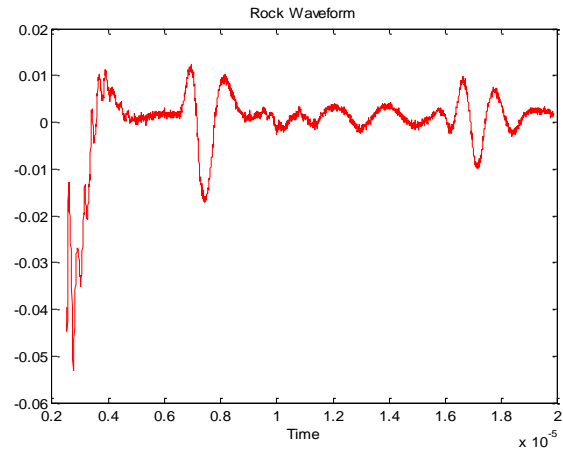
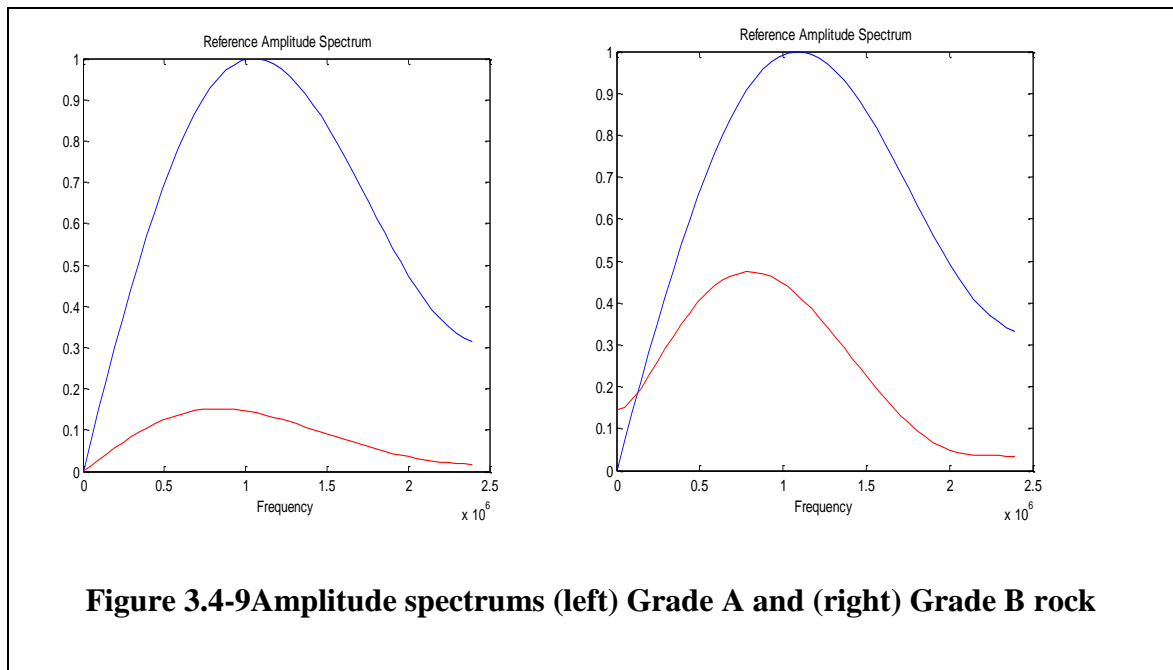


**Figure 3.4-8 Typical waveform for (top left) Grade A-Felsic norite and (top right) Grade B-Metatonalite and (bottom) Grade C rock-Basalt**

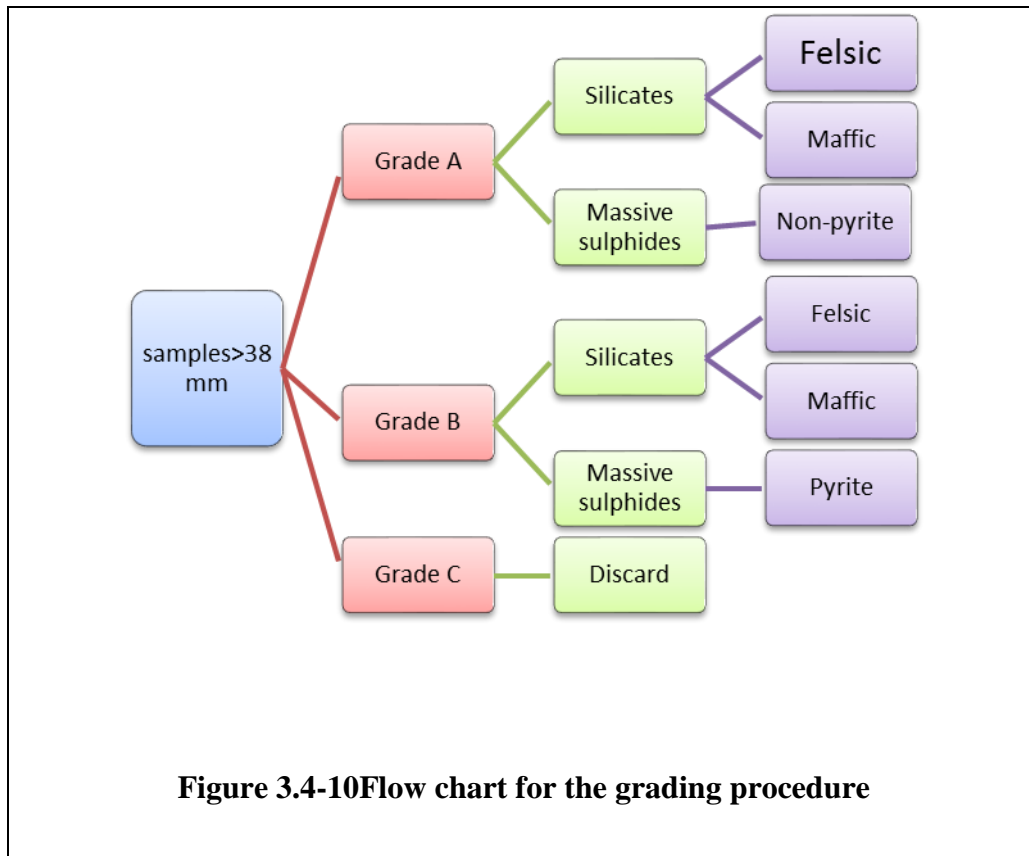


Grade A waveform shows that the signal is clearly distinguishable from noise. In Grade B, signal is also separable. However, noise is more pronounced in Grade B (comparison to Grade A). Grade C rock waveform mostly contains noise and signal is hard to detect. Therefore this type of samples are discarded for the current analysis (Figure 3.4-8).

The amplitude spectrum for Grade A is nicely started from zero and smooth curve. Non-zero offset is present in Grade B spectrum. Even though some of the amplitude spectra do not decay to zero (that is the trend or low frequency component is not completely removed), because the ratio of the slope is used, the results are still valid. 55 mm aluminum is used as reference in both grades which is denoted by blue color Figure 3.4-9.

### 3.4.5 Summary of the grading and grouping

The summary of the grading and grouping is shown in the following flowchart ([Figure 3.4-10](#))



### 3.5 Summary data:

The summary data which is included in [Appendix A](#) refers to the data that is used in the analysis after sorting them out from the whole database.

# Chapter 4

## Results and Discussion

In order to provide a guideline for seismic exploration and the choice of the seismic methods, it is necessary to analyze the elastic properties of the rocks. For the successful mineral exploration for massive sulphide deposits, it is necessary to analyze the physical and acoustic properties of a particular deposit because massive sulfides show large variations in elastic properties depending on mineralogy. Velocity and density by far have been given the most attention for the exploration of minerals. Attenuation along with velocity may provide more precise analysis. This chapter will discuss the changes and sensitivity of three parameters (velocity,  $Q$  and loss factor) with hydrostatic confining pressures for massive sulphides and felsic/mafic hosts. The relationship between these parameters and the rock-types and also how the individual parameters are related to each other will be discussed in detail. In addition, a sensitivity analysis is conducted to find out the correlation coefficient of the parameters that determine  $Q$ . The low and high pressure analyses are presented separately to observe changes in both pressure regimes and in which the mechanisms of attenuation may be different.

As described in Chapter 3, the whole dataset is graded in: Grade A, B and C to insure data quality. Grade C is discarded because the waveforms from these rocks do not contain sufficient signal for attenuation analysis. Velocity,  $Q$  and loss factor for Grade A

and B (silicates and massive sulphides for both the grades) are plotted separately. It is observed that they exhibit similar trends. Therefore no distinction is made between these two grades in upcoming analysis. Silicates are grouped into felsic and mafic and massive sulphides are grouped in to low and high pyrite rich rock samples. The following sections will demonstrate velocity, Q and loss factor with pressure for the ore and the host rocks.

#### 4.1 **Velocity versus pressure**

Velocity was measured for massive sulphides, felsic and mafic rock samples (dry condition) at various confining pressures up to 600 Mpa by the Pulse Transmission Technique. The average velocities for the groups of massive sulphides and silicates will be discussed in the following sections.

##### 4.1.1 *Velocity Vs. pressure for the four groups of massive sulphides*

In the database, massive sulphides contain mainly four types of sulphide minerals in individual state or in mixed ores . They are mainly: Chalcopyrite, Sphalerite, Pyrrhotite and Pyrite. Velocities of these sulphides are plotted against confining pressure (**Figure 4.1-1**). These figures are from both grade A and B. Grade A massive sulphides are mainly low pyrites and grade B sulphides are high pyrite. The bars denote standard deviations.

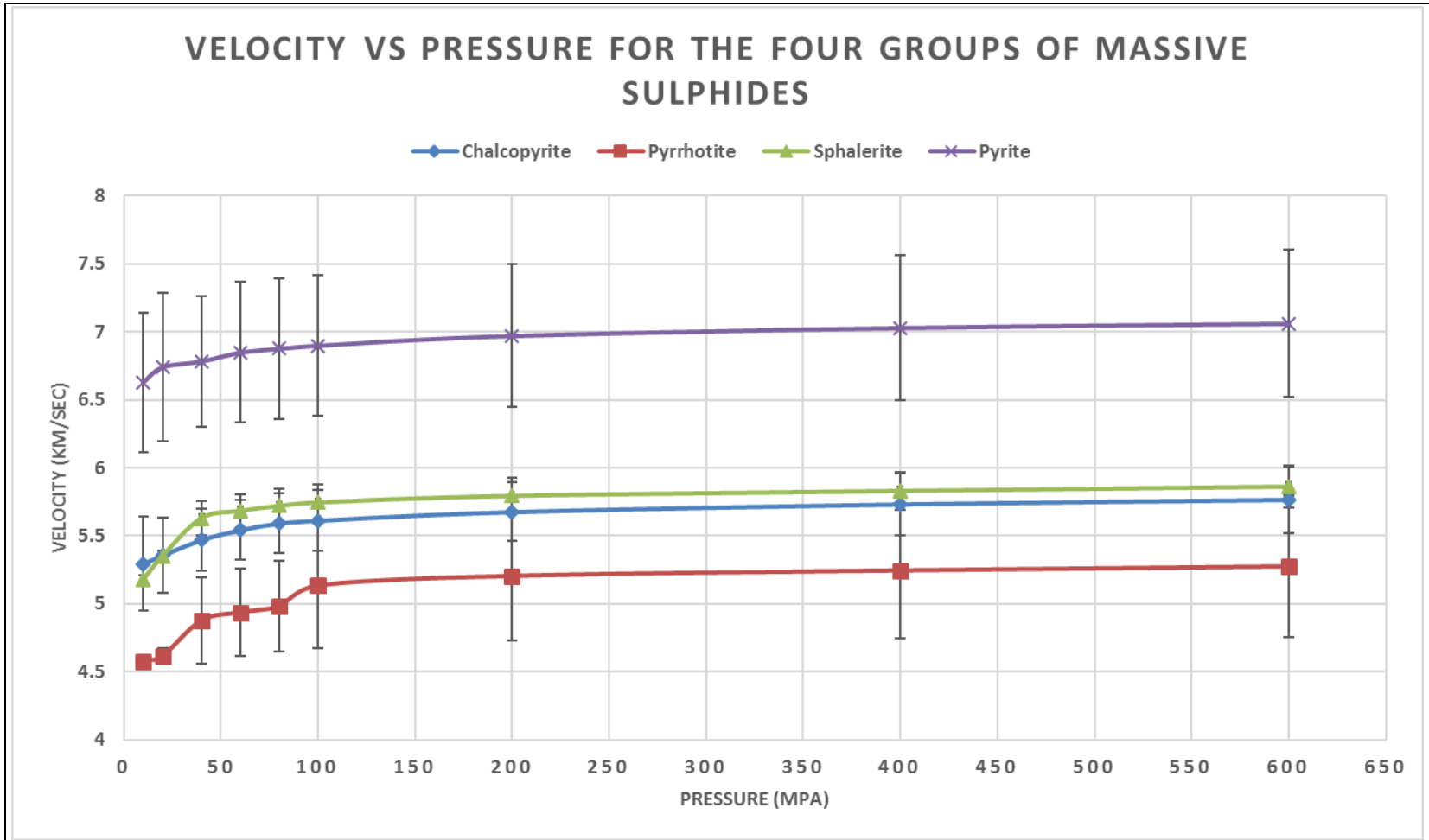


**Figure 4.1-1** Velocity vs. pressure for four groups of massive sulphides

This figure shows that pyrite rich sulphides have the highest velocity compared to other sulphides and are easily distinguishable from the rest of the massive sulphides. The range of velocity for pyrite rich samples is around 6.6-7.1 km/sec whereas other sulphides have the range of 4.50-5.80 km/sec. For all the sulphides, velocity has a positive correlation with pressure. From [Harvey's \(1998\)](#) study, as mentioned in literature review, it is understandable that the high velocity of pyrite rich sulphides is related to the crystal structure. Chalcopyrite, pyrrhotite and sphalerite rich samples have more or less similar densities and velocities hence they are grouped together into low pyrite group. The high and low pyrite sulphides are plotted with their associated hosts in [Figure 4.1-2](#). The standard deviation bars show uniform spread of the velocities from the mean for all the pressures.

#### 4.1.2 *Velocity for massive sulphides and silicates*

[Figure 4.1-2](#) shows average velocities with hydrostatic confining pressure up to 600 Mpa for massive sulphides (high and low-pyrite) and silicates (felsic and mafic). The velocity-pressure plots exhibit similar trend (velocity increases with pressure) for both the ore and the hosts.

## VELOCITY VS PRESSURE FOR MASSIVE SULPHIDES AND THE HOST ROCKS

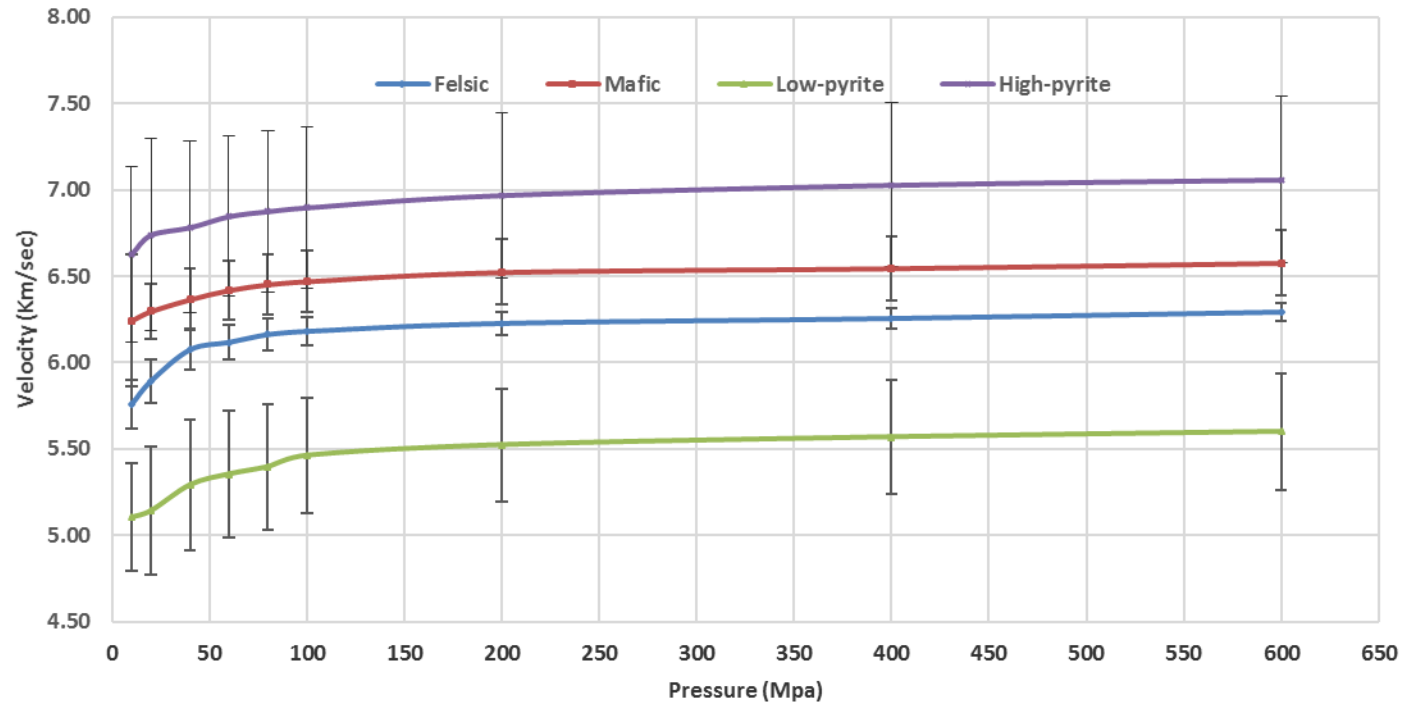


Figure 4.1-2 Velocity vs. pressure for silicate hosts (felsic and mafic) and massive sulphides (high and low pyrite)

Velocity increases rapidly below 100 MPa apparently due to the closure of micro cracks and grain boundaries (Birch, 1960). Above 100 Mpa, the increase in velocity with pressure is slow and linear. Close observation on Velocity-pressure plots show that the crack closure pressure might be around 100 Mpa. The results below 100 Mpa will be discussed further in Section 4.5.

Amongst the sulfides, pyrite-rich samples have the highest velocity and low-pyrite samples have the lowest velocities. Silicates fall in between these two sulphides. The range of velocities are shown in Table 4.4-1. The range shows that silicates have narrow range compared to massive sulphides. It is to be noted that, in this research we have not considered ultramafic rocks (UM). Ultramafics rocks can have velocities as high as pyrite (Figure 2.3.1). Felsic rocks have density around 2.72 g/cc which is lower than that of mafic rocks (around 2.92g/cc). Therefore the velocity in mafic should be greater than felsic, which is also observed in Figure 4.1-2, at 200 Mpa felsic has average velocity of 6.23 km/sec while mafic has 6.52 Km/sec. The acoustic properties of sulphides are different from that of silicates [Salisbury et al., 1996] which is also depicted in Figure 4.1-2. Massive sulphides have distinct velocity range compared to silicates. The velocities of felsic and mafic are very close to mean whereas massive sulphides have higher spread than the host rocks around the mean.

## 4.2 Q versus pressure

This section will discuss how attenuation changes with pressure for different rocks and their range of Q.

### 4.2.1 *Q Vs. pressure for the four groups of massive sulphides*

Chalcopyrite and pyrite rich sulphides share the same range of Q values and they have the similar trend except at low pressure (**Figure 4.2-1**). On the other hand sphalerite and pyrrhotite rich sulphides have similar range of Q. This actually opposes the velocity picture of **Figure 4.1-1**, where chalcopyrite and sphalerite have the similar range of velocity. Pyrrhotite and sphalerite have higher Q values than pyrite and chalcopyrite. Therefore seismic attenuation is higher in pyrite and chalcopyrite enrich sulphides.

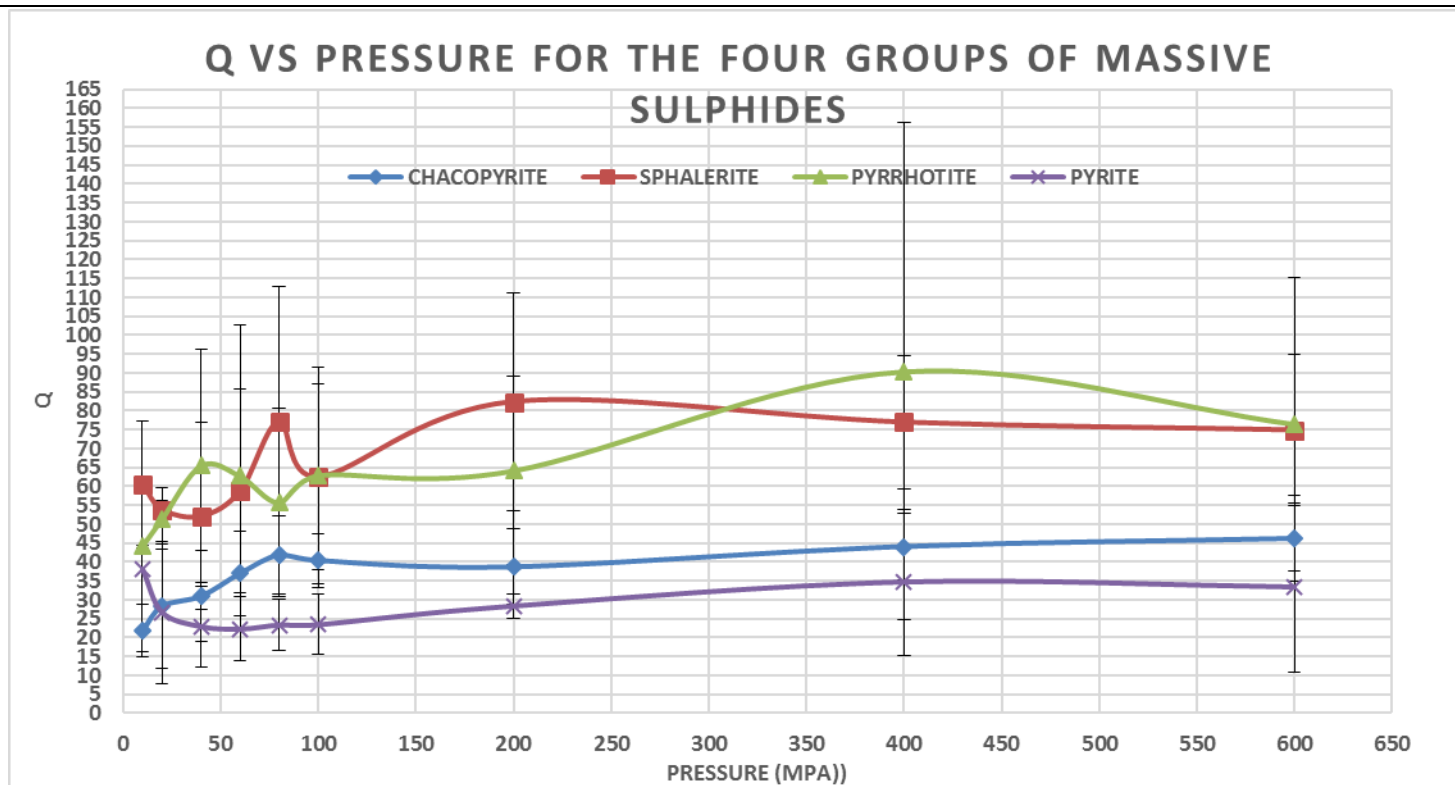


**Figure 4.2-1 Q vs pressure for four groups of massive sulphides**

Q increases (attenuation decreases) with pressure for sulphides with some exception in low pressure and also pyrrhotite and sphalerite rich samples have irregular trends of Q. If we observe the relation between the velocity ([Figure 4.1-1](#)) and Q ([Figure 4.2-1](#)) plots of sulphides, it shows that high pyrite sulphides has the highest velocity and the lowest Q and this inverse relation of Q and velocity regarding range also holds for other sulphides. However both velocity and Q have the similar increasing trend with pressure except some anomalous values at low pressure. The rate of change in Q is greater than velocity due to the sensitivity of attenuation to coupling between the transducer and the sample, source waveform, geological structure, reflection, beam spreading in small sized laboratory specimen etc. as mentioned by Butt (2001). Unlike velocity, Q has more uncertainty in the results. The high value of standard deviation indicates that the data points are spreaded out over a large range of values

Attenuation in high pyrite increases below 60 Mpa, this result of pyrite rich sulphides probably cannot be associated with crack closure. It is a possibility that it could be associated with differential crack closure but that is difficult to assess. It is mentioned in literature review that pyrite has a low Poisson's ratio compared to most of the other sulfide minerals. The Poisson's ratios for the common sulphides and felsic and mafic are tabulated below. These data are collected from [Harvey, \(1998\)](#).

**Table 4.2-1 Poisson's ratio of silicates and sulphide minerals**

	<b>Poisson's ratio</b>
<b>Felsic</b>	<b>0.26</b>
<b>Mafic</b>	<b>0.30</b>
<b>Pyrite</b>	<b>0.19</b>
<b>Chalcopyrite</b>	<b>0.35</b>
<b>Sphalerite</b>	<b>0.32</b>
<b>Pyrrhotite</b>	<b>0.23</b>

It is mentioned above that chalcopyrite, sphalerite and pyrrhotite have been grouped as low-pyrite due to their similar density and velocity. In this section  $Q$  for the four types of sulphides have been demonstrated. The following section will describe high and low pyrite sulphides along with the silicates.

#### 4.2.2 *Q for massive sulphides and silicates*

**Figure 4.2-2** and **4.2-3** are the plots of  $Q$  and  $(1/Q)$  respectively with confining pressure up to 600 Mpa. Silicates and massive sulphides are plotted on the same plot. The changes of  $Q$  with confining pressure is observed carefully.

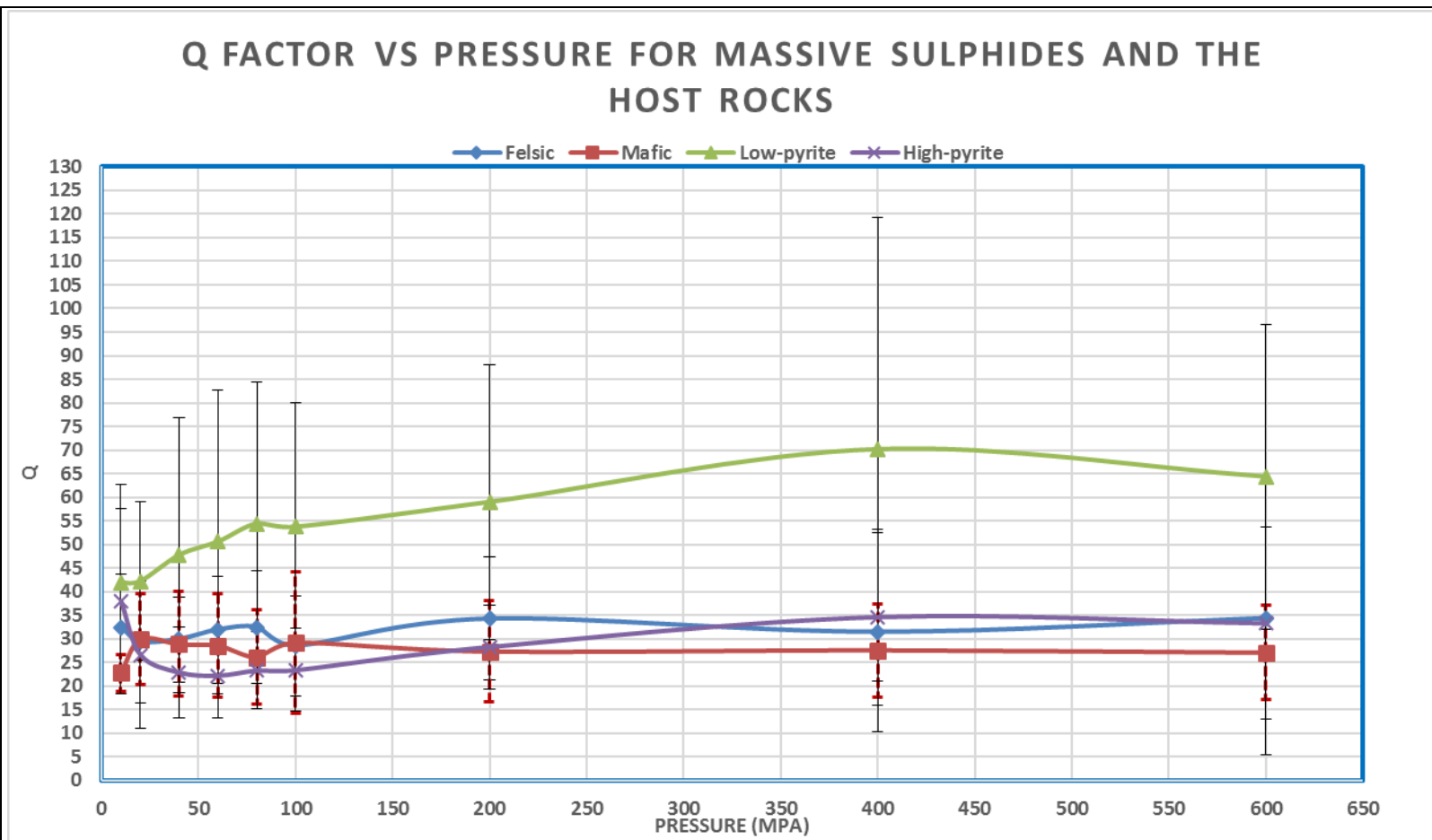


**Figure 4.2-2 Q vs pressure for silicate hosts (felsic and mafic) and massive sulphides (high and low pyrite)**

## 1/Q VS PRESSURE FOR MASSIVE SULPHIDE AND THE HOST ROCKS

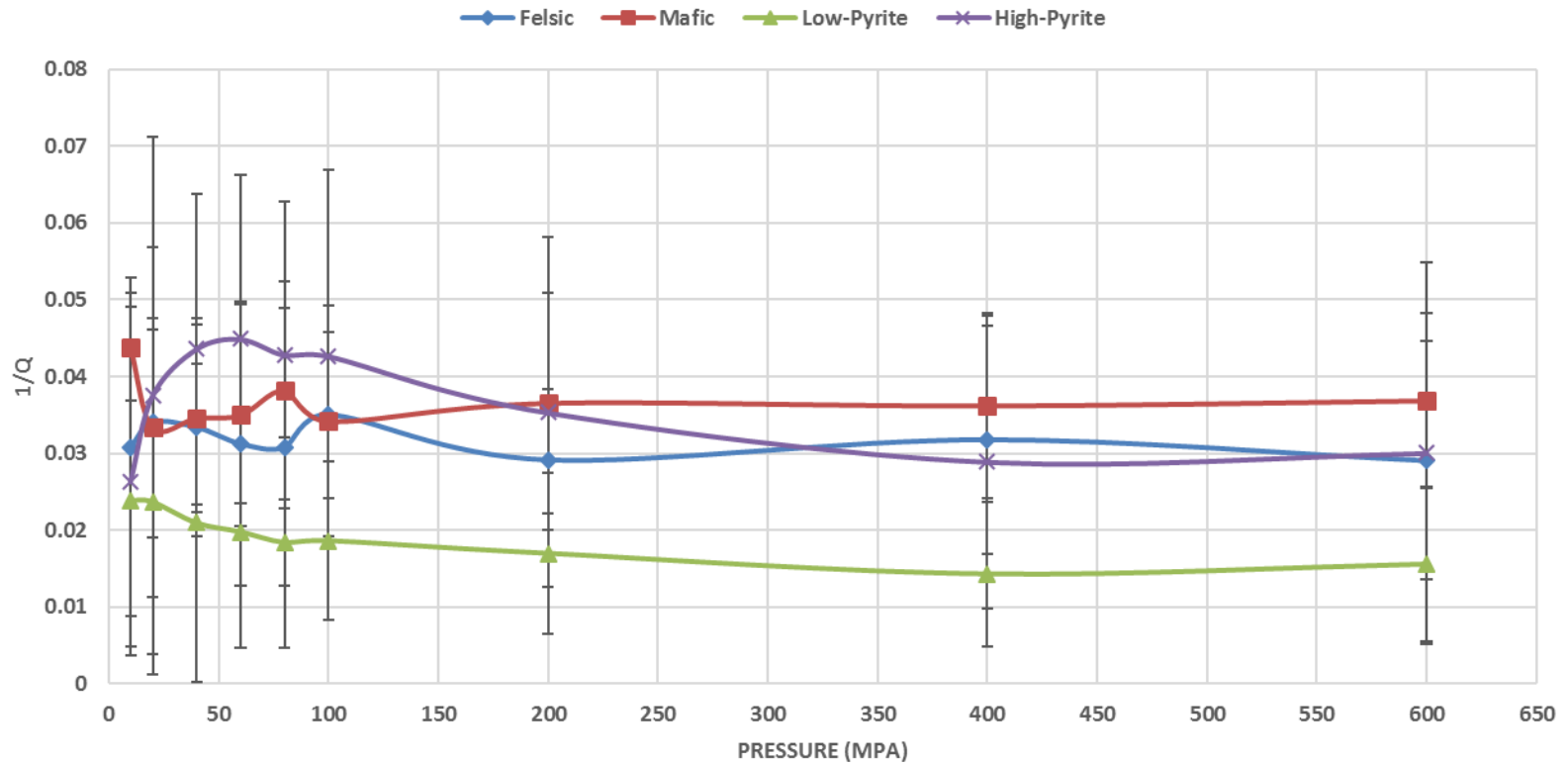


Figure 4.2-3 1/Q vs pressure for silicate hosts (felsic and mafic) and massive sulphides (high and low pyrite)

Q shows only modest pressure dependence (except for the low pyrite sulfides) and the low pressure results are not systematic. The lack of low pressure systematics suggests that the analysis technique may have issues at low pressure.

An increase in attenuation (Q decreases) is observed for high pyrites up to 60 Mpa, Above 60 Mpa attenuation decreases (Q increases) with pressure and there is a very slight increase in attenuation observed over 400 Mpa. In low pyrite attenuation decreases with pressure (Q increases) and above 400 Mpa there is a slight increase in attenuation similar to high pyrite. Little change is observed in Q with pressure for felsic and mafic silicates.

It seems that frictional dissipation likely dominates at low pressure regime and may approach very low values at high pressure. Intrinsic anelasticity might be present in both low (below 100 Mpa) and high pressure (above 100 Mpa) but dominant in high pressure regime.

Low pyrite sulphides have the highest Q values and wide range (41-70) while pyrite rich sulphides have the lowest and narrowest range (38-22).. The Q for silicates overlaps with high pyrite sulphides. Felsic rocks (28-35) have slightly higher Q values than mafic (26-30) rocks'. The ranges of Q are shown in the [Table 4.4-2](#).

Observing [Figure 4.2-2](#) or [4.2-3](#), low pyrite massive sulphide has distinct range and trend of Q which might separate them from host rocks and high pyrite. At high pressure, pyrite rich sulphides and their associated felsic and mafic hosts share the range of Q. Q might

have higher sensitivity with pressure for the ore, but due to the scatter in the results it might be a possibility.

### 4.3 Loss factor versus pressure

Loss factor is the energy loss of a seismic wave per unit distance at a given frequency. It is measured at 1 MHz frequency in this research. In addition to velocity and Q, the sensitivity of the loss factor with pressure is demonstrated in the following sections. From a mineral exploration perspective, loss factor is a more convenient parameter to estimate directly from seismic data than Q.

#### 4.3.1 *Loss factor Vs. pressure for four groups of massive sulphides*

**Figure 4.3-1** shows the changes of loss factor at 1 MHz with pressure for chalcopyrite, sphalerite, pyrrhotite and pyrite rich sulphides.

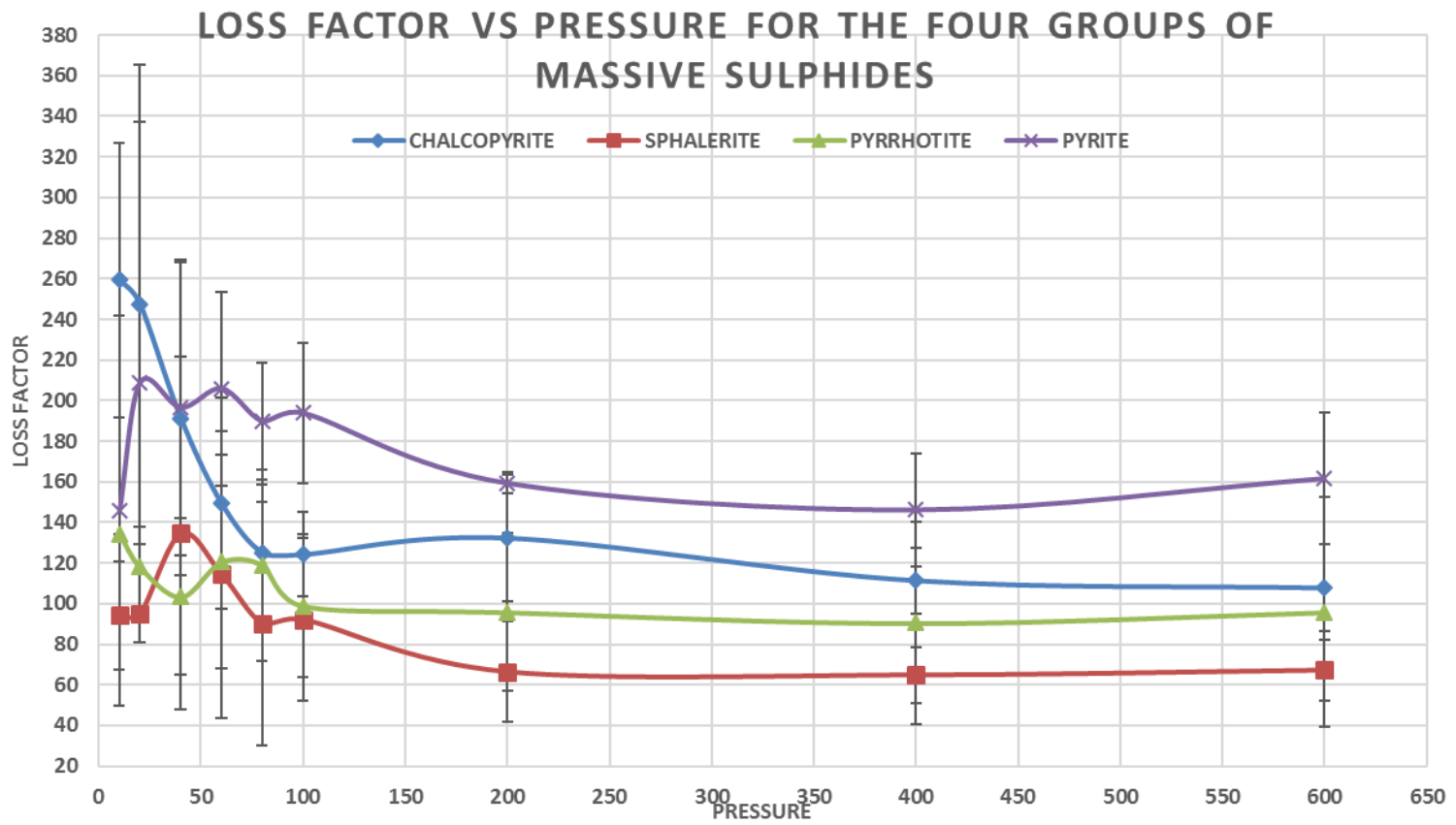


**Figure 4.3-1 Loss factor vs pressure for four groups of massive sulphides**

In general loss factor decreases with increasing pressure except some anomalous points in the low pressure. At higher pressure the change of loss becomes linear for chalcopyrite, pyrrhotite and sphalerite rich sulphides. As the pressure increases the pores and cracks diminish, therefore the propagating wave loses less energy in interacting the cracks and pores. It makes sense that loss factor decreases with increasing pressure and the presumed closure of the thin cracks. But in [Figure 4.2-3](#)  $1/Q$  vs. pressure, the relationship is a lot more complicated with some rocks showing increasing attenuation ( $1/Q$ ) and then decrease (high pyrite) with increasing pressure, some don't change much at all (host rocks) and one set (low pyrite) shows a clear decrease in attenuation with increased pressure. It appears that there is more scatter in the  $Q$  ( $1/Q$ ) measurements than the loss factor determinations.

High pyrite has the highest loss compared to other massive sulphides. The range of loss factor for each sulphides will be presented in [Table 4.4-1](#). Observing [Figure 4.3-1](#) (loss vs. pressure) and [Figure 4.2-1](#) ( $Q$  vs. pressure) of four groups of massive sulphides, it might be noted that individual massive sulphide has clear and distinct trend of loss factor unlike  $Q$  in high pressure.  $Q$  plots of pyrrhotite and sphalerite are not clearly separated. Further analysis on how  $Q$  and loss related will discussed in [Section 4.7.3](#).

#### 4.3.2 *Loss factor for massive sulphides and silicates*

[Figure 4.3-2](#) shows loss factor with pressure for massive sulphides and silicates.

## LOSS FACTOR VS PRESSURE FOR MASSIVE SULPHIDES AND THE HOST ROCKS

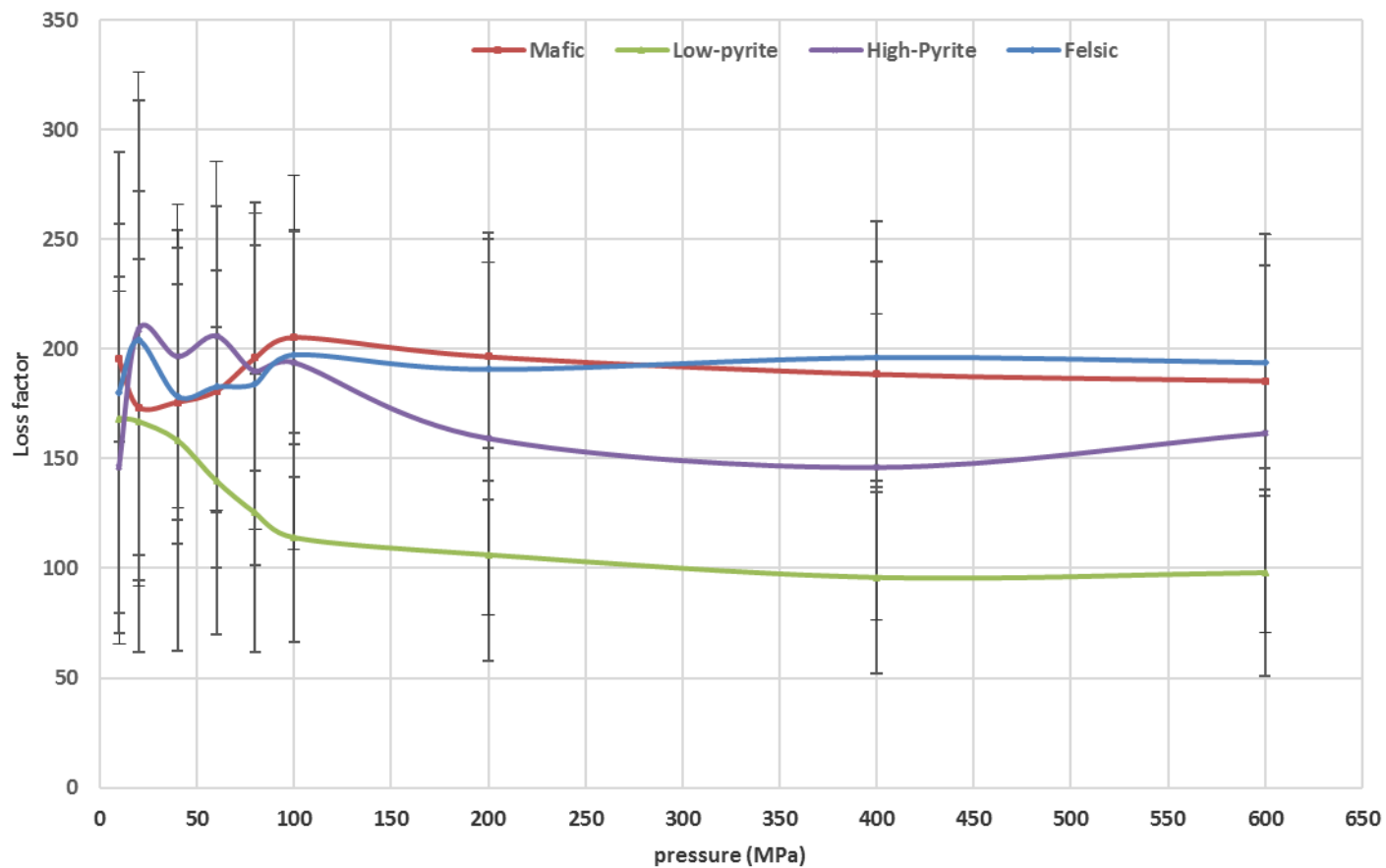


Figure 4.3-2 Q vs pressure for silicate hosts (felsic and mafic) and massive sulphides (high and low pyrite)

Loss of energy of seismic wave in massive sulphide decreases with pressure and remains almost linear for silicates over 100 Mpa. The major results drawn from [Figure 4.3-2](#) are that at high pressure the loss factor is lower in sulphides than in silicates and that low pyrite sulphides have lower loss factors than pyrite rich rocks. That is true for low pressures as well if the lowest pressure high pyrite sample is anomalous. Loss factor is almost the same for felsic and mafic silicates. The ranges of loss factor will be shown in [Table 4.4-2](#). An inverse relationship is observed between Q and loss factor ([Figure 4.2-2 and 4.3-2](#)) which will be shown later. From the standard deviation bars, loss factor has moderate scatter around the mean.

#### 4.4 Summary of the velocity, Q and Loss factor plots

This section will show the summary results from the plots previously discussed in [Section 4.1](#) through [4.3](#) in tabular format.

##### 4.4.1 *Summary results*

The range of velocity, Q and loss factor along with their trend in low and high pressure for the four groups of massive sulphides are tabulated in [Table 4.4-1](#). The same parameters are tabulated for high and low pyrite massive sulphides and felsic and mafic silicates in [Table 4.4-2](#).

**Table 4.4-1 Summary results for pyrite, chalcopyrite, sphalerite and pyrrhotite**

	Massive sulphide Groups	Velocity	Q	Loss factor
<b>Range</b>	<b>Pyrite</b>	<b>6.6-7.1</b>	<b>22-38</b>	<b>145-208</b>
	<b>Chalcopyrite</b>	<b>5.2-5.8</b>	<b>21-46</b>	<b>107-260</b>
	<b>Sphalerite</b>	<b>5.2-5.8</b>	<b>52-82</b>	<b>64-134</b>
	<b>Pyrrhotite</b>	<b>4.5-5.3</b>	<b>44-82</b>	<b>90-134</b>
<b>High pressure response &gt;100Mpa</b>	<b>Pyrite</b>	<b>Increasing</b>	<b>Increasing</b>	<b>Decreasing</b>
	<b>Chalcopyrite</b>	<b>Increasing</b>	<b>Increasing</b>	<b>Decreasing</b>
	<b>Sphalerite</b>	<b>Increasing</b>	<b>No defined trend</b>	<b>Decreasing</b>
	<b>Pyrrhotite</b>	<b>Increasing</b>	<b>No defined trend</b>	<b>Decreasing</b>
<b>Low pressure response &lt;100Mpa</b>	<b>Pyrite</b>	<b>Increasing</b>	<b>Decreasing</b>	<b>No defined trend</b>
	<b>Chalcopyrite</b>	<b>Increasing</b>	<b>Increasing</b>	<b>Decreasing</b>
	<b>Sphalerite</b>	<b>Increasing</b>	<b>No defined trend</b>	<b>No defined trend</b>
	<b>Pyrrhotite</b>	<b>Increasing</b>	<b>No defined trend</b>	<b>No defined trend</b>
<b>Remarks</b>		<p>*Velocity increases with pressure, the gradient is high in low pressure and low in high pressure.  **Pyrite has high velocity range compared to other Massive sulphides</p>	<p>*Pyrite has decreasing Q at low pressure and Q increases at high pressure. Chalcopyrite has increasing Q both at high and low pressure. Pyrrhotite and sphalerite have no defined trend</p>	<p>Loss factor decreases with increasing pressure above 100 Mpa. Below 100 Mpa the result does not show any trend except for chalcopyrite</p>

**Table 4.4-2 Summary results of Silicates and massive sulphides**

	Rocks	Velocity	Q	Loss factor
<b>Range</b>	Felsic	5.7-6.3	28-35	178-204
	Mafic	6.2-6.6	22-30	173-205
	Low pyrite	5.1-5.6	41-70	95-170
	High pyrite	6.6-7.1	22-38	145-208
<b>High pressure &gt;100Mpa response</b>	Felsic	Increasing	Almost linear	Mostly linear
	Mafic	Increasing	Almost linear	Decreasing
	Low pyrite	Increasing	Increasing	Decreasing
	High pyrite	Increasing	Increasing	Decreasing
<b>Low pressure &lt;100Mpa response</b>	Felsic	Increasing	No defined trend	Mostly linear
	Mafic	Increasing	No defined trend	Slightly increasing
	Low pyrite	Increasing	Increasing	Decreasing
	High pyrite	Increasing	Decreasing	Decreasing
<b>Remarks</b>		*higher velocity gradient at low pressure.	Q is more sensitive to massive pyrite rich and pyrite low samples	Wave undergoes greater loss in silicates and high pyrites

#### 4.5 Low pressure results

The high pressure results show better trend and clear distinction among the ores and host rocks. We assume this is due to the closure of the micro cracks (sections through [4.1](#) to [4.3](#)). At pressure below 100 Mpa (represents shallow depth), unclear trends in plots are observed. The plots from the previous sections will be shown here for pressure below <200 Mpa to observe closely the response of these parameters in low pressure. Frictional dissipation along the cracks and grain boundaries may govern the low pressure regime. [Figure 4.5-1](#) to [4.5-3](#) represents velocity, Q and loss factor with pressure respectively below 200 Mpa.

## VELOCITY VS PRESSURE (<200 MPA) FOR MASSIVE SULPHIDES AND THE HOST ROCKS

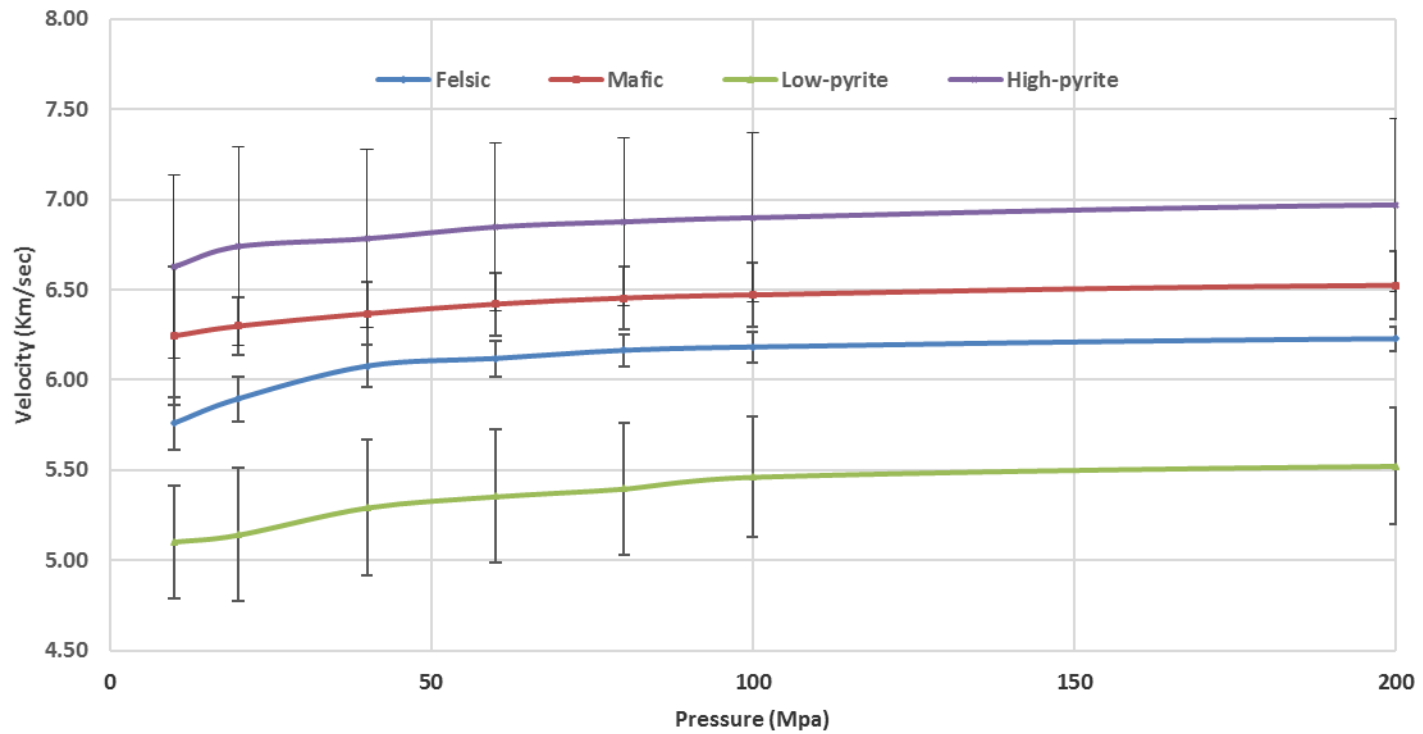
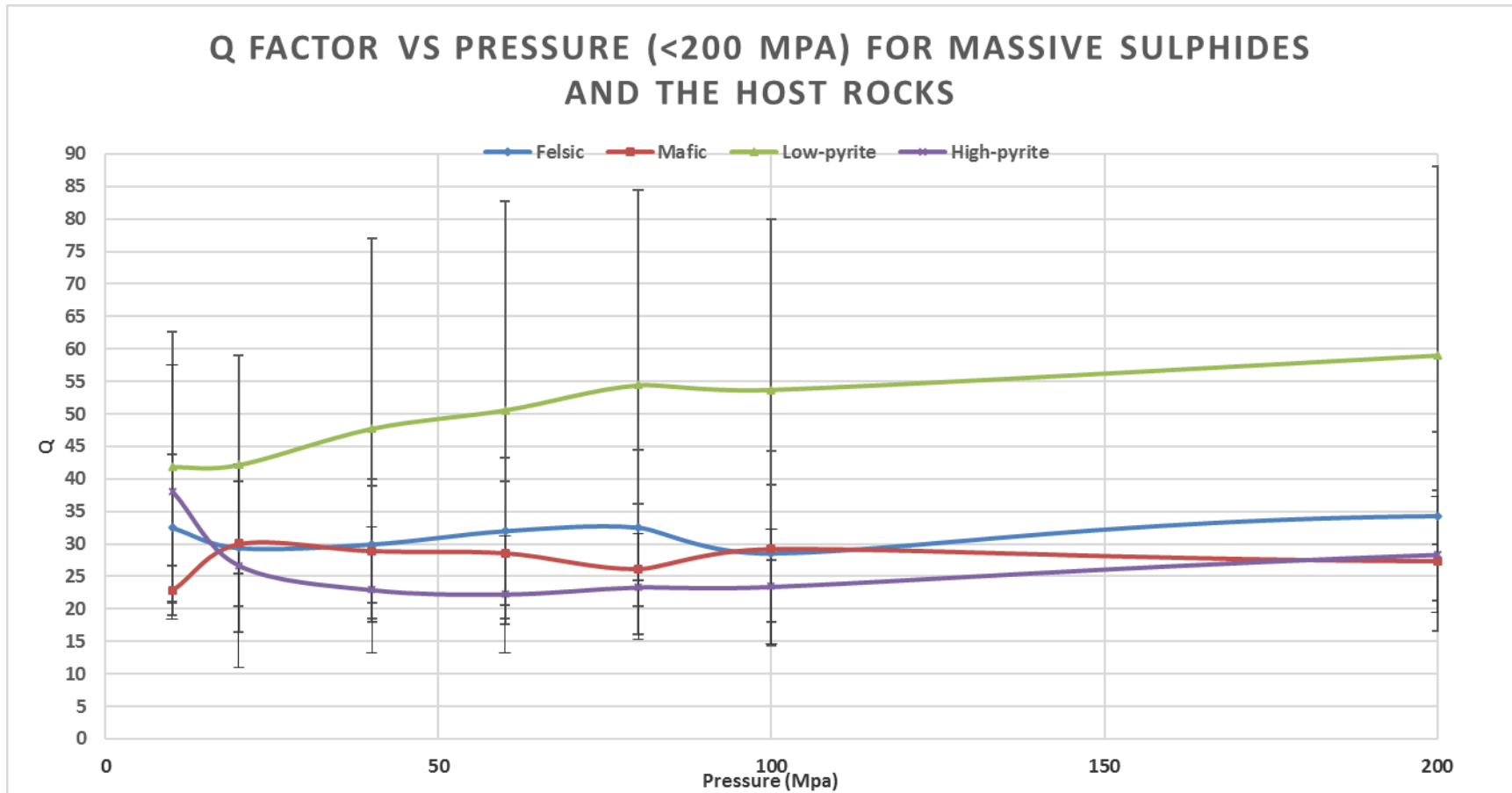


Figure 4.5-1 Velocity vs. pressure for silicate hosts (felsic and mafic) and massive sulphides (high and low pyrite) below 200 Mpa



**Figure 4.5-2 Q vs. pressure for silicate hosts (felsic and mafic) and massive sulphides (high and low pyrite) below 200 Mpa**

### LOSS FACTOR VS PRESSURE (<200 MPA) FOR MASSIVE SULPHIDES AND THE HOST ROCKS

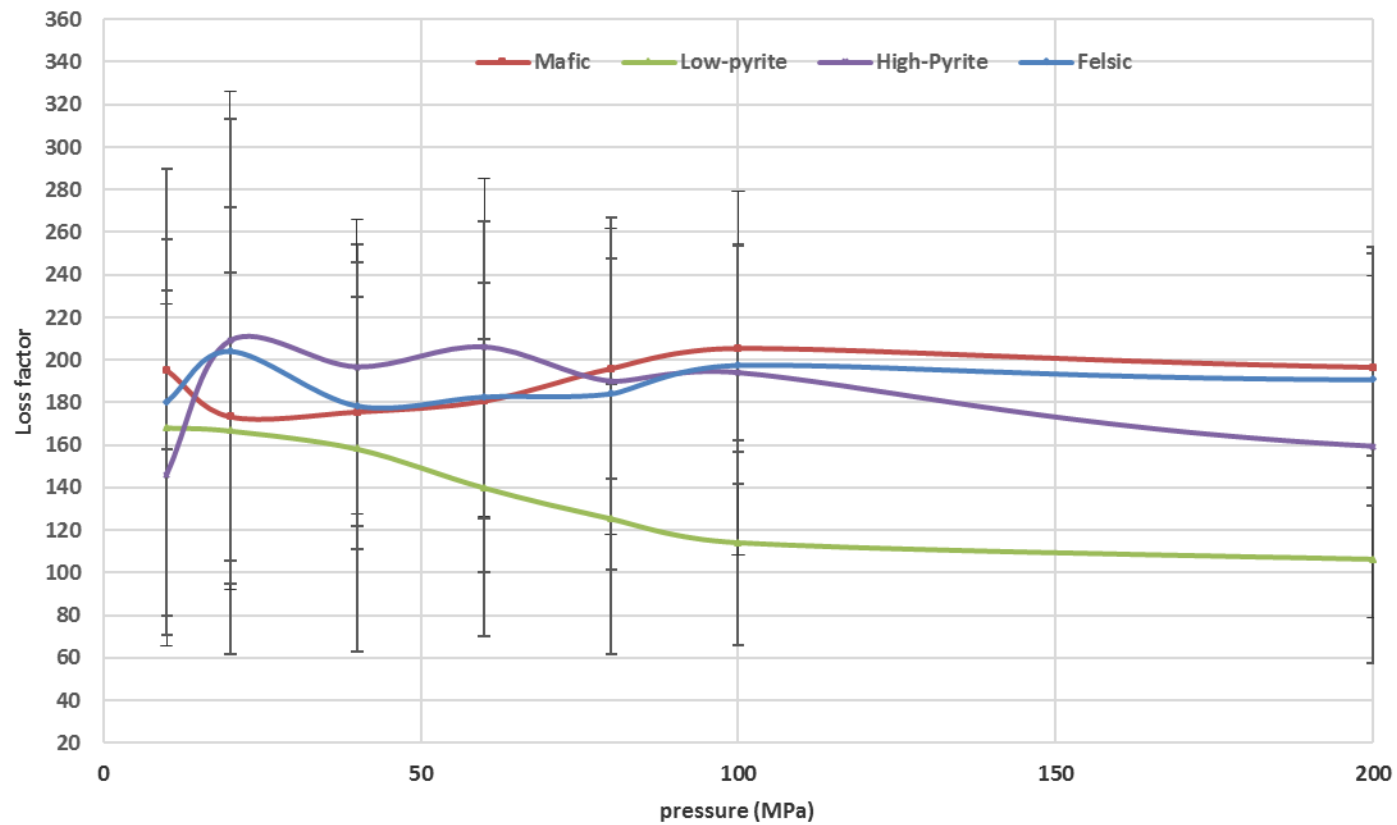


Figure 4.5-3 Loss factor vs. pressure for silicate hosts (felsic and mafic) and massive sulphides (high and low pyrite) below 200 Mpa

The thing that stands out in these graphs is the anomalous behaviour of the low pyrite sulphides with respect to both Q and loss factor. Low pyrite has increasing Q throughout the pressure range. Q for massive pyrite decreases (attenuation increases) up to 60 Mpa and over 60 Mpa Q starts to increase (attenuation decreases). There is no definite trend of Q in host rocks. Below 100 Mpa, low pyrite has decreasing loss factor with pressure while other rocks does not have any defined trend for loss.

Velocity gradient with pressure is higher below 100 Mpa. As mentioned earlier 100 Mpa might be the crack closure pressure in the current case, therefore, greater changes are observed below that pressure. Velocity maintains positive correlation with pressure throughout the low and high pressure zone.

#### **4.6 Sensitivity Analysis by Monte Carlo Approach: Sensitivity of Q for Silicates and Massive sulphides**

To understand the sensitivity of Q to velocity, sample length and slope of the spectral ratio curve, an analysis will be carried out in this section. This will measure the sensitivity of Q to each parameter (sample length, velocity and the slope of the spectral ratio curve).

From the spectral ratio technique ([Section 3.3.2](#)), the equation of Q is as follows:

$$Q = \frac{\pi x}{cm} \dots\dots\dots (4.1)$$

Where,

x=sample length,

c=velocity,

m=slope [slope of the plot of  $\ln \left( \frac{A_1(f)}{A_2(f)} \right)$  Vs frequency]

On the right hand side of Equation 4.1, there are three variables: sample length, velocity and the slope of the spectral ratio curve. Among these three parameters, which one is more sensitive is not known. To identify the sensitivity of the above mentioned parameters of Equation 4.1 a sensitivity analysis is conducted. Velocity and slope are inversely related to Q and length of the rock sample is proportional to Q.

[Gardner et al., \(1981\)](#) suggested a way to rank the parameters according to their contribution. A simple correlation co-efficient derived from Monte Carlo simulations is the simple way to rank parameters. Linear correlation can be determined on the input and output parameters by the Pearson's correlation co-efficient denoted by r. The details of the technique will be available at [Gardner et al., 1981](#)

$$r_{xy} = \frac{\sum_{i=1}^N (x_{ij} - \bar{x}_j)(y_i - \bar{y})}{[\sum_{i=1}^N (x_{ij} - \bar{x}_j)^2]^{1/2} [\sum_{i=1}^N (y_i - \bar{y})^2]^{1/2}} \dots \dots \dots (4.2)$$

The value of r determines the sensitivity of each parameter. The parameter with highest r value will be the most sensitive parameter on the right hand side of equation 4.1. The positive value of r represents that the parameter is positively correlated with Q and negative value of r represents inverse correlation of the parameter with Q.

Sensitivity analysis is done on the data containing massive sulphides and host silicate rocks. The type of distributions and the distribution parameters for the sample length, velocity and slope are tabulated in **Table 4.6-1** and **Figure 4.6-1 (A), (B)** and **(C)** shows the distribution.

**Table 4.6-1 Distribution type and parameter for Grade A rock data**

Grade A rock data	Distribution	Distribution parameter
Sample length	Normal	Mean=44.1422, Standard deviation=4.27443
Velocity	Log normal	Mean=, 1.84601 Standard deviation=0.054109
slope	Weibull	a= 9.68827E-7, b=1.886

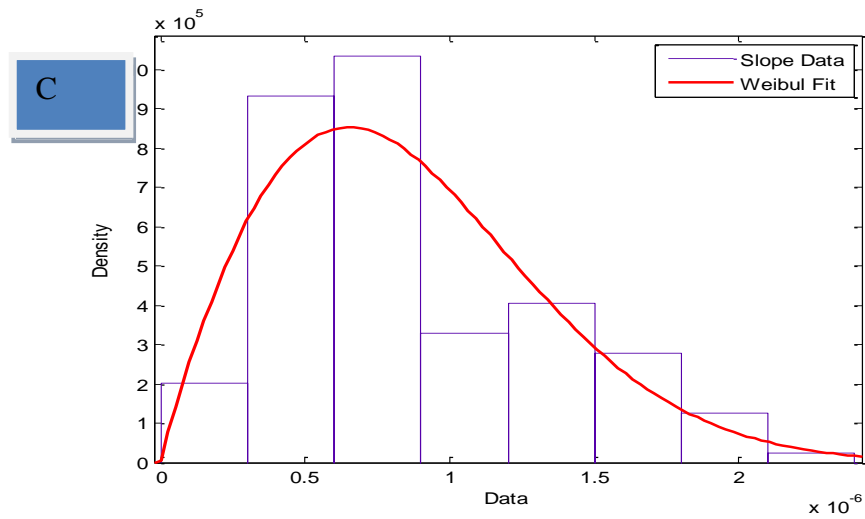
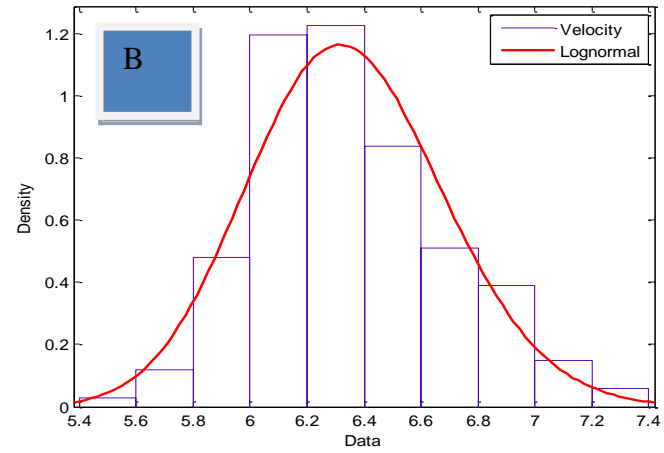
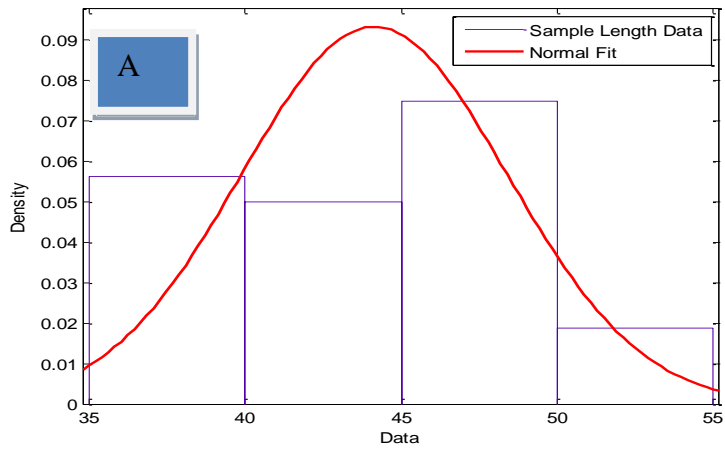


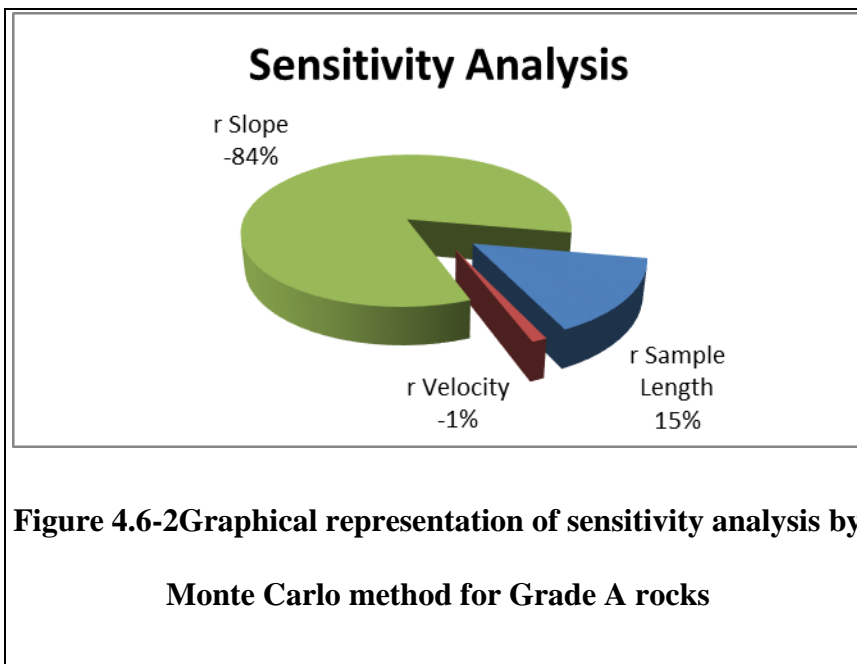
**Figure 4.6-1 Distribution of (A) sample length, (B) velocity, (C) slope**

The best fit distribution was chosen based on maximum log likelihood value of Normal, Lognormal and Weibull. Length of the rock samples has normal distribution. Velocity has lognormal and slope has Weibull distribution. The correlation coefficients,  $r$  for sample length, velocity and slope are tabulated in **Table 4.6-2**. This table shows that the highest value of  $r$  is for slope (0.3447) and the lowest value of  $r$  is for velocity 0.0057. please note that the negative of the  $r$  value means those parameters (velocity and slope) are inversely related with  $Q$ . According to the  $r$  value, in the equation 4.1  $Q$  is most sensitive to slope and least sensitive to velocity. A slight change in slope will cause higher change in  $Q$ .

**Table 4.6-2 Correlation coefficient of sample length, velocity and slope on  $Q$**

<b>Parameter</b>	<b>Correlation</b>	<b>Normalized Correlation</b>
<b>r Sample Length</b>	<b>0.0622</b>	<b>0.15</b>
<b>r Velocity</b>	<b>-0.0051</b>	<b>-0.01</b>
<b>r Slope</b>	<b>-0.3447</b>	<b>-0.84</b>

**Figure 4.6-2** is the graphical representations of the coefficients. The sensitivity analysis shows that the most sensitive parameter is the slope of the spectral ratio curve and its contribution to Q is 84%. Velocity has contribution of 1% and sample length has 15% contribution again negative values represent inverse correlation.



#### 4.7 Relationship among the parameters

Previous sections show the response of velocity, attenuation and loss factor with pressure. Depending on the rock type, the sensitivity of these parameters to pressure may vary. This section will demonstrate and establish a relation of attenuation and loss factor with velocity as well relation between Q and loss factor for massive sulphide and silicates.

Joint interpretation of the parameters will provide base information of applying attenuation and loss factor in exploration of massive sulphides.

#### 4.7.1 *Velocity and Q*

Q is plotted against velocity in [Figure 4.7-1](#) for massive sulphides and the host rocks.

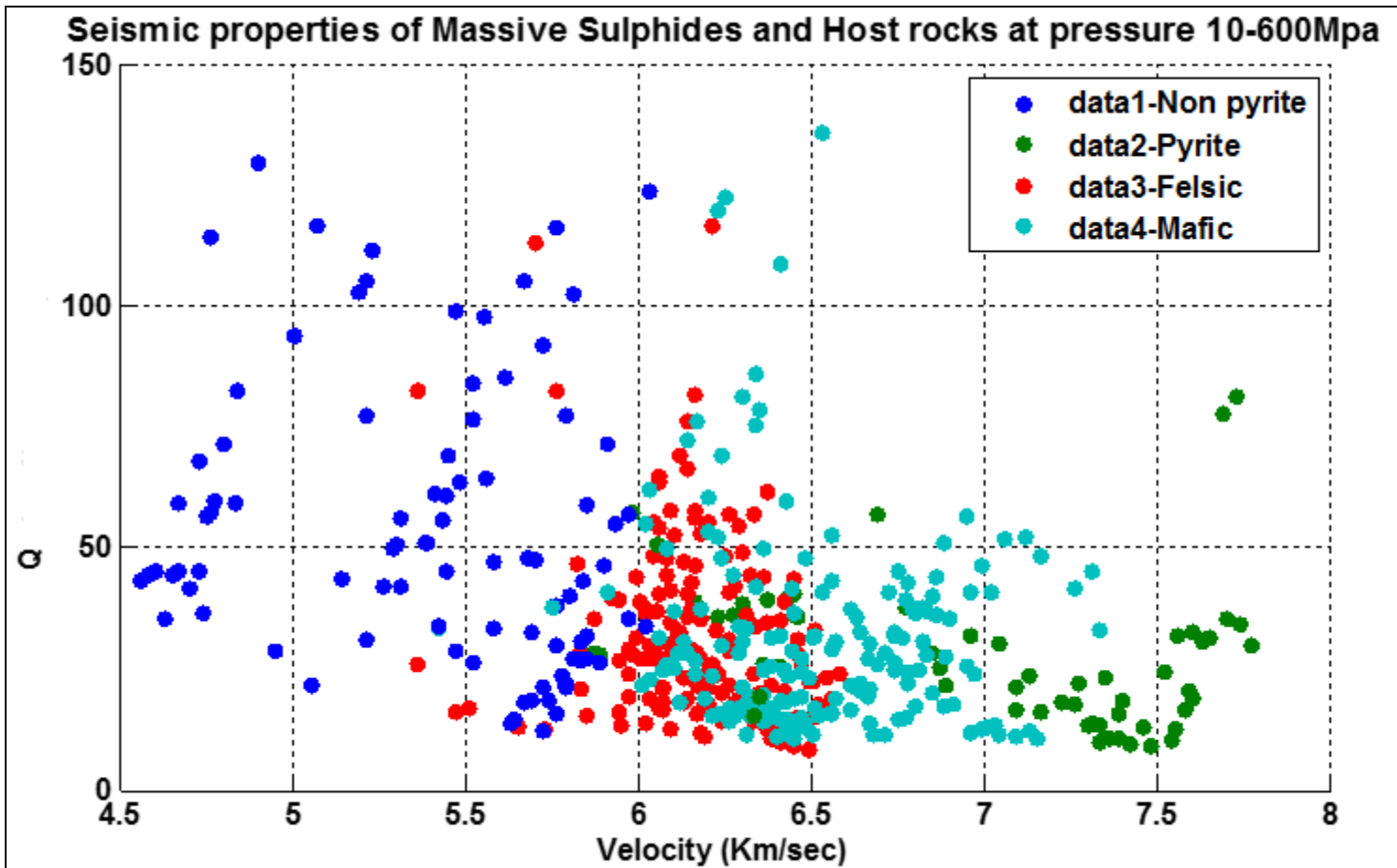


Figure 4.7-1 Q Vs Velocity for Massive Sulphides (Pyrite and Non pyrite) and Host rocks (Felsic and mafic) at pressures ranging from 10-600Mpa

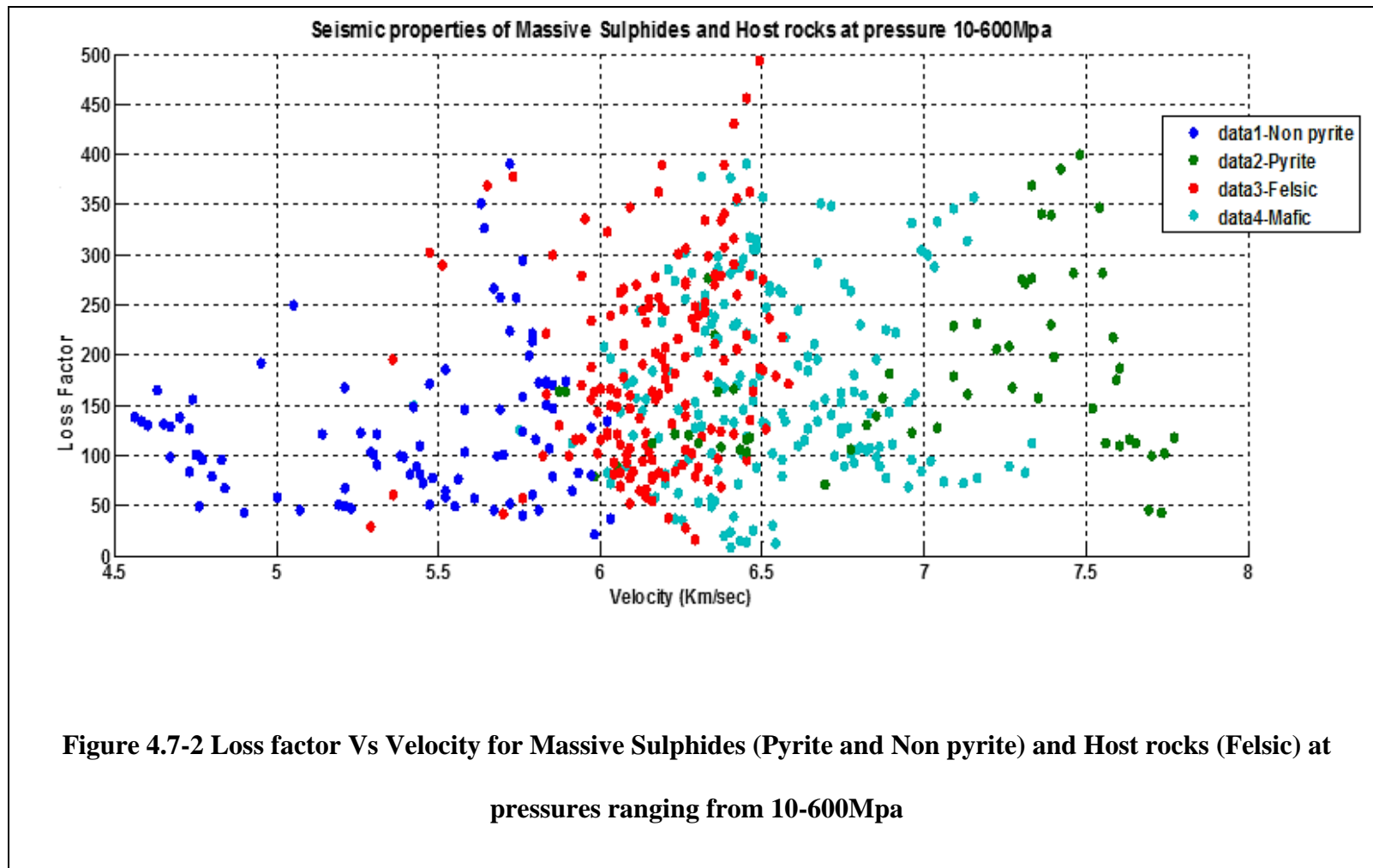
The outcomes express that seismic parameter Q can identify massive sulphide from their associated hosts and also separate high and low pyrite. The figure demonstrates the following points,

- Velocity separates high and low pyrite sulphides very well from each other and also from the host rocks (felsic and mafic). The range of velocity for high pyrites is the highest around 7-7.8 km/sec and for the low pyrites, velocities are around 4.5-6 km/sec. Felsic and mafic have shared range of velocity (around 6-7 km/sec). The ranges of velocity clearly depict that massive sulphide is distinguishable from the host rocks.
- In terms of Q factor, low pyrite has broad range of Q values (around 25-125), Q is low for the high pyrites (10-35) and felsic and mafic have shared their Q value, ranging from 10 to 60.
- Visual observation shows that Q for low pyrite sulphides spreads to a wide region (This is also demonstrated in the greater pressure dependence of Q for the low sulphides in the Q Vs Pressure graph) while Q is not extensive for high pyrite sulphides. Felsic and mafic is hard to separate from each other as they have shared their Q range. Previously it was observed from Q Vs. Pressure plots that high and low pyrite have distinct Q and low pyrites have much higher Q values than the host rocks. Q-factor in pyrite rich sulphides are typically much lower than low pyrites. Host rocks and pyrite rich sulphides might be difficult to distinguish depending on Q factor only.

- Joint interpretation of velocity and Q can provide better resolution for differentiating massive sulphide and the hosts.
- **Figure 4.7-1** provides four zones (low pyrite, high pyrite, felsic and mafic). Felsic and mafic rocks share the zones but that is completely understandable due to presence of some intermediate rocks.

#### 4.7.2 *Velocity and Loss factor*

Loss factor is plotted against velocity for massive sulphides and the host rocks in **Figure 4.7-2**.



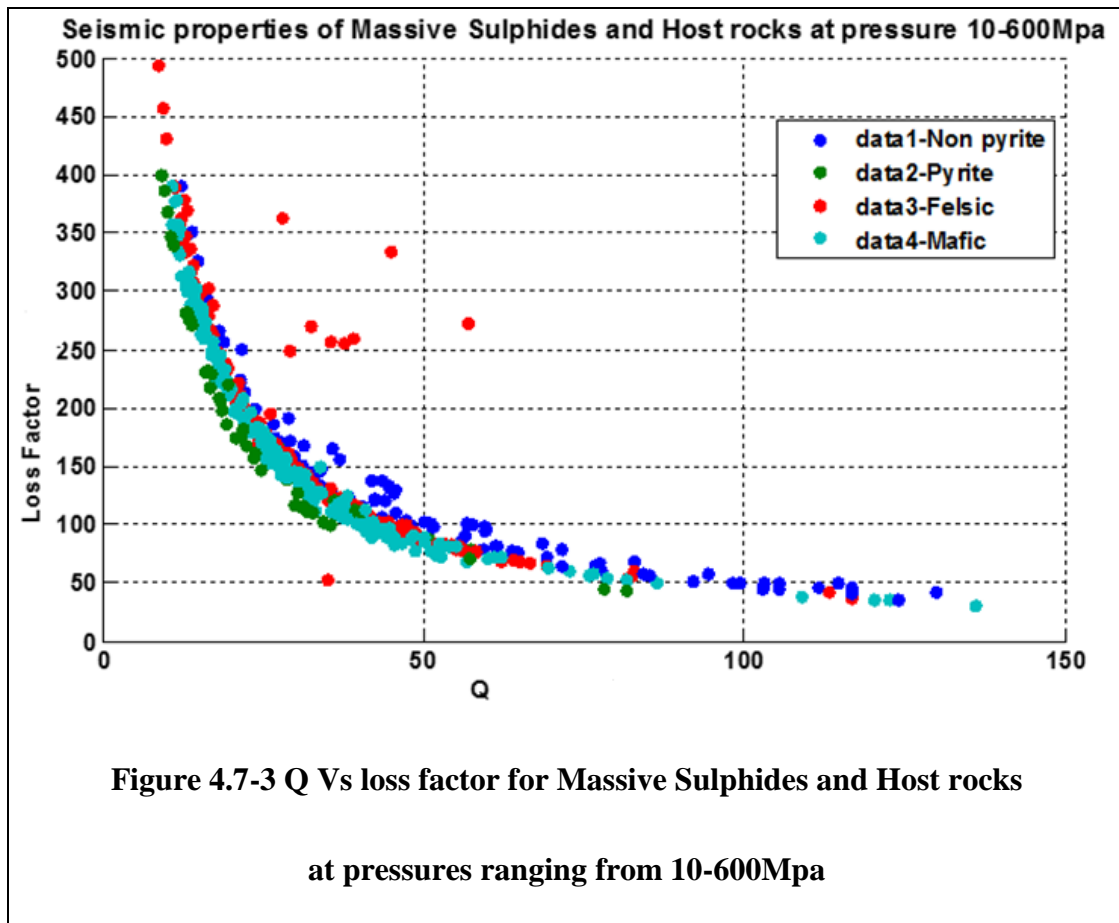
Again this might aid in understanding ore and the host prior to seismic exploration. Majority of the low pyrite data have lower loss compared to high pyrite. The ranges of velocity are described previously for Q vs. Velocity plot.

In a general view there are 3 zones observed both in **Figure 4.7-1** and **4.7-2**

- Dark Blue Non pyrite zone: with low velocity, high Q , low loss and,
- Green Pyrite zone: with high velocity, low Q, high loss and
- Red felsic and Light Blue mafic zone in between sulphides: which has same range of Q and loss but separated by velocity.

#### 4.7.3 *Loss factor and Q*

Loss factors are plotted against Q in **Figure 4.7-3**.

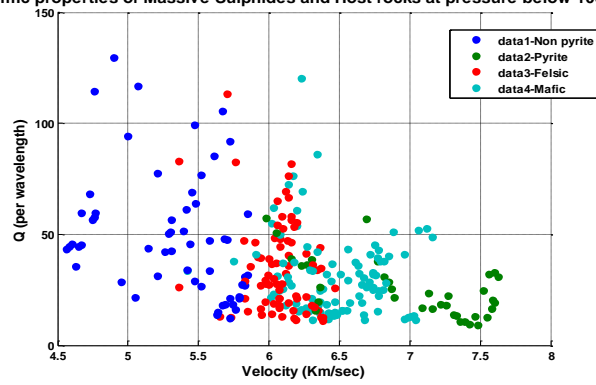


This shows an inverse relationship between the loss factor and Q. Measurement of Q requires consideration of many parameters and also due to Q being a very sensitive parameter, it is difficult to measure. On the other hand loss factor can be measured easily. The relationship between loss and Q might be employed in measuring Q from loss factor.

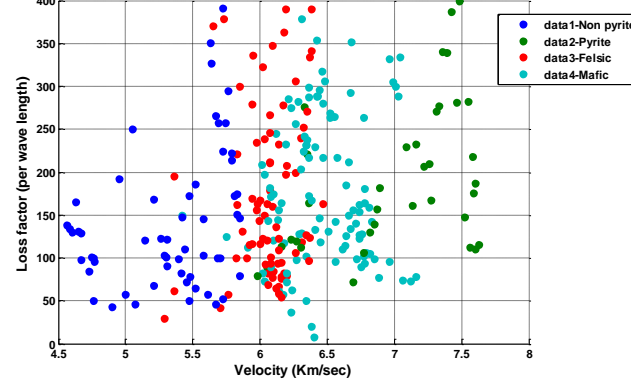
#### 4.7.4 *Low and high pressure response*

Previous [sections \(4.7.1-4.7.3\)](#) considered pressure range of 10-600 Mpa. These plots are further plotted for two different range of pressure [(0-100MPa) and (100-600Mpa)] to observe the relationship of the parameters and the rock types at low and high pressures separately (**Figure 4.7-4** and **4.7-5**) represent the plots for low and high pressure respectively.

Seismic properties of Massive Sulphides and Host rocks at pressure below 100 Mpa



Seismic properties of Massive Sulphides and Host rocks at pressure below 100 Mpa



Seismic properties of Massive Sulphides and Host rocks at pressure below 100 Mpa

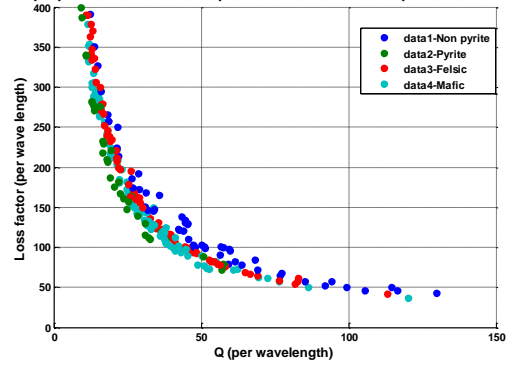
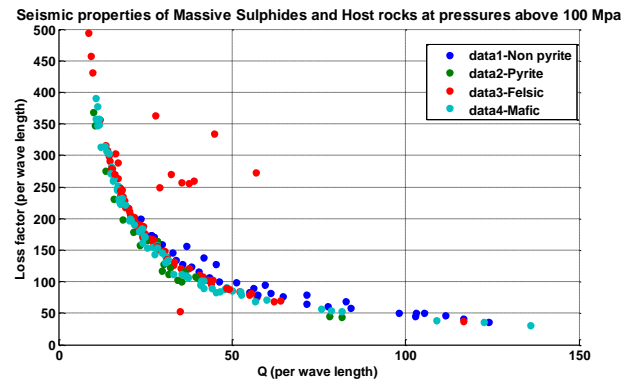
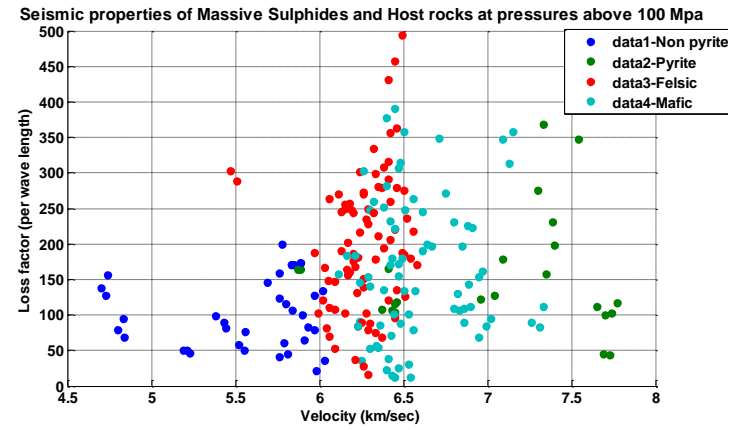
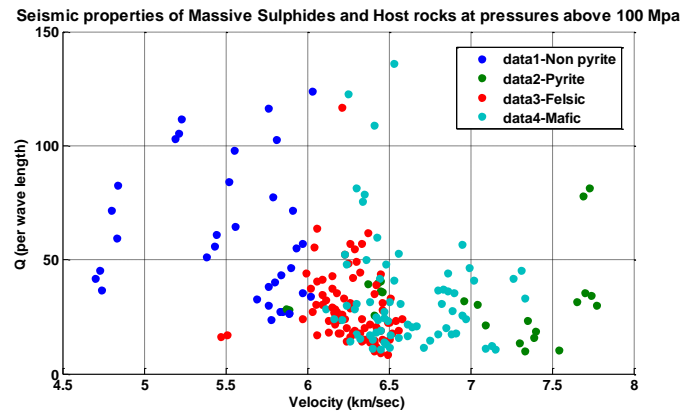


Figure 4.7-4 Q Vs Velocity (Top left), Loss Vs Velocity (Top right) and Loss Vs Q

(Bottom)for Massive Sulphides (Pyrite and Non pyrite) and Host rocks (Felsic and mafic) at pressures ranging from 10-100Mpa



**Figure 4.7-5** Vs Velocity (Top left), Loss Vs Velocity (Top right) and Loss Vs Q (Bottom)for Massive Sulphides (Pyrite and Non pyrite) and Host rocks (Felsic and mafic) at pressures ranging from 100-600 Mpa

These plots [(Q vs. Velocity), (Loss factor vs. Velocity), and (Loss factor vs. Q)] do not show difference for high and low pressure. Due to greater data points, low pressure plots shows large spread. As high and low pressure results have similar response, the standard considered for high pressure data analysis might be assumed same for the low pressure analysis. If the analytic values (velocity, Q and loss factor) of rock samples (unknown) collected from the shallow depths matches with the characteristics value of a particular rock group (known) at high pressure analysis, then it can be implied that the collected sample rock (unknown) follows the same rock group (known) of high pressure analysis.

# Chapter 5

## Conclusion

Due to the high demand for minerals, detection and delineation of massive sulphide ore deposits are of great interest. High resolution seismic techniques (particularly tomography) are currently being used for imaging massive sulphide. Velocity and density have been extensively studied for massive sulphides to characterize the acoustic impedance. Velocity and density do not always uniquely characterize massive sulphides. The discrimination of massive sulphides and the host rock with identical or common velocity will be unclear. Therefore in addition to velocity and density analysis, seismic attenuation may be considered for the better delineation of the ore. The literature survey indicates that seismic attenuation has not been considered so far for massive sulphide characterization. The aim of this research is to assess seismic attenuation and loss factor to provide information on ore and the host that will help to identify massive sulphide deposits. Velocity, attenuation and loss factors were analyzed for massive pyrite rich and pyrite poor sulphides and the host rocks. In the previous chapter, their sensitivity with pressure was observed along with the relation among the parameters. This chapter will briefly mention the findings from the analysis and discuss some recommendations for future work.

## 5.1 Findings from the analysis:

The response of velocity with pressure shows clear trends. Velocities of massive sulphides and the host rocks have a positive correlation with pressure. Massive pyrite rich and pyrite low sulphides have the highest and lowest range of velocities respectively. Velocities of the host rocks (felsic and mafic) falls in between the high and low pyrite sulphides (please note that ultramafic rocks have not been considered here which have velocities as high as pyrite rich sulphides). The velocity gradient for both the ore and hosts is higher at low pressure (below 100 Mpa) and becomes almost linear with increase in pressure possibly due to the closure of micro cracks and grain boundaries.

The picture of  $Q$  is much more complicated than velocity. The changes in  $Q$  with pressure for the sulphides is more sensitive than that of velocity. Among the sulphides seismic attenuation is higher (lower  $Q$ ) in pyrite and chalcopyrite rich sulphides compared to pyrrhotite and sphalerite. Pyrite rich sulphides have the highest velocity and the lowest  $Q$  range. Individual sulphides also show this inverse relation of velocity and  $Q$  in terms of their range. Generally  $Q$  has increasing trends (decreasing attenuation) with pressure for sulphides except some anomalous results at low pressure. Sulphides with high pyrite content have increasing attenuation with pressure up to 60 Mpa. This unusual behaviour of high pyrite sulphides might be related with differential crack closure or presence of perpendicular cracks in the direction of the wave propagation which might be difficult to characterize. After observing the individual sulphides, they are grouped in to

two major groups: low and high pyrite sulphides. Attenuation with pressure for pyrite rich sulphides and the host rocks shows moderate change.. Low pyrite sulphides show increasing Q with pressure and change is much noticeable. Pyrite- rich sulphides and the host have overlapping Q. Much more scatter is observed in the Q plots for both the ore and the hosts compared to their velocity plots.

Loss factor has decreasing trends with pressure. Over 200 Mpa, the change in loss factor becomes linear. As the pores and cracks starts to close with pressure increase, the loss factor decreases. The changes of attenuation ( $1/Q$ ) is much more complicated than that of loss factor. Attenuation ( $1/Q$ ) does not show clear decrease with pressure like loss factor for high pyrite and host rocks. However, low pyrite shows decrease in attenuation with pressure. The important conclusion from these observations is that Q measurement has more scatter compared to that of loss factor. The loss of energy of seismic waves is higher in host rocks compared to the sulphides. Felsic and mafic have almost similar range of loss.

The response of the above mentioned three parameters in both high and low pressure is observed carefully. High pressure results have better trends. On the other hand due to the presence of micro cracks and pores the low pressure results (Q and loss factor) show unclear trends. From the analysis of Q-plots it might be that frictional dissipation dominates at the low pressure and may reach very low value at higher pressure. On the other hand intrinsic anelasticity may dominate in the high pressure region. Close

observation of low pressure results depict anomalous behaviour of low pyrite sulphides with respect to Q and loss factor. As mentioned in the previous chapter, 100 Mpa might be the crack closure pressure in the current case. Therefore, greater changes are observed below that pressure.

The relationship among the parameters might be aid in understanding the host and the ore prior to seismic exploration. The joint interpretation of (velocity and Q) or (velocity and loss factor) provides four zones: low and high pyrite sulphides are on two ends and felsic and mafic hosts are in the middle zone. Velocity separated low and high pyrite massive sulphides as they have the lowest and the highest range respectively. Felsic and mafic hosts are also separable in velocity range from each other and from the sulphides. Q separates low and high pyrite. Low pyrite has broad range of Q while high pyrite has very narrow range. This separates them well from each other. Felsic and mafic has overlapping Q range with each other and also with high pyrite and hard to distinguish from sulphides based on Q only. Q might provide higher resolution along with velocity. The correlation among the velocity, Q and the rock-type is the base knowledge that is required before attempting multi-parameter tomography (or joint inversion of velocity and attenuation). This works set the basis for the next step (tomography).

Loss factor and Q have an exponential decay relationship. Loss is inversely proportional to Q. Therefore joint interpretation of loss factor and velocity provides opposite picture from that of the Q and velocity. This relationship among the loss factor and Q can

provide measurement advantage.  $Q$  can be measured from the loss factor which is easy to measure and does not require consideration of many parameters as in the case of  $Q$  measurement. These joint interpretations show similar response in both the high (>100 Mpa) and low (<100Mpa) pressures.

## 5.2 Future recommendations

Following are some future recommendations:

- Current research considers dry samples only. Attenuation can be measured for the saturated rocks to better represent in situ conditions.
- Attenuation for the compressional wave was measured in this research. Measurement of shear wave velocity, attenuation and loss factor along with the compressional wave can be carried out to observe the ratio of  $V_p/V_s$  and  $Q_p/Q_s$ .

This experiment was conducted at ultrasonic frequencies, extrapolation of this data to seismic frequencies will provide broad spectrum.

## Bibliography

Al-Sinawi, S. A. (1968). *An Investigation of Body Wave Velocities, Attenuation and Elastic Parameters of Rocks Subjected to Pressure at Room Temperature* (Doctoral dissertation, Saint Louis University).

Birch, F., and Bancroft, D., 1938, Elasticity and internal friction in a long column of granite: *Bull. SSA*, (28), 243-254.

Birch, F., 1960, The Velocity of Compressional Waves in Rocks to 10 Kilobars, Part 1: *Journal of Geophysical Research*, 65 (4), 1083-1095.

Butt, S. D., Mukherjee, C., & Lebars, G. (2000). Evaluation of acoustic attenuation as an indicator of roof stability in advancing headings. *International Journal of Rock Mechanics and Mining Sciences*, 37(7), 1123-1131.

Butt, S. D. (2001). Experimental measurement of P-wave attenuation due to fractures over the 100 to 300 kHz bandwidth. *pure and applied geophysics*, 158(9-10), 1783-1796.

Carcione, J. M., Helbig, K., & Helle, H. B. (2003). Effects of pressure and saturating fluid on wave velocity and attenuation in anisotropic rocks. *International Journal of Rock Mechanics and Mining Sciences*, 40(3), 389-403.

Christensen, N. I. (1985). Measurements of dynamic properties of rock at elevated temperatures and pressures. *ASTM STP*, 869, 93-107.

Collins, F., & Lee, C. C. (1956). Seismic wave attenuation characteristics from pulse experiments. *Geophysics*, 21(1), 16-40.

Demerling, C., (2004). An investigation of finite-difference seismic modelling applied to massive sulphide exploration, Memorial University of Newfoundland.

Donald, A., Butt, S. D., Iakevlov, S., 2004. Adaptation of triaxial cell for ultrasonic P-wave attenuation, velocity and acoustic emissions measurements. *Int. J. Rock Mech. Min. Sci.* 41 (6), 1001-1011.

Duff, D., Hurich, C., & Deemer, S. (2012). Seismic properties of the Voisey's Bay massive sulfide deposit: Insights into approaches to seismic imaging. *Geophysics*, 77(5), WC59-WC68.

Duffy, T. S., & Anderson, D. L. (1989). Seismic velocities in mantle minerals and the mineralogy of the upper mantle. *Journal of Geophysical Research: Solid Earth (1978–2012)*, *94*(B2), 1895-1912.

Eaton, D., Milkereit, B., and Adam, E., 1997, 3-D seismic exploration, in Gubins, A., Ed., Proc. Exploration 97: 4<sup>th</sup> Dec. Internat. Conf. on Mineral Expl., 65–78.

Eaton, D., Milkereit, B., and Salisbury, M., 2003a, Hardrock Seismic Exploration: Mature Technologies Adapted to New Exploration Targets, Society of Exploration Geophysicists, Geophysical Developments No. 10, pp. 1-6.

Frempong, P., Butt, S., and Donald, A., 2005, Frequency Dependent Spectral Ratio Technique for Q Estimation: Rainbow in the Earth-2nd International Workshop, Lawrence Berkeley laboratory, Berkeley, California.

Gardner, G. H. F., Wyllie, M. R. J., & Droschak, D. (1964). Effects of pressure and fluid saturation on the attenuation of elastic waves in sands. *Journal of Petroleum Technology*, *16*(02), 189-198.

Gardner, R. H., O'Neill, R. V., Mankin, J. B., and Carney, J. H., 1981, "A comparison of sensitivity analysis and error analysis based on a stream ecosystem model," *Ecol. Modell.*, *12*, 173-190.

Gingerich, J. C., Mathews, I.W., Peshko, M. J., 2000. The Development of new exploration technologies at Noranda: Seeing More with hyperspectral and Deeper with 3-D seismic. Prospectors and Developers Association of Canada international Convention, March 5-10. 2000, Toronto.

Gordon, R. B., & Davis, L. A. (1968). Velocity and attenuation of seismic waves in imperfectly elastic rock. *Journal of Geophysical Research*, 73(12), 3917-3935.

Greenhalgh, S. A., Mason, I. M., 1997. Seismic imaging with application to mine layout and development. In: Gubins, A. G. (Ed.), *Geophysics and Geochemistry at the Millennium: Proc. Exploraion 97*. GEOFX Publishers, Toronto, Canada, pp. 585-598.

Harvey, C. W. (1998). Shear wave velocities of sulphide-bearing assemblages as determined from high-pressure laboratory measurements. Dalhousie University.

Holliger, K., & Bührenmann, J. (1996). Attenuation of broad-band (50–1500 Hz) seismic waves in granitic rocks near the Earth's surface. *Geophysical research letters*, 23(15), 1981-1984.

Johnston, D. H., Toksöz, M. N., & Timur, A. (1979). Attenuation of seismic waves in dry and saturated rocks: II. Mechanisms. *Geophysics*, 44(4), 691-711.

Johnston, D. H., and Toksöz, M. N., 1980, Ultrasonic P and S wave Attenuation in Dry and Saturated Rocks under Pressure: *Journal of Geophysical Research*, vol. 85, no. B2, pp. 925-936.

Kaneko, K., Inoue, I., Sassa, K., & Ito, I. (1979, January). Monitoring the stability of rock structures by means of acoustic wave attenuation. In *4th ISRM Congress*. International Society for Rock Mechanics.

Khondakar, L. Y., Butt, S. D., & Hurich, C. A. (2010, January). Investigation of P-wave attenuation of massive sulfide and host rocks. In *2010 SEG Annual Meeting*. Society of Exploration Geophysicists.

Klíma, K., Vaněk, J., & Pros, Z. (1964). The attenuation of longitudinal waves in diabase and greywacke under pressures up to 4 kilobars. *Studia Geophysica et Geodaetica*, 8(3), 247-254.

Levykin, A. I. (1965). Longitudinal and transverse wave absorption and velocity in rock specimens at multilateral pressures up to 4000 kg/cm<sup>2</sup>. *USSR Geophys Ser Engl Transl Phys Solid Earth*, 1, 94-98.

Malehmir, A., Andersson, M., Lebedev, M., Urosevic, M., & Mikhaltsevitch, V. (2013). Experimental estimation of velocities and anisotropy of a series of Swedish crystalline rocks and ores. *Geophysical Prospecting*, *61*(1), 153-167.

Meglis, I. L., Greenfield, R. J., Engelder, T., & Graham, E. K. (1996). Pressure dependence of velocity and attenuation and its relationship to crack closure in crystalline rocks. *Journal of Geophysical Research: Solid Earth (1978–2012)*, *101*(B8), 17523-17533.

Milkereit, B., Eaton, D., Wu, J., Perron, G., Salisbury, M., Berrer, E., and Morrison, G., 1996, Seismic imaging of massive sulfide deposits: Part II. Reflection seismic profiling: *Econ. Geol.*, *91*, 829– 834.

Milkereit, B., & Eaton, D. (1998). Imaging and interpreting the shallow crystalline crust. *Tectonophysics*, *286*(1), 5-18.

Molina, J. P., & Wack, B. (1982). Crack field characterization by ultrasonic attenuation—preliminary study on rocks. In *International Journal of Rock Mechanics and Mining Sciences & Geomechanics Abstracts* (Vol. 19, No. 6, pp. 267-278). Pergamon.

Pyrak-Nolte, L. J., Myer, L. R., & Cook, N. G. (1990). Transmission of seismic waves across single natural fractures. *Journal of Geophysical Research: Solid Earth (1978–2012)*, *95*(B6), 8617-8638.

Rybach, L., & Buntebarth, G. (1982). Relationships between the petrophysical properties density, seismic velocity, heat generation, and mineralogical constitution. *Earth and Planetary Science Letters*, *57*(2), 367-376.

Salisbury, M. H., Milkereit, B., and Bleeker, W., 1996, Seismic imaging of massive sulfide deposits: Part I. Rock properties: *Econ. Geol.*, *91*, 821–828.

Salisbury, M. H., Milkereit, B., Ascough, G., Adair, R., Matthews, L., Schmitt, D. R., & Wu, J. (2000). Physical properties and seismic imaging of massive sulfides. *Geophysics*, *65*(6), 1882-1889.

Salisbury, M., and Snyder, D., 2007, Applications of seismic methods to mineral exploration, in Goodfellow, W.D., ed., *Mineral deposits of Canada—A synthesis of major deposit- types, district metallogeny, the evolution of geological provinces, and exploration methods*: Geological Association of Canada, Mineral Deposits Division, Special Publication 5, p. 971–982.

Sarma, L. P., & Ravikumar, N. (2000). Q-factor by spectral ratio technique for strata evaluations. *Engineering geology*, *57*(1), 123-132.

Stainsby, S. D., & Worthington, M. H. (1985). Q estimation from vertical seismic profile data and anomalous variations in the central North Sea. *Geophysics*, 50(4), 615-626.

Telford, W. M., Geldart, L. P., Sheriff, R. E., 1995, *Applied Geophysics*, 2<sup>nd</sup> ed. U.S.A., Cambridge University Press.

Tonn, R., 1989. Comparison of seven methods for the computation of 'Q'. *Phys. Earth. Planet. Inter.* 55, 259-268.

Toksöz, M. N., Johnston, D. H., & Timur, A. (1979). Attenuation of seismic waves in dry and saturated rocks: I. Laboratory measurements. *Geophysics*, 44(4), 681-690.

Vanorio, T., Virieux, J., Capuano, P., & Russo, G. (2005). Three-dimensional seismic tomography from P wave and S wave microearthquake travel times and rock physics characterization of the Campi Flegrei Caldera. *Journal of Geophysical Research: Solid Earth (1978–2012)*, 110(B3).

Walsh, J. B., Brace, W. F., and Wawersik, W. R., 1970, Attenuation of stress waves in Ceder City quartz diorite: Air Force Weapons Lab. Tech. rep. AFWL-TR-70-8.

Winkler, K. W., and Plona, T. J., 1982, Technique for Measuring Ultrasonic Velocity and Attenuation Spectra in Rocks under Pressure: *Journal of Geophysical Research*, 87 (B13), 776-780.

## **Appendix A (Rock Properties)**

A-1 Grade A: physical properties of silicates

Rock name	Sample Id	Suite Location	Weight (gm)	Length (mm)	Diameter (mm)	Volume (mm <sup>3</sup> )	Density (g/cc)
Granophyre	10117	Sudbury Samples (second suite)	63.56	45.35	22.55	22.40	2.83
Tuff	10130	Sudbury Samples (second suite)	53.75	49.55	22.69	19.92	2.69
Granophyre	10142	Sudbury Samples (second suite)	57.90	46.60	22.75	21.59	2.68
Tuff	10190	Sudbury Samples (second suite)	62.06	45.38	22.75	22.03	2.81
Granophyre	10193	Sudbury Samples (second suite)	58.19	48.03	22.75	21.56	2.69
Granophyre	10195	Sudbury Samples (second suite)	60.08	48.58	22.74	22.16	2.71
Tuff	10196	Sudbury Samples (second suite)	63.43	47.82	22.75	22.47	2.82
Felsic norite	52845	Sudbury Samples (second suite)	68.44	48.52	25.08	23.88	2.86
Diorite	603841	Noranda-Louvicort	55.96	39.93	25.34	20.16	2.78
Andesite	604961	Noranda, Quebec	60.22	43.01	25.35	21.71	2.77
Andesite	604966	Noranda, Quebec	59.31	41.78	25.33	21.01	2.82
Andesite	604967	Noranda, Quebec	59.26	41.77	25.36	21.14	2.80
Tuff	52847-4	Sudbury Samples (second suite)	67.59	50.52	24.94	24.71	2.73
Gneiss	60064-10	Sudbury Samples (second suite)	65.49	48.97	24.89	23.77	2.75
Diabase	60064-11	Sudbury Samples (second suite)	63.69	42.06	24.89	20.40	3.12
Norite	60064-4	Sudbury Samples (second suite)	69.78	50.15	24.88	24.29	2.87
Breccia	60064-5	Sudbury Samples (second suite)	66.26	48.13	24.89	23.34	2.83
Breccia	60064-6	Sudbury Samples (second suite)	72.58	50.60	24.89	24.51	2.96
Gneiss	60064-7	Sudbury Samples (second suite)	72.80	48.72	24.89	23.75	3.06
Granophyre	60066-2	Sudbury Samples (second suite)	59.85	44.87	24.89	21.64	2.76
Felsic norite	60066-6	Sudbury Samples (second suite)	53.01	39.73	24.62	18.84	2.81
Rhyodacite	604959xy	Noranda, Quebec	54.66	39.40	25.34	19.92	2.74
Rhyodacite	604959z	Noranda, Quebec	53.53	38.76	25.35	19.53	2.74

A-1 Grade A: physical properties of silicates (continued)

Rock name	Sample Id	Suite Location	Weight (g)	Length (mm)	Diameter (mm)	Volume (mm <sup>3</sup> )	Density (g/cc)
Rhyodacite	604960xy	Noranda, Quebec	53.65	38.95	25.35	19.72	2.72
Rhyodacite	604963xy	Noranda, Quebec	54.88	39.53	25.34	19.90	2.76
Norite	85597-14	Inco-Sudbury Basin	57.30	38.54	24.07	18.42	3.11
Norite	85597-15	Inco-Sudbury Basin	60.42	40.42	24.67	19.33	3.12
Hornblend	BNB96-062	Yelloknife, Bucket#1	57.53	39.07	25.28	19.65	2.93
Metatonalite	BNB97-018	Kapuskasing, Ont	52.06	38.40	25.32	19.67	2.70
Anorthosite	KAP88-3A	Kapuskasing, Ont	53.22	40.23	24.66	Missing	Missing
Anorthosite	KAP88-3B	Kapuskasing, Ont	56.49	42.58	24.66	20.48	2.76
Anorthosite	L6z	Ecsot'96 Labrador	58.42	46.60	25.33	20.85	2.80

A-2 Grade A: velocities (km/sec) of silicates at pressures 10-600 MPa

Rock name	Sample Id	Suite Location	10 Mpa	20 Mpa	40 Mpa	60 Mpa	80 Mpa	100 Mpa	200 Mpa	400 Mpa	600 Mpa
Granophyre	10117	Sudbury Samples (second suite)	6.09	6.21	6.26	6.29	6.31	6.32	c	6.42	6.46
Tuff	10130	Sudbury Samples (second suite)	5.74	5.86	5.97	6.01	6.03	6.05	6.09	6.15	6.18
Granophyre	10142	Sudbury Samples (second suite)	5.92	6.05	6.11	6.14	6.17	6.19	6.26	6.32	6.37
Tuff	10190	Sudbury Samples (second suite)	5.83	5.94	5.99	6.00	6.02	6.03	6.06	6.11	6.15
Granophyre	10193	Sudbury Samples (second suite)	5.63	5.76	5.86	5.90	5.91	5.93	5.97	6.03	6.06
Granophyre	10195	Sudbury Samples (second suite)	C	5.83	5.97	6.03	6.07	6.09	6.13	6.19	6.23
Tuff	10196	Sudbury Samples (second suite)	6.18	6.19	6.22	6.23	6.24	6.25	c	6.32	6.35
Felsic norite	52845	Sudbury Samples (second suite)	6.12	6.34	6.47	6.52	6.55	6.57	6.61	6.64	6.67
Diorite	603841	Noranda-Louvicort	Missing	c	c	c	c	c	c	6.23	6.25
Andesite	604961	Noranda, Quebec6.03	c	c	c	c	c	c	c	6.40	6.41
Andesite	604966	Noranda, Quebec	6.03	6.06	6.10	6.13	6.16	6.18	6.24	6.29	6.30
Andesite	604967	Noranda, Quebec	Missing	6.20	6.24	6.27	6.29	6.31	6.38	6.44	6.48
Tuff	52847-4	Sudbury Samples (second suite)	6.14	6.26	6.31	6.34	6.36	6.37	6.41	6.46	6.51
Gneiss	60064-10	Sudbury Samples (second suite)	5.94	6.07	6.14	6.17	6.18	6.19	6.24	6.26	6.29
Diabase	60064-11	Sudbury Samples (second suite)	C	6.34	6.51	6.67	6.74	6.78	6.85	6.88	6.91

A-2 Grade A: velocities (km/sec) of silicates at pressures 10-600 MPa (continued)

Rock name	Sample Id	Suite Location	10 Mpa	20 Mpa	40 Mpa	60 Mpa	80 Mpa	100 Mpa	200 Mpa	400 Mpa	600 Mpa
Norite	60064-4	Sudbury Samples (second suite)	c	6.33	6.38	6.41	6.44	6.45	6.50	6.53	6.57
Breccia	60064-5	Sudbury Samples (second suite)	c	6.36	6.41	6.42	6.43	6.44	6.47	6.50	6.54
Breccia	60064-6	Sudbury Samples (second suite)	6.56	6.63	6.72	6.75	6.77	6.78	6.82	6.86	6.90
Gneiss	60064-7	Sudbury Samples (second suite)	c	6.52	6.64	6.71	6.74	6.76	6.80	6.83	6.86
Granophyre	60066-2	Sudbury Samples (second suite)	6.14	6.20	6.30	6.35	6.37	6.38	6.41	6.46	6.50
Felsic norite	60066-6	Sudbury Samples (second suite)	c	6.31	6.42	6.46	6.47	6.48	6.51	6.56	6.61
Rhyodacite	604959xy	Noranda, Quebec	6.04	6.06	6.09	6.12	6.14	6.16	6.21	6.26	6.29
Rhyodacite	604959z	Noranda, Quebec	c	5.83	5.87	5.90	5.92	5.94	5.99	6.04	6.09
Rhyodacite	604960xy	Noranda, Quebec	Missing	6.05	6.08	6.10	6.13	6.16	6.25	6.30	6.33
Rhyodacite	604963xy	Noranda, Quebec	5.99	6.00	6.03	6.05	6.07	6.09	6.17	6.23	6.26
Norite	85597-14	Inco-Sudbury Basin	6.69	6.74	6.79	6.82	6.85	6.88	6.95	6.99	7.02
Norite	85597-15	Inco-Sudbury Basin	6.77	6.96	6.99	7.01	7.03	7.04	7.09	7.13	7.15
Hornblend	BNB96-062	Yelloknife, Bucket#1	missing	c	6.26	6.30	6.34	6.36	6.42	6.47	6.49
Anorthosite	KAP88-3A	Kapuskasing, Ont	c	6.66	6.74	6.78	6.81	6.83	6.89	6.95	6.97
Anorthosite	KAP88-3B	Kapuskasing, Ont	c	6.61	6.96	7.06	7.12	7.16	7.26	7.31	7.33
Anorthosite	L6z	Ecsoot'96 Labrador	Missing	5.42	5.75	5.91	6.02	6.08	6.24	6.36	6.43
Average			6.11	6.21	6.30	6.34	6.37	6.39	6.47	6.48	6.51

A-3 Grade A: Q for silicates at pressures 10-600 MPa

Rock name	Sample Id	Suite Location	10 Mpa	20 Mpa	40 Mpa	60 Mpa	80 Mpa	100 Mpa	200 Mpa	400 Mpa	600 Mpa
Granophyre	10117	Sudbury Samples (second suite)	missing	missing	missing	missing	missing	missing	c	38.98	27.96
Tuff	10130	Sudbury Samples (second suite)	missing	missing	missing	missing	missing	missing	34.89	29.19	35.46
Granophyre	10142	Sudbury Samples (second suite)	missing	missing	missing	missing	missing	missing	56.97	44.75	missing
Tuff	10190	Sudbury Samples (second suite)	missing	missing	missing	missing	missing	missing	63.88	32.33	37.56
Granophyre	10193	Sudbury Samples (second suite)	missing	missing	missing	missing	missing	missing	24.27	27.14	17.10
Granophyre	10195	Sudbury Samples (second suite)	c	21.11	19.50	18.91	16.85	12.88	18.18	17.80	24.08
Tuff	10196	Sudbury Samples (second suite)	missing	missing	missing	missing	missing	missing	c	17.70	20.29
Felsic norite	52845	Sudbury Samples (second suite)	18.21	18.60	19.45	15.85	15.73	19.1	21.74	20.64	20.84

A-3 Grade A: Q for silicates at pressures 10-600 MPa (continued)

Rock name	Sample Id	Suite Location	10 Mpa	20 Mpa	40 Mpa	60 Mpa	80 Mpa	100 Mpa	200 Mpa	400 Mpa	600 Mpa
Diorite	603841	Noranda-Louvicort	missing	c	c	c	c	c	c	52.28	122.54
Andesite	604961	Noranda, Quebec6.03	c	c	c	c	c	c	c	181.66	108.94
Andesite	604966	Noranda, Quebec	22.98	31.46	25.48	30.84	26.98	37.54	29.90	28.29	30.68
Andesite	604967	Noranda, Quebec	missing	60.78	69.46	44.67	34.02	33.57	31.55	41.79	47.95
Tuff	52847-4	Sudbury Samples (second suite)	40.49	41.21	36.46	34.02	44.15	34.66	35.11	31.23	33.03
Gneiss	60064-10	Sudbury Samples (second suite)	16.45	18.26	19.10	15.88	12.17	11.30	14.50	16.10	19.02
Diabase	60064-11	Sudbury Samples (second suite)	C	42.13	32	30.55	24.96	24.55	20.26	17.55	17.70
Norite	60064-4	Sudbury Samples (second suite)	C	17.81	25.54	32.03	28.99	36.65	31.43	40.99	30.87
Breccia	60064-5	Sudbury Samples (second suite)	c	24.84	18.52	14.75	14.69	14.32	13.75	11.71	325.09
Breccia	60064-6	Sudbury Samples (second suite)	29.26	35.94	40.93	45.23	39.51	42.97	3069	36.51	35.48

A-3 Grade A: Q for silicates at pressures 10-600 MPa (continued)

Rock name	Sample Id	Suite Location	10 Mpa	20 Mpa	40 Mpa	60 Mpa	80 Mpa	100 Mpa	200 Mpa	400 Mpa	600 Mpa
Gneiss	60064-7	Sudbury Samples (second suite)	c	15.57	22.23	28.60	32.00	31.55	36.91	37.27	44.27
Granophyre	60066-2	Sudbury Samples (second suite)	36.08	21.23	18.02	15.88	12.81	12.53	13.45	15.11	15.25
Felsic norite	60066-6	Sudbury Samples (second suite)	c	11.43	11.99	13.30	15.03	13.74	16.96	15.80	16.83
Rhyodacite	604959xy	Noranda, Quebec	48.55	64.94	57.97	69.18	76.34	81.74	116.72	154.32	265.02
Rhyodacite	604959z	Noranda, Quebec	c	28.92	35.47	46.48	39.72	39.32	44.32	55.51	41.61
Rhyodacite	604960xy	Noranda, Quebec	missing	37.25	44.58	52.75	47.39	46.47	48.49	49.15	57.18
Rhyodacite	604963xy	Noranda, Quebec	31.76	38.99	30.14	27.71	25.21	27.91	28.35	52.27	31.23
Norite	85597-14	Inco-Sudbury Basin	26.12	32.92	37.98	38.02	40.41	51.07	56.75	46.48	40.87
Norite	85597-15	Inco-Sudbury Basin	15.28	11.81	12.80	12.98	13.43	11.61	11.09	12.20	10.67
Hornblend	BNB96-062	Yelloknife, Bucket#1	missing	c	16.98	21.32	18.60	19.80	24.91	27.18	23.31
Anorthosite	KAP88-3A	Kapuskasing, Ont	c	27.38	26.31	22.31	25.12	28.12	27.56	25.57	24.25
Anorthosite	KAP88-3B	Kapuskasing, Ont	c	37.4	41.1	51.91	52.59	48.69	41.91	45.25	33.1
Anorthosite	L6z	Ecsoot'96 Labrador	missing	33.73	37.95	40.97	55.06	50.03	48.28	49.96	59.91
Average			25.52	30.62	30.43	31.48	30.94	31.74	34.91	41.06	53.94

A-4 Grade A: loss factors for silicates at pressures 10-600 MPa

Rock name	Sample Id	Suite Location	10 Mpa	20 Mpa	40 Mpa	60 Mpa	80 Mpa	100 Mpa	200 Mpa	400 Mpa	600 Mpa
Granophyre	10117	Sudbury Samples (second suite)	missing	missing	missing	missing	missing	missing	c	260.14	363.34
Tuff	10130	Sudbury Samples (second suite)	missing	missing	missing	missing	missing	missing	52.59	248.99	257.13
Granophyre	10142	Sudbury Samples (second suite)	missing	missing	missing	missing	missing	missing	273.55	334.62	missing
Tuff	10190	Sudbury Samples (second suite)	missing	missing	missing	missing	missing	missing	70.49	270.04	255.95
Granophyre	10193	Sudbury Samples (second suite)	missing	missing	missing	missing	missing	missing	188.32	166.75	263.29
Granophyre	10195	Sudbury Samples (second suite)	c	221.74	234.44	239.37	266.81	347.83	244.83	247.69	181.93
Tuff	10196	Sudbury Samples (second suite)	missing	missing	missing	missing	missing	missing	c	243.89	211.82
Felsic norite	52845	Sudbury Samples (second suite)	244.84	231.41	216.82	263.98	264.91	217.49	189.86	199.06	196.34

A-4 Grade A: loss factors for silicates at pressures 10-600 MPa (continued)

Rock name	Sample Id	Suite Location	10 Mpa	20 Mpa	40 Mpa	60 Mpa	80 Mpa	100 Mpa	200 Mpa	400 Mpa	600 Mpa
Diorite	603841	Noranda-Louvicort	missing	c	c	c	c	c	c	83.78	35.63
Andesite	604961	Noranda, Quebec6.03	c	c	c	c	c	c	c	23.47	39.08
Andesite	604966	Noranda, Quebec	196.95	143.14	174.67	144.36	164.19	117.62	146.25	153.37	141.19
Andesite	604967	Noranda, Quebec	missing	72.41	62.96	97.44	127.54	128.82	135.57	101.39	87.82
Tuff	52847-4	Sudbury Samples (second suite)	109.77	105.77	118.60	126.53	97.19	123.59	121.26	135.26	126.89
Gneiss	60064-10	Sudbury Samples (second suite)	279.22	246.15	232.73	278.49	362.83	389.95	301.54	270.72	228.14
Diabase	60064-11	Sudbury Samples (second suite)	C	102.16	130.99	133.89	162.23	163.96	196.60	226.00	223.11
Norite	60064-4	Sudbury Samples (second suite)	C	242.00	167.49	132.92	146.17	118.67	133.58	101.95	134.55
Breccia	60064-5	Sudbury Samples (second suite)	C	172.69	229.83	288.19	288.95	295.94	306.64	358.43	357.45
Breccia	60064-6	Sudbury Samples (second suite)	142.16	114.53	99.20	89.97	102.02	93.66	130.37	108.95	111.45

A-4 Grade A: loss factors for silicates at pressures 10-600 MPa (continued)

Rock name	Sample Id	Suite Location	10 Mpa	20 Mpa	40 Mpa	60 Mpa	80 Mpa	100 Mpa	200 Mpa	400 Mpa	600 Mpa
Gneiss	60064-7	Sudbury Samples (second suite)	c	268.84	184.90	140.93	126.52	127.94	108.72	107.19	89.86
Granophyre	60066-2	Sudbury Samples (second suite)	123.19	207.33	240.33	270.63	334.49	341.24	316.57	279.56	275.32
Felsic norite	60066-6	Sudbury Samples (second suite)	c	378.29	354.39	317.54	280.52	306.54	247.59	263.24	245.27
Rhyodacite	604959xy	Noranda, Quebec	93.05	69.34	77.29	64.46	58.21	54.19	37.64	28.25	16.37
Rhyodacite	604959z	Noranda, Quebec	c	161.84	131.06	99.51	116.05	116.84	102.78	81.39	107.69
Rhyodacite	604960xy	Noranda, Quebec	missing	121.07	100.68	84.81	93.92	95.32	90.03	88.13	75.38
Rhyodacite	604963xy	Noranda, Quebec	143.45	116.65	150.14	162.76	178.30	160.53	155.97	83.79	139.58
Norite	85597-14	Inco-Sudbury Basin	165.17	122.96	105.82	105.24	98.57	77.67	69.18	83.99	95.10
Norite	85597-15	Inco-Sudbury Basin	263.73	331.97	304.94	299.89	289.00	333.88	346.98	313.70	357.72
Hornblend	BNB96-062	Yelloknife, Bucket#1	missing	c	256.73	203.16	231.45	216.67	170.60	155.19	180.38
Anorthosite	KAP88-3A	Kapuskasing, Ont	c	149.65	153.89	180.38	159.49	142.07	143.71	153.54	161.46
Anorthosite	KAP88-3B	Kapuskasing, Ont	c	110.38	95.39	74.46	72.87	78.27	89.67	82.49	112.15
Anorthosite	L6z	Ecsoot'96 Labrador	missing	149.26	125.07	112.70	82.32	89.72	90.58	85.88	70.83
Average			175.25	174.53	171.67	170.04	178.46	179.93	165.24	172.29	159.92

A-5 Grade A: slope data for silicates at pressures 10-600 MPa

Rock name	Sample Id	Suite Location	10 Mpa (10 <sup>-7</sup> )	20 Mpa (10 <sup>-7</sup> )	40 Mpa (10 <sup>-7</sup> )	60 Mpa (10 <sup>-7</sup> )	80 Mpa (10 <sup>-7</sup> )	100 Mpa (10 <sup>-7</sup> )	200Mpa (10 <sup>-7</sup> )	400Mpa (10 <sup>-7</sup> )	600 Mpa (10 <sup>-7</sup> )
Granophyre	10117	Sudbury Samples (second suite)	missin g	missing	missing	missing	missing	missing	c	5.693	7.888
Tuff	10130	Sudbury Samples (second suite)	missin g	missing	missing	missing	missing	missing	7.327	8.670	7.102
Granophyre	10142	Sudbury Samples (second suite)	missin g	missing	missing	missing	missing	missing	4.105	5.177	missing
Tuff	10190	Sudbury Samples (second suite)	missin g	missing	missing	missing	missing	missing	3.683	7.216	6.156
Granophyre	10193	Sudbury Samples (second suite)	missin g	missing	missing	missing	missing	missing	10.413	9.221	14.559
Granophyre	10195	Sudbury Samples (second suite)	c	12.402	13.112	13.388	14.922	19.454	13.693	13.845	10.175
Tuff	10196	Sudbury Samples (second suite)	missin g	missing	missing	missing	missing	missing	c	13.428	11.662
Felsic norite	52845	Sudbury Samples (second suite)	13.677	12.927	12.112	14.746	14.798	12.145	10.606	11.112	10.968

A-5 Grade A: slope data for silicates at pressures 10-600 MPa (continued)

Rock name	Sample Id	Suite Location	10 Mpa (10 <sup>-7</sup> )	20 Mpa (10 <sup>-7</sup> )	40 Mpa (10 <sup>-7</sup> )	60 Mpa (10 <sup>-7</sup> )	80 Mpa (10 <sup>-7</sup> )	100 Mpa (10 <sup>-7</sup> )	200 Mpa (10 <sup>-7</sup> )	400 Mpa (10 <sup>-7</sup> )	600 Mpa (10 <sup>-7</sup> )
Diorite	603841	Noranda-Louvicort	missing	c	c	c	c	c	c	3.852	1.638
Andesite	604961	Noranda, Quebec6.03	c	c	c	c	c	c	c	1.162	1.935
Andesite	604966	Noranda, Quebec	9.473	6.885	8.402	6.944	7.898	5.658	7.034	7.377	6.791
Andesite	604967	Noranda, Quebec	missing	3.482	3.028	4.686	6.133	6.195	6.519	4.876	4.223
Tuff	52847-4	Sudbury Samples (second suite)	6.385	6.152	6.898	7.395	5.653	7.189	7.053	7.867	7.380
Gneiss	60064-10	Sudbury Samples (second suite)	15.742	13.877	13.121	15.701	20.456	21.985	17.001	15.263	12.862
Diabase	60064-11	Sudbury Samples (second suite)	C	4.947	6.343	6.484	7.856	7.939	9.520	10.944	10.804
Norite	60064-4	Sudbury Samples (second suite)	C	13.973	9.670	7.674	8.439	6.852	7.712	5.886	7.769
Breccia	60064-5	Sudbury Samples (second suite)	C	9.570	12.735	15.969	16.011	16.399	16.992	19.861	18.014
Breccia	60064-6	Sudbury Samples (second suite)	8.281	6.672	5.779	5.206	5.943	5.456	7.595	6.347	6.493

A-5 Grade A: slope data for silicates at pressures 10-600 MPa (continued)

Rock name	Sample Id	Suite Location	10 Mpa (10 <sup>-7</sup> )	20 Mpa (10 <sup>-7</sup> )	40 Mpa (10 <sup>-7</sup> )	60 Mpa (10 <sup>-7</sup> )	80 Mpa (10 <sup>-7</sup> )	100 Mpa (10 <sup>-7</sup> )	200 Mpa (10 <sup>-7</sup> )	400 Mpa (10 <sup>-7</sup> )	600 Mpa (10 <sup>-7</sup> )
Gneiss	60064-7	Sudbury Samples (second suite)	c	15.081	10.371	7.905	7.176	6.098	6.013	5.040	5.010
Granophyre	60066-2	Sudbury Samples (second suite)	6.364	10.710	12.415	13.981	17.279	17.628	16.354	14.441	14.223
Felsic norite	60066-6	Sudbury Samples (second suite)	c	17.304	16.210	14.524	12.831	14.021	11.325	12.041	12.219
Rhyodacite	604959xy	Noranda, Quebec	4.221	3.145	3.506	2.924	2.641	2.458	1.708	1.281	0.743
Rhyodacite	604959z	Noranda, Quebec	c	7.222	5.849	4.444	5.179	5.214	4.586	3.632	4.806
Rhyodacite	604960xy	Noranda, Quebec	missing	5.429	4.515	3.803	4.212	4.275	4.031	3.952	3.381
Rhyodacite	604963xy	Noranda, Quebec	6.528	5.309	6.833	7.407	8.115	7.306	7.098	3.814	6.352

A-5 Grade A: slope data for silicates at pressures 10-600 MPa (continued)

Rock name	Sample Id	Suite Location	10 Mpa (10 <sup>-7</sup> )	20 Mpa (10 <sup>-7</sup> )	40 Mpa (10 <sup>-7</sup> )	60 Mpa (10 <sup>-7</sup> )	80 Mpa (10 <sup>-7</sup> )	100 Mpa (10 <sup>-7</sup> )	200 Mpa (10 <sup>-7</sup> )	400 Mpa (10 <sup>-7</sup> )	600 Mpa (10 <sup>-7</sup> )
Norite	85597-14	Inco-Sudbury Basin	6.929	5.456	4.695	4.670	4.374	3.446	3.071	3.050	4.220
Norite	85597-15	Inco-Sudbury Basin	12.273	15.448	14.191	13.956	13.449	15.537	16.147	14.598	16.646
Hornblend	BNB96-062	Yelloknife, Bucket#1	missing	c	11.584	9.138	10.411	9.746	7.674	6.98	8.113
Anorthosite	KAP88-3A	Kapuskasing, Ont	c	6.931	7.128	8.355	7.387	6.580	6.656	7.111	7.478
Anorthosite	KAP88-3B	Kapuskasing, Ont	c	5.411	4.676	3.650	3.573	3.837	4.397	4.044	5.498
Anorthosite	L6z	Ecsot'96 Labrador	missing	8.008	6.710	6.046	4.416	4.813	4.860	4.608	3.800
Average			8.446	8.494	8.689	8.650	9.090	9.188	8.305	8.206	8.091

A-6 Grade B: physical properties of silicates

Rock name	Sample Id	Suite Location	Weight (gm)	Length (mm)	Diameter (mm)	Volume (mm <sup>3</sup> )	Density (g/cc)
Granophyre	10649	Sudbury Samples (second suite)	61.09	47.23	22.72	22.46	2.72
Andesite	604962	Sudbury Samples (second suite)	58.57	41.53	25.34	21.00	2.79
Andesite	604965	Noranda, Quebec	65.64	56.35	25.38	23.52	2.79
Diorite	17-79-1751	Noranda, Quebec	55.42	39.06	25.33	19.64	2.82
Rhyolite	181679z	Sturgeon Lake- Noranda Mining	57.13	42.41	25.35	21.33	2.68
Magnate	181696xy	Noranda 99-Bathu2.76rst	76.03	39.04	25.36	19.52	3.89
Tuff	52847-1	Noranda 99-Bathurst	68.86	51.47	24.87	24.97	2.76
Tuff	52847-2	Sudbury Samples (second suite)	65.54	48.93	24.93	23.77	2.76
Tuff	52847-3	Sudbury Samples (second suite)	66.64	49.79	24.93	24.21	2.75
Granophyre	52847-7	Sudbury Samples (second suite)	65.17	49.72	24.96	24.31	2.68

A-6 Grade B: physical properties of silicates (continued)

Rock name	Sample Id	Suite Location	Weight (gm)	Length (mm)	Diameter (mm)	Volume (mm <sup>3</sup> )	Density (g/cc)
Quartz gabbro	5988-1	Sudbury Samples (second suite)	68.66	48.37	25.05	23.76	2.89
Gneiss	60064-12	Sudbury Samples (second suite)	64.90	49.67	24.90	24.10	2.69
Felsic norite	60064-2	Sudbury Samples (second suite)	62.25	44.85	24.87	21.66	2.87
Breccia	60064-3	Sudbury Samples (second suite)	58.55	43.92	24.87	21.24	2.76
Breccia	60064-6-TOP	Sudbury Samples (second suite)	68.44	50.65	24.89	24.58	2.78
Gneiss	60064-8	Sudbury Samples (second suite)	58.70	43.03	24.57	20.35	2.88
Granophyre	60066-1	Sudbury Samples (second suite)	70.14	51.35	24.89	24.90	2.82
Quartz gabbro	60066-3	Sudbury Samples (second suite)	69.53	51.27	24.87	24.77	2.81
Quartz gabbro	60066-4	Sudbury Samples (second suite)	68.28	47.11	24.87	22.74	2.78

A-6 Grade B: physical properties of silicates (continued)

Rock name	Sample Id	Suite Location	Weight (gm)	Length (mm)	Diameter (mm)	Volume (mm <sup>3</sup> )	Density (g/cc)
Greywacke	BA 4301-8A-BOT	Sudbury Samples (second suite)	96.51	47.43	24.75	34.63	2.79
Greywacke	BA 4301-8A-TOP	Sudbury Samples 41.93(second suite)	91.82	47.03	24.74	33.76	2.72
Metatonalite	BNB97-018Az	Sudbury Samples (second suite)	56.90	40.40	25.34	21.11	2.70
Metatonalite	BNB97-018Bx	Yellowknife Bucket#4	54.54	44.10	25.34	20.31	2.68
Medium grained Gneiss	BNB97-021Az	Yellowknife Bucket#2	58.82	46.64	25.24	22.19	2.65
Anorthosite	L6xy	Labrador-Nakvakfjord Nain	65.61	44.91	25.32	23.46	2.80
Metbasalt	LG-196x-23	Liscomb complex	59.35	44.10	24.60	21.30	2.79

A-7 Grade B: velocities (km/sec) of silicates at pressures 10-600 MPa

Rock name	Sample Id	Suite Location	10 Mpa	20 Mpa	40 Mpa	60 Mpa	80 Mpa	100 Mpa	200 Mpa	400 Mpa	600 Mpa
Granophyre	10649	Sudbury Samples (second suite)	5.90	6.00	6.06	6.08	6.10	6.11	6.15	6.18	6.21
Andesite	604962	Sudbury Samples (second suite)	Missing	c	c	c	6.38	6.40	6.47	6.53	6.56
Andesite	604965	Noranda, Quebec	6.08	6.10	6.14	6.17	6.20	6.23	6.30	6.34	6.35
Diorite	17-79-1751	Noranda, Quebec	6.03	c	c	6.34	c	c	c	c	c
Rhyolite	181679z	Sturgeon Lake-Noranda Mining	C	c	c	c	c	c	c	5.47	5.51
Magnate	181696xy	Noranda 99-Bathu2.76rst	C	c	c	c	c	c	5.95	6.10	6.16
Tuff	52847-1	Noranda 99-Bathurst	C	C	6.28	6.30	6.31	6.32	6.35	6.38	6.42
Tuff	52847-2	Sudbury Samples (second suite)	C	C	6.34	6.36	6.37	6.38	6.41	6.45	6.49
Tuff	52847-3	Sudbury Samples (second suite)	C	C	6.22	6.24	6.25	6.26	6.29	6.33	6.37

A-7 Grade B: velocities (km/sec) of silicates at pressures 10-600 MPa (continued)

Rock name	Sample Id	Suite Location	10 Mpa	20 Mpa	40 Mpa	60 Mpa	80 Mpa	100 Mpa	200 Mpa	400 Mpa	600 Mpa
Granophyre	52847-7	Sudbury Samples (second suite)	C	C	6.08	6.14	6.16	6.18	6.22	6.26	6.28
Quartz gabbro	5988-1	Sudbury Samples (second suite)	C	C	6.14	6.19	6.21	6.23	6.26	6.30	6.32
Gneiss	60064-12	Sudbury Samples (second suite)	5.36	5.76	6.07	6.19	6.28	6.26	6.33	6.38	6.42
Felsic norite	60064-2	Sudbury Samples (second suite)	C	5.96	6.01	6.04	6.06	6.07	6.11	6.16	6.21
Breccia	60064-3	Sudbury Samples (second suite)	C	c	c	6.27	c	6.32	6.38	6.42	6.45
Breccia	60064-6-TOP	Sudbury Samples (second suite)	C	6.17	6.28	6.33	6.35	6.36	6.40	6.45	6.48
Gneiss	60064-8	Sudbury Samples (second suite)	c	6.56	6.64	6.66	6.67	6.68	6.71	6.75	6.80
Granophyre	60066-1	Sudbury Samples (second suite)	C	c	6.41	6.44	6.46	6.47	6.50	6.54	6.58

A-7 Grade B: velocities (km/sec) of silicates at pressures 10-600 MPa (continued)

Rock name	Sample Id	Suite Location	10 Mpa	20 Mpa	40 Mpa	60 Mpa	80 Mpa	100 Mpa	200 Mpa	400 Mpa	600 Mpa
Quartz gabbro	60066-3	Sudbury Samples (second suite)	C	6.24	c	6.34	6.36	6.37	c	6.43	6.47
Quartz gabbro	60066-4	Sudbury Samples (second suite)	C	c	c	c	6..35	6.36	6.40	6.43	6.45
Greywacke	BA 4301-8A-BOT	Sudbury Samples (second suite)	C	c	5.94	5.97	5.98	6.00	6.05	6.13	6.20
Greywacke	BA 4301-8A-TOP	Sudbury Samples 41.93(second suite)	C	c	c	c	c	c	6.09	6.16	6.20
Metatonalite	BNB97-018Az	Sudbury Samples (second suite)	5.29	c	5.70	5.76	c	c	c	6.02	6.06
Metatonalite	BNB97-018Bx	Yellowknife Bucket#4	Missing	Missin	Missing	Missing	Missing	c	c	6.45	6.49
Medium grained Gneiss	BNB97-021Az	Yellowknife Bucket#2	5.65	5.73	5.85	5.95	6.02	6.07	6.17	6.24	6.28
Anorthosite	L6xy	Labrador-Nakvakfjord Nain	Missing	c	c	6.06	6.16	6.20	6.29	6.37	6.45
Metbasalt	LG-196x-23	Liscomb complex	C	5.36	5.82	6.02	6.12	6.19	6.41	6.52	6.56
Average			5.72	5.99	6.12	6.19	6.24	6.26	6.30	6.31	6.35

A-8 Grade B: Q for silicates at pressures 10-600 MPa

Rock name	Sample Id	Suite Location	10 Mpa	20 Mpa	40 Mpa	60 Mpa	80 Mpa	100 Mpa	200 Mpa	400 Mpa	600 Mpa
Granophyre	10649	Sudbury Samples (second suite)	Missing	Missing	Missing	Missing	Missing	Missing	42.93	27.44	26.20
Andesite	604962	Sudbury Samples (second suite)	Missing	c	c	c	213.36	530.59	164.32	135.95	52.67
Andesite	604965	Noranda, Quebec	26.12	37.18	72.56	76.45	53.72	120.14	81.63	75.59	78.57
Diorite	17-79-1751	Noranda, Quebec	62.15	C	c	86.21	c	c	c	c	c
Rhyolite	181679z	Sturgeon Lake-Noranda Mining	C	c	c	c	c	c	c	16.45	17.12
Magnate	181696xy	Noranda 99-Bathurst	C	c	c	c	c	c	11.24	20.76	24.65
Tuff	52847-1	Noranda 99-Bathurst	C	C	Missing	Missing	Missing	17.13	15.29	13.90	11.94
Tuff	52847-2	Sudbury Samples (second suite)	C	C	Missing	Missing	Missing	10.96	9.87	9.25	8.51

A-8 Grade B: Q for silicates at pressures 10-600 MPa (continued)

Rock name	Sample Id	Suite Location	10 Mpa	20 Mpa	40 Mpa	60 Mpa	80 Mpa	100 Mpa	200 Mpa	400 Mpa	600 Mpa
Tuff	52847-3	Sudbury Samples (second suite)	C	C	Missing	Missing	Missing	14.24	17.44	14.40	15.34
Granophyre	52847-7	Sudbury Samples (second suite)	C	C	48.06	66.56	57.98	53.28	33.35	28.76	42.38
Quartz gabbro	5988-1	Sudbury Samples (second suite)	C	C	28.42	18.91	15.37	15.95	14.39	17.42	15.58
Gneiss	60064-12	Sudbury Samples (second suite)	26.04	missing	21.35	missing	missing	21.9	24.13	21.98	20.64
Felsic norite	60064-2	Sudbury Samples (second suite)	C	missing	21.72	missing	missing	24.74	28.41	24.09	23.87
Breccia	60064-3	Sudbury Samples (second suite)	C	c	c	c	c	19.28	17.02	18.30	19.10
Breccia	60064-6-TOP	Sudbury Samples (second suite)	C	missing	15.4	missing	missing	14.36	11.3	10.82	13.35
Gneiss	60064-8	Sudbury Samples (second suite)	c	43.34	32.60	19.37	13.97	11.60	11.67	14.91	17.42
Granophyre	60066-1	Sudbury Samples (second suite)	C	c	missing	missing	missing	25.79	22.64	23.27	24.22
Quartz gabbro	60066-3	Sudbury Samples (second suite)	C	missing	c	missing	missing	c	c	23.66	24.55
Quartz gabbro	60066-4	Sudbury Samples (second suite)	C	c	c	c	18.06	14.93	14.93	15.13	285.91
Greywacke	BA 4301-8A-BOT	Sudbury Samples (second suite)	C	c	27.07	23.37	27.92	27.25	30.42	23.37	24.93

A-8 Grade B: Q for silicates at pressures 10-600 MPa (continued)

Rock name	Sample Id	Suite Location	10 Mpa	20 Mpa	40 Mpa	60 Mpa	80 Mpa	100 Mpa	200 Mpa	400 Mpa	600 Mpa
Greywacke	BA 4301-8A-TOP	Sudbury Samples (second suite)	C	c	c	c	c	c	30.41	26.98	23.59
Metatonalite	BNB97-018Az	Sudbury Samples (second suite)	177.17	c	113.1	82.58	c	c	c	37.57	40.65
Metatonalite	BNB97-018Bx	Yellowknife Bucket#4	Missin g	Missi ng	Missing	Missing	Missing	c	c	19.22	22.44
Medium grained Gneiss	BNB97-021Az	Yellowknife Bucket#2	13.05	12.57	15.54	13.63	14.05	21.20	21.84	20.23	18.45
Anorthosite	L6xy	Labrador-Nakvakfjord Nain	Missin g	c	c	54.34	56.46	55.37	54.93	62.04	43.97
Metbasalt	LG-196x-23	Liscomb complex	C	82.78	47.11	36.83	32.64	22.33	14.63	17.69	19.08
Average			60.91	43.96	40.27	48.43	32.24	28.85	24.51	35.93	38.20

A-9 Grade B: Loss factors for silicates at pressures 10-600 MPa

Rock name	Sample Id	Suite Location	10 Mpa	20 Mpa	40 Mpa	60 Mpa	80 Mpa	100 Mpa	200 Mpa	400 Mpa	600 Mpa
Granophyre	10649	Sudbury Samples (second suite)	Missing	Missing	Missing	Missing	Missing	Missing	103.36	160.89	167.73
Andesite	604962	Sudbury Samples (second suite)	Missing	c	c	c	20.04	8.03	25.67	30.73	78.97
Andesite	604965	Noranda, Quebec	171.80	120.30	61.25	570.85	81.93	36.46	53.06	56.94	54.69
Diorite	17-79-1751	Noranda, Quebec	72.82	C	c	49.92	c	c	c	c	c
Rhyolite	181679z	Sturgeon Lake-Noranda Mining	C	c	c	c	c	c	c	303.27	289.23
Magnate	181696xy	Noranda 99-Bathu2.76rst	C	c	c	c	c	c	407.95	215.48	179.71
Tuff	52847-1	Noranda 99-Bathurst	C	C	Missing	Missing	Missing	252.04	281.12	307.73	356.07
Tuff	52847-2	Sudbury Samples (second suite)	C	C	Missing	Missing	Missing	390.14	431.42	457.34	494.09
Tuff	52847-3	Sudbury Samples (second suite)	C	C	Missing	Missing	Missing	306.18	248.71	299.36	279.31
Granophyre	52847-7	Sudbury Samples (second suite)	C	C	93.38	66.77	76.40	82.87	131.56	151.55	102.54
Quartz gabbro	5988-1	Sudbury Samples (second suite)	C	C	156.35	233.12	285.85	274.66	302.91	248.67	260.36
Gneiss	60064-12	Sudbury Samples (second suite)	195.52	missing	210.58	missing	missing	199.01	178.68	194.55	205.92

A-9 Grade B: Loss factors for silicates at pressures 10-600 MPa (continued)

Rock name	Sample Id	Suite Location	10 Mpa	20 Mpa	40 Mpa	60 Mpa	80 Mpa	100 Mpa	200 Mpa	400 Mpa	600 Mpa
Felsic norite	60064-2	Sudbury Samples (second suite)	C	missing	209.08	missing	missing	181.74	157.18	183.87	184.07
Breccia	60064-3	Sudbury Samples (second suite)	C	c	c	c	c	223.99	251.32	232.32	221.49
Breccia	60064-6-TOP	Sudbury Samples (second suite)	C	missing	282.11	missing	missing	298.87	377.24	390.83	315.37
Gneiss	60064-8	Sudbury Samples (second suite)	c	95.98	126.05	211.54	292.75	352.17	348.48	271.22	230.38
Granophyre	60066-1	Sudbury Samples (second suite)	C	c	missing	missing	missing	163.56	185.39	179.32	171.24
Quartz gabbro	60066-3	Sudbury Samples (second suite)	C	missing	c	missing	missing	c	c	179.33	171.82
Quartz gabbro	60066-4	Sudbury Samples (second suite)	C	c	c	c	237.99	287.46	281.86	14.84	12.89
Greywacke	BA 4301-8A-BOT	Sudbury Samples (second suite)	C	c	169.71	155.64	163.41	166.87	148.26	190.47	176.52
Greywacke	BA 4301-8A-TOP	Sudbury Samples (second suite)	C	c	c	c	c	c	147.35	164.17	186.58
Metatonalite	BNB97-018Az	Sudbury Samples (second suite)	29.11	c	42.330	57.36	c	c	c	120.65	110.77
Metatonalite	BNB97-018Bx	Yellowknife Bucket#4	Missing	Missing	Missing	Missing	Missing	c	c	220.17	187.39

A-9 Grade B: Loss factors for silicates at pressures 10-600 MPa (continued)

Rock name	Sample Id	Suite Location	10 Mpa	20 Mpa	40 Mpa	60 Mpa	80 Mpa	100 Mpa	200 Mpa	400 Mpa	600 Mpa
Medium grained Gneiss	BNB97-021Az	Yellowknife Bucket#2	370.06	378.83	300.32	336.42	322.67	212.02	202.51	216.21	235.46
Anorthosite	L6xy	Labrador-Nakvakfjord Nain	Missing	c	c	82.87	78.47	79.49	78.98	69.05	96.22
Metbasalt	LG-196x-23	Liscomb complex	C	61.49	99.52	123.06	136.59	197.39	290.97	236.64	218.00
Average			167.86	164.15	159.15	141.62	169.61	206.28	220.67	203.83	201.21

A-10 Grade B: slope data for silicates at pressures 10-600 MPa

Rock name	Sample Id	Suite Location	10 Mpa (10 <sup>-7</sup> )	20 Mpa (10 <sup>-7</sup> )	40 Mpa (10 <sup>-7</sup> )	60 Mpa (10 <sup>-7</sup> )	80 Mpa (10 <sup>-7</sup> )	100 Mpa (10 <sup>-7</sup> )	200 Mpa (10 <sup>-7</sup> )	400 Mpa (10 <sup>-7</sup> )	600 Mpa (10 <sup>-7</sup> )
Granophyre	10649	Sudbury Samples (second suite)	Missing	Missing	Missing	Missing	Missing	Missing	5.620	8.749	9.120
Andesite	604962	Sudbury Samples (second suite)	Missing	c	c	c	0.958	0.384	1.227	1.470	3.776
Andesite	604965	Noranda, Quebec	9.167	6.420	3.268	3.087	4.372	1.946	2.832	3.038	2.919
Diorite	17-79-1751	Noranda, Quebec	3.275	C	c	2.245	c	c	c	c	c
Rhyolite	181679z	Sturgeon Lake- Noranda Mining	C	c	c	c	c	c	c	14.808	14.122
Magnite	181696xy	Noranda 99- Bathu2.76rst	C	c	c	c	c	c	18.336	9.685	8.077
Tuff	52847-1	Noranda 99- Bathurst	C	C	Missing	Missing	Missing	14.935	16.658	18.235	21.110
Tuff	52847-2	Sudbury Samples (second suite)	C	C	Missing	Missing	Missing	21.977	24.303	25.763	27.833
Tuff	52847-3	Sudbury Samples (second suite)	C	C	Missing	Missing	Missing	17.551	14.257	17.160	16.011
Granophyre	52847-7	Sudbury Samples (second suite)	C	C	5.345	3.822	4.373	4.744	7.531	8.675	5.870
Quartz gabbro	5988-1	Sudbury Samples (second suite)	C	C	8.707	12.928	15.918	15.295	16.868	13.848	14.499
Gneiss	60064-12	Sudbury Samples (second suite)	11.181	c	12.042	c	c	11.380	10.218	11.125	11.776

A-10 Grade B: slope data for silicates at pressures 10-600 MPa (continued)

Rock name	Sample Id	Suite Location	10 Mpa (10 <sup>-7</sup> )	20 Mpa (10 <sup>-7</sup> )	40 Mpa (10 <sup>-7</sup> )	60 Mpa (10 <sup>-7</sup> )	80 Mpa (10 <sup>-7</sup> )	100 Mpa (10 <sup>-7</sup> )	200 Mpa (10 <sup>-7</sup> )	400 Mpa (10 <sup>-7</sup> )	600 Mpa (10 <sup>-7</sup> )
Felsic norite	60064-2	Sudbury Samples (second suite)	C	missing	10.796	missing	missing	9.383	8.116	9.494	15.488
Breccia	60064-3	Sudbury Samples (second suite)	C	c	c	c	c	11.326	12.708	11.747	11.200
Breccia	60064-6- TOP	Sudbury Samples (second suite)	C	missing	16.451	missing	missing	17.428	21.998	22.791	18.390
Gneiss	60064-8	Sudbury Samples (second suite)	c	4.755	6.245	10.480	14.503	17.447	17.264	13. 436	11.431
Granophyre	60066-1	Sudbury Samples (second suite)	C	c	missing	missing	missing	9.670	10.960	10.602	10.124
Quartz gabbro	60066-3	Sudbury Samples (second suite)	C	missing	c	missing	missing	c	c	10.585	10.142
Quartz gabbro	60066-4	Sudbury Samples (second suite)	C	c	c	c	12.908	15.591	15.287	15.507	17.807
Greywacke	BA 4301- 8A-BOT	Sudbury Samples (second suite)	C	c	9.268	8.499	8.923	9.113	8.096	10.401	9.639
Greywacke	BA 4301- 8A-TOP	Sudbury Samples (second suite)	C	c	c	c	c	c	7.978	8.889	10.013
Metatonalite	BNB97- 018Az	Sudbury Samples (second suite)		c	2.043	2.769	c	c	c	5.824	5.347

A-10 Grade B: slope data for silicates at pressures 10-600 MPa (continued)

Rock name	Sample Id	Suite Location	10 Mpa (10 <sup>-7</sup> )	20 Mpa (10 <sup>-7</sup> )	40 Mpa (10 <sup>-7</sup> )	60 Mpa (10 <sup>-7</sup> )	80 Mpa (10 <sup>-7</sup> )	100 Mpa (10 <sup>-7</sup> )	200 Mpa (10 <sup>-7</sup> )	400 Mpa (10 <sup>-7</sup> )	600 Mpa (10 <sup>-7</sup> )
Metatonalite	BNB97-018Bx	Yellowknife Bucket#4	Missing	Missing	Missing	Missing	Missing	c	c	10.241	8.716
Medium grained Gneiss	BNB97-021Az	Yellowknife Bucket#2	18.789	19.234	15.243	17.081	16.383	10765	10.282	10.977	11.955
Anorthosite	L6xy	Labrador-Nakvakfjord Nain	Missing	5.076	4.714	4.450	4.213	4.269	4.241	3.708	5.167
Metbasalt	LG-196x-23	Liscomb complex	C	3.180	5.146	6.363	7.063	10.206	15.044	12.236	11.272

A-11 Grade A: velocities (km/sec) of massive silphides at pressures 10-600 MPa

Rock name	Sample Id	Suite Location	10 Mpa	20 Mpa	40 Mpa	60 Mpa	80 Mpa	100 Mpa	200 Mpa	400 Mpa	600 Mpa
Chalcopyrite	KC-486xy	Kidd creek	4.95	5.05	5.21	5.26	5.29	5.31	5.38	5.43	5.44
Chalcopyrite	SEL-202	Selbaie	5.64	5.72	5.76	5.79	5.81	5.83	5.89	5.97	6.02
Chalcopyrite	SEL-204	Selbaie	c	5.30	5.44	5.58	5.68	5.70	5.76	5.80	5.84
Pyrrhotite	Inco-9-1	Inco-Sudbury basin	Missing	Missing	Missing	Missing	Missing	5.85	5.91	5.98	6.03
Pyrrhotite	Inco-9-2	Inco-Sudbury basin	Missing	Missing	5.42	5.47	5.52	5.58	5.69	5.76	5.83
Pyrite ore	Sel-103	Selbaie	c	7.48	7.55	7.58	7.59	7.60	7.65	7.69	7.73
Pyrite ore	Sel-105	Selbaie	7.31	7.46	7.52	7.56	7.60	7.63	7.70	7.74	7.77
Pyrite-chalcopyrite ore	Sel-506	Selbaie	5.98	6.05	6.16	6.23	6.27	6.30	6.37	6.43	6.45
Pyrrhotite	T-30826xy	Thompson	4.58	4.67	4.73	4.75	4.76	4.77	4.80	4.83	4.84
Pentlandite-pyrrhotite ore	Inco-12-2	Inco-Sudbury basin	C	4.56	4.60	4.63	4.65	4.67	4.70	4.73	4.74
Pentlandite-pyrrhotite ore	Inco-12-4	Inco-Sudbury basin	c	c	4.76	4.90	5.00	5.07	5.19	5.21	5.23
Massive sphalerite ore	KC-316xy	Kidd creek	5.21	5.31	5.41	5.45	5.47	5.48	5.52	5.55	5.56
Sphalerite	Sel-303	Selbaie	5.14	5.39	5.52	5.61	5.67	5.72	5.76	5.79	5.81
Sphalerite-chalcopyrite-pyrite ore	Sel-503	Selbaie	C	C	5.74	5.79	5.83	5.85	5.90	5.93	5.97
Average			5.54	5.70	5.68	5.74	5.78	5.81	5.87	5.92	5.95

A-12 Grade A: Q for massive silphides at pressures 10-600 MPa

Rock name	Sample Id	Suite Location	10 Mpa	20 Mpa	40 Mpa	60 Mpa	80 Mpa	100 Mpa	200 Mpa	400 Mpa	600 Mpa
Chalcopyrite	KC-486xy	Kidd creek	28.73	21.61	31.19	42.34	50.14	42.38	51.16	56.10	61.14
Chalcopyrite	SEL-202	Selbaie	14.81	12.21	16.05	21.24	27.24	30.96	26.66	35.64	33.81
Chalcopyrite	SEL-204	Selbaie	C	50.97	45.49	47.26	48.02	47.67	38.18	40.39	43.54
Pyrrhotite	Inco-9-1	Inco-Sudbury basin	Missing	Missing	Missing	Missing	Missing	59.17	71.55	211.87	123.87
Pyrrhotite	Inco-9-2	Inco-Sudbury basin	Missing	Missing	33.99	28.98	26.53	33.66	32.96	29.87	27.36
Pyrite ore	Sel-103	Selbaie	c	9.12	12.81	1650	20.53	19.19	31.72	78.08	81.67
Pyrite ore	Sel-105	Selbaie	13.76	12.98	24.61	31.99	32.66	30.83	35.42	34.36	29.88
Pyrite-chalcopyrite ore	Sel-506	Selbaie	57.44	50.79	39.18	35.99	36.35	38.57	39.45	39.99	40.65
Pyrrhotite	T-30826xy	Thompson	44.39	59.48	68.29	56.66	57.61	59.79	71.53	59.36	82.78
Pentlandite-pyrrhotite ore	Inco-12-2	Inco-Sudbury basin	c	43.41	45.47	35.62	44.59	45.40	41.91	45.41	36.84
Pentlandite-pyrrhotite ore	Inco-12-4	Inco-Sudbury basin	c	c	114.48	129.77	94.21	116.63	103.08	105.29	111.55
Massive sphalerite ore	KC-316xy	Kidd creek	77.38	56.36	61.35	69.15	99.28	63.81	84.11	98.12	64.56
Sphalerite	Sel-303	Selbaie	43.88	51.36	76.71	85.22	105.48	92.04	116.57	77.62	102.80
Sphalerite-chalcopyrite-pyrite ore	Sel-503	Selbaie	C	C	18.48	22.03	26.82	31.83	46.38	55.10	57.25
Average			40.06	36.83	45.24	47.90	51.50	50.85	56.48	69.09	64.12

A-13 Grade A: loss factors for massive silphides at pressures 10-600 MPa

Rock name	Sample Id	Suite Location	10 Mpa	20 Mpa	40 Mpa	60 Mpa	80 Mpa	100 Mpa	200 Mpa	400 Mpa	600 Mpa
Chalcopyrite	KC-486xy	Kidd creek	191.85	250.07	167.90	122.51	102.88	121.26	99.13	89.57	82.05
Chalcopyrite	SEL-202	Selbaie	326.69	390.77	295.21	221.91	172.38	151.17	173.78	128.23	134.07
Chalcopyrite	SEL-204	Selbaie	C	101.01	110.26	103.47	100.05	100.42	124.09	116.48	107.32
Pyrrhotite	Inco-9-1	Inco-Sudbury basin	Missing	Missing	Missing	Missing	Missing	78.83	64.53	21.54	36.53
Pyrrhotite	Inco-9-2	Inco-Sudbury basin	Missing	Missing	148.14	172.13	186.31	145.29	145.49	158.61	171.09
Pyrite ore	Sel-103	Selbaie	c	399.99	282.18	218.14	175.16	187.07	112.44	45.44	43.22
Pyrite ore	Sel-105	Selbaie	271.31	281.84	147.43	112.84	109.95	116.01	100.05	102.61	117.52
Pyrite-chalcopyrite ore	Sel-506	Selbaie	79.44	88.80	113.05	121.72	119.74	112.29	108.59	106.12	104.06
Pyrrhotite	T-30826xy	Thompson	134.22	98.23	84.48	101.39	99.51	95.68	79.48	95.18	68.10
Pentlandite-pyrrhotite ore	Inco-12-2	Inco-Sudbury basin	c	137.86	130.47	165.44	131.59	128.70	138.54	127.05	156.28
Pentlandite-pyrrhotite ore	Inco-12-4	Inco-Sudbury basin	c	c	50.08	42.91	57.93	46.15	51.00	49.74	46.77
Massive sphalerite ore	KC-316xy	Kidd creek	67.68	91.17	82.21	72.40	50.24	78.03	58.77	50.11	76.02
Sphalerite	Sel-303	Selbaie	120.98	98.57	64.44	57.08	45.63	51.83	40.64	60.72	45.68
Sphalerite-chalcopyrite-pyrite ore	Sel-503	Selbaie	C	C	257.26	213.91	174.52	146.056	99.73	83.52	79.84
Average			170.31	193.83	148.70	132.76	117.37	111.38	99.73	88.21	90.61

A-14 Grade B: velocities (km/sec) of massive silphides at pressures 10-600 MPa

Rock name	Sample Id	Suite Location	10 Mpa	20 Mpa	40 Mpa	60 Mpa	80 Mpa	100 Mpa	200 Mpa	400 Mpa	600 Mpa
Pyrite	Sel-5	Selbaie	c	c	c	c	c	c	c	7.30	7.33
Pyrite ore	Sel-101	Selbaie	7.13	7.27	7.33	7.36	7.39	7.42	7.54	c	c
Pyrite ore	Sel-104	Selbaie	c	C	7.09	7.16	7.22	7.26	7.35	7.39	7.40
Pyrite ore	KC-470Bz	Kidd Creek	c	c	c	c	c	c	c	5.87	5.89
Pyrite-chalcopyrite ore	Sel-502	Selbaie	c	c	c	6.33	6.35	6.36	6.41	6.45	6.46
Sphalerite	Sel-302	Selbaie	c	c	5.63	5.67	5.69	5.72	5.78	5.85	5.89
Pyrite-sphalerite ore	Sel0505	Selbaie	6.69	6.77	6.82	6.85	6.87	6.89	6.96	7.04	7.09
Average			6.91	7.02	6.72	6.67	6.70	6.73	6.81	6.65	6.68

A-15 Grade B: Q for massive silphides at pressures 10-600 MPa

Rock name	Sample Id	Suite Location	10 Mpa	20 Mpa	40 Mpa	60 Mpa	80 Mpa	100 Mpa	200 Mpa	400 Mpa	600 Mpa
Pyrite	Sel-5	Selbaie	c	c	c	c	c	c	c	13.57	10.09
Pyrite ore	Sel-101	Selbaie	23.69	22.36	13.42	10.88	10.87	9.51	10.41	c	c
Pyrite ore	Sel-104	Selbaie	c	C	16.75	16.41	18.32	17.95	23.48	15.96	18.59
Pyrite ore	KC-470Bz	Kidd Creek	c	c	c	c	c	c	c	28.36	28.27
Pyrite-chalcopyrite ore	Sel-502	Selbaie	c	c	c	15.60	19.46	26.18	25.61	36.41	35.80
Sphalerite	Sel-302	Selbaie	c	c	13.81	18.08	18.61	21.22	23.65	27.33	26.63
Pyrite-sphalerite ore	Sel0505	Selbaie	56.99	37.99	30.80	28.52	25.27	21.76	32.10	30.29	21.52
Average			40.34	30.18	18.70	17.89	18.51	19.32	23.05	25.32	23.48

A-16 Grade B: loss factors for massive silphides at pressures 10-600 MPa

Rock name	Sample Id	Suite Location	10 Mpa	20 Mpa	40 Mpa	60 Mpa	80 Mpa	100 Mpa	200 Mpa	400 Mpa	600 Mpa
Pyrite	Sel-5	Selbaie	c	c	c	c	c	c	c	275.36	369.07
Pyrite ore	Sel-101	Selbaie	161.52	167.87	277.47	340.87	339.84	386.67	347.64	c	C
Pyrite ore	Sel-104	Selbaie	c	C	229.74	232.24	206.34	209.34	158.09	231.29	198.31
Pyrite ore	KC-470Bz	Kidd Creek	c	c	c	c	c	c	c	163.93	163.90
Pyrite-chalcopyrite ore	Sel-502	Selbaie	c	c	c	276.37	220.85	163.87	166.21	116.19	118.01
Sphalerite	Sel-302	Selbaie	c	c	350.32	266.14	257.70	224.83	199.64	170.70	173.96
Pyrite-sphalerite ore	Sel0505	Selbaie	71.57	106.11	129.89	139.69	157.18	182.03	122.13	127.96	178.82
Average			116.55	136.99	247.01	251.07	236.38	233.35	198.74	180.91	200.34

## **Appendix B (Loss Factor)**

## Loss factor derivation and relationship with Q :

Loss factor derivation by Dr. Stephen D. Butt, Professor at Faculty of Engineering and Applied Science (Oil and Gas Engineering/ Drilling and Geomechanics) Memorial University of Newfoundland.

$$\text{Loss factor (dB/m)} = \frac{20 \log_{10} \left( \frac{A_0}{A_1} \right)}{x}$$

Where,

$A_0$  = the initial amplitude,

$A_1$  = amplitude after passing through the specimen

$x$  = specimen length in meter.

From theory:

$$A_1 = A_0 \exp - \frac{\pi x f}{cQ}$$

Where,  $f$  = frequency and  $Q$  = Quality factor

$$\Rightarrow \frac{A_1}{A_0} = \exp - \frac{\pi x f}{cQ}$$

$$\Rightarrow \ln \left( \frac{A_1}{A_0} \right) = - \frac{\pi x f}{cQ}$$

$$\text{Or } \ln\left(\frac{A_0}{A_1}\right) = \frac{\pi x f}{cQ}$$

$$\text{From the spectral ratio fit, } SR_{slope} = \frac{\pi x}{cQ} = S$$

$$\text{Therefore, } \ln\left(\frac{A_0}{A_1}\right) = Sf$$

$$\text{And } \log\left(\frac{A_0}{A_1}\right) = \ln\left(\frac{A_0}{A_1}\right) * \log_e$$

$$\Rightarrow \log\left(\frac{A_0}{A_1}\right) = \log_e * Sf$$

$$\text{Loss factor (dB/m)} = \frac{20 \log_e * Sf}{x}$$

Select a standard frequency of  $f=1 \text{ MHz}=1 \times 10^6 \text{ Hz}$

$$\Rightarrow \text{Loss factor} = \frac{20 \log_e * 1 \times 10^6 * S}{x}$$

$$\text{Hence, Loss factor (dB/m @ 1 MHz)} = 5.4366 \times 10^7 * \frac{S}{x}$$

**Relation between Q and loss factor:**

$$S = \frac{\pi x}{cQ}$$

$$\text{Therefore, Loss factor} = \frac{20 \log_e * 1 \times 10^6 * \pi}{cQ}$$